Taxonomy of *Aspergillus* series *Versicolores*: species reduction and lessons learned about intraspecific variability

F. Sklenář[1,2*], K. Glässnerová[1], Ž. Jurjević[3], J. Houbraken[4], R.A. Samson[4], C.M. Visagie[5], N. Yilmaz[5], J. Gené[6], J. Cano[6], A.J. Chen[7], A. Nováková[2], T. Yaguchi[8], M. Kolařík[2], V. Hubka[1,2,8*]

[1]*Department of Botany, Faculty of Science, Charles University, Prague, Czech Republic;* [2]*Laboratory of Fungal Genetics and Metabolism, Institute of Microbiology, Czech Academy of Sciences, Prague, Czech Republic;* [3]*EMSL Analytical, Cinnaminson, New Jersey, USA;* [4]*Westerdijk Fungal Biodiversity Institute, Utrecht, The Netherlands;* [5]*Department of Biochemistry, Genetics, and Microbiology, Forestry and Agricultural Biotechnology Institute, University of Pretoria, Pretoria, South Africa;* [6]*Unitat de Micologia, Facultat de Medicina i Ciències de la Salut, IISPV, Universitat Rovira i Virgili, Reus, Spain;* [7]*Microbiome Research Center, Moon (Guangzhou) Biotech Ltd., Guangzhou, China;* [8]*Medical Mycology Research Center, Chiba University, Chuo-ku, Chiba, Japan*

**Corresponding author*: V. Hubka, vit.hubka@gmail.com; F. Sklenář, frantisek.sklenar@natur.cuni.cz

Abstract: *Aspergillus* series *Versicolores* members occur in a wide range of environments and substrates such as indoor environments, food, clinical materials, soil, caves, marine or hypersaline ecosystems. The taxonomy of the series has undergone numerous re-arrangements including a drastic reduction in the number of species and subsequent recovery to 17 species in the last decade. The identification to species level is however problematic or impossible in some isolates even using DNA sequencing or MALDI-TOF mass spectrometry indicating a problem in the definition of species boundaries. To revise the species limits, we assembled a large dataset of 518 strains. From these, a total of 213 strains were selected for the final analysis according to their calmodulin (*CaM*) genotype, substrate and geography. This set was used for phylogenetic analysis based on five loci (*benA*, *CaM*, *RPB2*, *Mcm7*, *Tsr1*). Apart from the classical phylogenetic methods, we used multispecies coalescence (MSC) model-based methods, including one multilocus method (STACEY) and five single-locus methods (GMYC, bGMYC, PTP, bPTP, ABGD). Almost all species delimitation methods suggested a broad species concept with only four species consistently supported. We also demonstrated that the currently applied concept of species is not sustainable as there are incongruences between single-gene phylogenies resulting in different species identifications when using different gene regions. Morphological and physiological data showed overall lack of good, taxonomically informative characters, which could be used for identification of such a large number of existing species. The characters expressed either low variability across species or significant intraspecific variability exceeding interspecific variability. Based on the above-mentioned results, we reduce series *Versicolores* to four species, namely *A. versicolor, A. creber*, *A. sydowii* and *A. subversicolor*, and the remaining species are synonymized with either *A. versicolor* or *A. creber*. The revised descriptions of the four accepted species are provided. They can all be identified by any of the five genes used in this study. Despite the large reduction in species number, identification based on phenotypic characters remains challenging, because the variation in phenotypic characters is high and overlapping among species, especially between *A. versicolor* and *A. creber*. Similar to the 17 narrowly defined species, the four broadly defined species do not have a specific ecology and are distributed worldwide. We expect that the application of comparable methodology with extensive sampling could lead to a similar reduction in the number of cryptic species in other extensively studied *Aspergillus* species complexes and other fungal genera.

Key words: *Aspergillus creber*, *Aspergillus sydowii*, *Aspergillus versicolor*, indoor fungi, multispecies coalescent model, osmotolerance, species delimitation, sterigmatocystin

Citation: Sklenář F, Glässnerová K, Jurjević Ž, Houbraken J, Samson RA, Visagie CM, Yilmaz N, Gené J, Cano J, Chen AJ, Nováková A, Yaguchi T, Kolařík M, Hubka V (2022). Taxonomy of *Aspergillus* series *Versicolores*: species reduction and lessons learned about intraspecific variability. *Studies in Mycology* **102**: 53–93. doi: 10.3114/sim.2022.102.02

Received: 29 June 2022 ; **Accepted:** 26 October 2022; **Effectively published online:** 16 November 2022

Corresponding editor: J.Z. Groenewald

INTRODUCTION

Aspergillus is an important genus of filamentous fungi with almost 450 accepted species and a large number of newly described species every year since the advent of molecular phylogenetics (Houbraken *et al.* 2020). The taxonomy of the clade comprising *A. versicolor* and related species has been turbulent and the clade is now recognized as series *Versicolores* within the section *Nidulantes*. Originally, the '*Aspergillus versicolor* group' was introduced by Thom & Church (1926) and later revised by Thom & Raper (1945) who accepted four species. Raper & Fennell (1965) then expanded the group to 18 species, but only two of those species remained in the series in its current form. Because group is not a recognized taxonomic rank, Gams *et al.* (1985) replaced groups with sections and created section *Versicolores*. Kozakiewicz (1989) reallocated seven species from section *Versicolores* to other sections based on the evaluation of conidial surface ornamentation using scanning electron microscope. Klich (1993) revised the section using cluster analysis by average linkage based on macro- and micromorphological measurements. As a result, the species removed by Kozakiewicz (1989) were transferred back to the section and the section was expanded again to contain 23 species. Peterson (2008) performed the first comprehensive revision of *Aspergillus* using DNA sequence data, including data from *benA*, *CaM*, *RPB2* and ITS-LSU region of rDNA. The preceding conceptions of the section were shattered as only *A. versicolor* and *A. sydowii* remained in the phylogenetically defined section. Other species were transferred into different sections, mainly sections *Usti* and *Nidulantes*. In addition, the whole section was considered superfluous because of its internal phylogenetic position within section *Nidulantes*. Jurjević *et al.* (2012) analyzed strains closely related to *A. versicolor* and *A. sydowii* which were collected mainly

Studies in Mycology

from the indoor environments in the USA, and obtained from the NRRL culture collection. They performed a phylogenetic analysis based on DNA sequences from six loci, accepted *A. amoenus*, *A. protuberus*, *A. sydowii*, *A. tabacinus* and *A. versicolor* as section members and proposed nine new species. As a result, the number of accepted species increased to 14. The authors also suggested that the section rank should be retained because it forms a monophyletic cluster, and the designation is broadly used in practice. Hubka *et al.* (2016) considered the concept of section *Versicolores* untenable as it formed only a clade within section *Nidulantes*, confirming the result of Peterson (2008). Houbraken *et al.* (2020) expanded the classification of *Aspergillus* with the series rank and reduced section *Versicolores* to series level. Since the expansion of series *Versicolores* by Jurjević *et al.* (2012), three additional species have been described, increasing the total number of accepted species to 17. Visagie *et al.* (2014) described *A. griseoaurantiacus* from house dust in Micronesia, Thailand and Mexico, Tsang *et al.* (2016) described *A. hongkongensis* from a human clinical sample collected in Hong Kong, and Jakšić Despot *et al.* (2017) described *A. pepii* from indoor air in a grain mill in Croatia.

The representatives of series *Versicolores* are often described as ubiquitous because they are frequently isolated from a wide range of substrates, mainly soil, indoor environments, food, feed, plants, caves, and clinical material (Domsch *et al.* 2007, Pitt & Hocking 2009, Jurjević *et al.* 2012, Zahradnik *et al.* 2013, Siqueira *et al.* 2016, Nováková *et al.* 2018). Series *Versicolores* members are xerophilic, which means that they can grow on substrates with a low water activity (a_w < 0.9) (Janda-Ulfig *et al.* 2009, González-Abradelo *et al.* 2019). The abundant presence of these species in indoor environments and bioaerosols increases their potential to pose health risks to humans (Micheluz *et al.* 2015, Géry *et al.* 2021). The spores of these species can cause allergies, aggravate asthma and they are associated with sick building syndrome (Schwab & Straus 2004, Géry *et al.* 2022). Almost all species can also produce mycotoxins, most notably sterigmatocystin, which is recognized as a potential carcinogen (class 2B - possible human carcinogen) (Veršilovskis & De Saeger 2010, Rank *et al.* 2011, Jurjević *et al.* 2013, Jakšić Despot *et al.* 2017). There are also numerous reports on the isolation of series *Versicolores* species from human and animal clinical specimens and rare cases of proven or suspected infections (Siqueira *et al.* 2016, Bongomin *et al.* 2018, Borgohain *et al.* 2019, Jia *et al.* 2019, Swain *et al.* 2020).

There are many studies reporting the isolation of bioactive compounds from series *Versicolores*, showing the great potential of these fungi for biotechnology, *e.g.* diphenyl ethers with antimicrobial and cytotoxic activity from *A. tennesseensis*, beta-glucosidase applicable in cellulose degradation from *A. versicolor*, or chitinase with antifungal activity from *A. griseoaurantiacus* (Kato *et al.* 2015, Li *et al.* 2018, Shehata *et al.* 2018, Sakhri *et al.* 2019, Danagoudar *et al.* 2021, Dobolyi *et al.* 2021, Huang *et al.* 2021). Genome sequences for seven species from the series have been deposited to the NCBI GenBank database [accessed 23rd of March 2022]. Among the most notable findings, the sterigmatocystin biosynthetic gene cluster was found to be absent for *A. sydowii*, explaining the inability of this species to produce this mycotoxin (Rank *et al.* 2011). Additionally, mating-type loci (both *MAT-1-1-1* and *MAT-1-2-1*), which are crucial for sexual development, are present in the genomes of series *Versicolores* species, suggesting their heterothallic mode of reproduction, even though the sexual state is yet to be observed (De Vries *et al.* 2017).

The correct identification of series *Versicolores* species is of great importance as evidenced by their diverse above-mentioned significances. However, a large part of these species cannot be identified morphologically due to their similarity or high intraspecific variability (Jurjević *et al.* 2012, Siqueira *et al.* 2016, Géry *et al.* 2021). Additionally, the broadly used identification method MALDI-TOF MS (matrix-assisted laser desorption ionization time-of-flight mass spectrometry) is not able to discriminate species within the series. This significantly limits the possibilities of correct identification, especially in clinical practices (Vidal-Acuña *et al.* 2018, Imbert *et al.* 2019, Shao *et al.* 2022). There is also increasing evidence that some isolates cannot be reliably identified with sequence data because BLAST similarity searches with different genes result in different identifications (our observations and personal communication). These problems may indicate that the concept of species is too narrow and motivated the present taxonomic revision.

One requirement of the species delimitation methods, which often fails to be met in studies involving fungi, is the presence of within-species variability which is ensured by the quality of sampling in terms of geography and/or substrates (Ahrens *et al.* 2016, Sklenář *et al.* 2020). Without large enough depth of sampling, boundaries between intraspecific and interspecific variability can easily be misinterpreted. Thanks to the omnipresence of series *Versicolores* and the ease of their isolation, these species represent the perfect model group for studying species limits on a large scale. For this study, we assembled a collection of more than 500 isolates from various substrates and continents. A subset of genetically unique isolates was subjected to the detailed analysis by various phylogenetic methods building upon the previous studies using this approach for *Aspergillus* (Sklenář *et al.* 2017, Hubka *et al.* 2018, Sklenář *et al.* 2021). Aside from the phylogenetic part, we also studied traditional phenotypic characters including micromorphology, macromorphology on eight cultivation media, and the growth rate at different temperatures and in an osmotic gradient. The synthesis of the resulting data and the consideration of practical taxonomic implications have led to the proposal of a drastic reduction in the number of species as detailed below.

MATERIALS AND METHODS

Strains

Some strains and/or DNA sequences were obtained from previously published studies of Jurjević *et al.* (2012) and Siqueira *et al.* (2016), which focused on the indoor environment and clinical material in the USA, respectively. Furthermore, we included strains from various countries and substrates deposited in culture collections such as CBS culture collection housed at the Westerdijk Fungal Biodiversity Institute (WI), working collection DTO of the Food and Indoor Mycology department housed at the WI, Culture Collection of Fungi, Department of Botany, Charles University (CCF, Czech Republic), working collections of the Applied Mycology group (CN) and the Forestry and Agricultural Biotechnology Institute (CMW) at the University of Pretoria (South Africa), and China General Microbiological Culture Collection Center (CGMCC, China). Additionally, we supplemented the dataset with newly isolated strains mainly originating from the indoor environment and caves. The isolation techniques mostly followed the procedures described by Jurjević *et al.* (2015), Nováková *et al.* (2012) and Nováková *et al.* (2018). Detailed information about the provenance of strains is listed in Table 1.

Table 1. *Aspergillus* series *Versicolores* strains examined in this study.

Species	Strain No.[1]	Provenance (locality, substrate, year of isolation, isolator/collector)	GenBank/ENA/DDBJ accession Nos.					
			ITS	*benA*	*CaM*	*RPB2*	*Mcm7*	*Tsr1*
A. creber	**NRRL 58592^T = IBT 32277^T = DTO 225-G7^T = CBS 145749^T**	USA, CA, indoor air, 2008, Ž. Jurjević	NR_135442	JN853980	JN854043	JN853832	JQ301890	JN853887
	EMSL 4757	USA, MO, Festus, basement, swab, 2018, Ž. Jurjević	–	ON807803	ON807940	ON808233	ON808106	ON808375
	NRRL 58672	USA, GA, indoor air, 2009, Ž. Jurjević	–	JN853992	JN854055	JN853844	JN854122	JN853878
	UTHSCSA 09-3357 = FMR 14151	USA, PA, bronchoalveolar lavage, 2009, D.A. Sutton	LN898684	LN898838	LN898761	LN898915	ON808105	ON808374
	NRRL 58675	USA, OH, indoor air, 2009, Ž. Jurjević	–	JN853994	JN854058	JN853847	JN854124	JN853891
	NRRL 58612	USA, NJ, indoor air, 2009, Ž. Jurjević	–	JN853990	JN854051	JN853840	JN854121	JN853880
	UTHSCSA 03-2409 = FMR 14132	USA, TX, hospital air, 2003, D.A. Sutton	LN898681	LN898835	LN898758	LN898912	ON808104	–
	NRRL 58607	USA, PA, indoor air, 2009, Ž. Jurjević	–	JN853989	JN854050	JN853839	JN854120	JN853890
	UTHSCSA 10-1327 = FMR 14201	USA, MN, human nail, 2010, D.A. Sutton	LN898687	LN898841	LN898764	LN898918	ON808103	–
	DTO 180-A5 = KAS 3914	South Africa, house dust, 2010, C.M. Visagie	–	ON807802	ON807939	ON808232	ON808102	ON808373
	NRRL 58601	USA, NJ, indoor air, 2009, Ž. Jurjević	–	JN853987	JN854047	JN853836	JN854119	JN853882
	S 478	Spain, Cueva del Tesoro, cave sediment, 2012, A. Nováková	–	ON807801	ON807938	ON808231	ON808101	ON808372
	DTO 357-E7	Netherlands, cystic fibrosis patient, between 2011–2013, collector unknown	–	ON807800	ON807937	ON808230	ON808100	ON808371
	NRRL 58673	USA, GA, indoor air, 2009, Ž. Jurjević	–	JN853993	JN854056	JN853845	JN854123	JN853889
	DTO 319-E4 = IBT 26409	Greenland, Pakitsoq, ice sample (approximately 11500 years old), 2014, J.C. Frisvad	–	ON807799	ON807936	ON808229	ON808099	ON808370
	S 216	Romania, Magura Cave, bat guano, 2009, A. Nováková	–	ON807798	ON807935	ON808228	ON808098	ON808369
	DTO 319-D6 = IBT 22306	USA, MD, indoor air, 2014, B. Jarvis	–	ON807797	ON807934	ON808227	ON808097	ON808368
	EMSL 4775	USA, WA, Shoreline, bathroom - swab, 2018, Ž. Jurjević	–	ON807796	ON807933	ON808226	ON808096	ON808367
	NRRL 58587	USA, CA, indoor air, 2008, Ž. Jurjević	–	JN853985	JN854042	JN853831	JN854118	JN853886
	CGMCC 3.05281	China, fruit peel, 1999, collector unknown	–	ON807795	ON807932	ON808225	ON808095	ON808366
	S 448	Spain, Cueva del Tesoro, cave sediment, 2012, A. Nováková	–	ON807794	ON807931	ON808224	ON808094	ON808365
	S 321	Slovakia, Demanovská Peace Cave, dead marten, 2011, A. Nováková	–	ON807793	ON807930	ON808223	ON808093	ON808364
	CMW-IA 29 = CMW 58631 = CN 090-F5	South Africa, Goeiehoek Silo, Gauteng, soybean, 2020, S. Bezuidenhout	–	ON807792	ON807929	ON808222	ON808092	ON808363
	UTHSCSA 14-188 = FMR 14168	USA, DE, bronchoalveolar lavage, 2014, D.A. Sutton	LN898685	LN898839	LN898762	LN898916	ON808091	–
	EMSL 4759	USA, NY, Buffalo, bathroom wall - swab, 2018, Ž. Jurjević	–	ON807791	ON807928	ON808221	ON808090	ON808362
	NRRL 58670	USA, NJ, indoor air, 2009, Ž. Jurjević	–	JN853991	JN854053	JN853842	–	JN853888
	NRRL 58584	USA, PA, indoor air, 2008, Ž. Jurjević	–	JN853984	JN854041	JN853830	–	JN853894
	NRRL 13147 = CBS 145753 = DTO 225-F4 (ex-type of *A. venenatus*)	USA, TN, toxic dairy cattle feed, 1984, B.W. Horn	JQ301896	JN854003	JN854014	JN853803	JN854129	JN853876
	EMSL 4847	USA, NJ, Trenton, office building – indoor air, 2018, Ž. Jurjević	–	ON807809	ON807947	ON808240	ON808113	ON808382

Table 1. (Continued).

Species	Strain No.[1]	Provenance (locality, substrate, year of isolation, isolator/ollector)	GenBank/ENA/DDBJ accession Nos.					
			ITS	*benA*	*CaM*	*RPB2*	*Mcm7*	*Tsr1*
	NRRL 35641 = CBS 145750 = DTO 225-G5 = IBT 32284 (ex-type of *A. puulaauensis*)	USA, HI, dead hardwood branch, 2003, D.T. Wicklow	JQ301893	JN853979	JN854034	JN853823	JN854127	JN853895
	CCF 5173	Czech Republic, Prague, mouse excrements in seed store, 2000, J. Hubert	–	OP762559	ON807946	OP762579	OP762565	OP762573
	UTHSCSA 11-1436 = FMR 14159	USA, WA, bronchoalveolar lavage, 2014, D.A. Sutton	LN898715	LN898869	LN898792	LN898946	OP688453	–
	S 376	Spain, Cueva del Tesoro, cave sediment, 2012, A. Nováková	–	ON807808	ON807945	ON808238	ON808111	ON808380
	DTO 321-G4	Netherlands, polyethylene foil, 2014, J. Houbraken	–	ON808380	ON807944	ON808237	ON808110	ON808379
	S 344	Slovakia, Šingliarova Abyss, organic matter in cave, 2008, A. Nováková	–	ON807806	ON807943	ON808236	ON808109	ON808378
	NRRL 58602	USA, WV, indoor air, 2009, Ž. Jurjević	–	JN853999	JN854048	JN853837	JN854128	JN853896
	S 191	Romania, Meziad Cave, bat droppings, 2009, A. Nováková	–	ON807805	ON807942	ON808235	ON808108	ON808377
	DTO 324-F6	Netherlands, cystic fibrosis patient, 2014, collector unknown	–	ON807804	ON807941	ON808234	ON808107	ON808376
	CGMCC 3.07849	China, 2005, substrate unknown, 2005, collector unknown	–	ON807790	ON807927	ON808220	ON808089	ON808361
	NRRL 58593	USA, CA, indoor air, 2008, Ž. Jurjević	–	JN853998	JN854044	JN853833	JN854111	JN853869
	DTO 019-A3	USA, NJ, soil, isolation date and collector unknown	–	ON807789	ON807926	ON808219	ON808088	ON808360
	UTHSCSA 10-479 = FMR 14153	USA, OH, hospital air, 2010, D.A. Sutton	LN898695	LN898849	LN898772	LN898926	ON808087	ON808359
	NRRL 230	China, soy sauce, 1917, Round	–	JN853973	JN854023	JN853812	JN854109	JN853867
	NRRL 4642	Unknown, 1969	EF652467	JN853975	EF652379	EF652203	JN854110	JN853868
	NRRL 227 = CBS 599.65 = ATCC 16853 = IMI 211379 (ex-type of *A. cvjetkovicii*)	USA, New Jersey, soil, 1915, G.W. Wilson	EF652440	EF652264	EF652352	EF652176	JN854108	JN853866
	CMW-IA 30 = CMW 58632 = CN 093-G3	South Africa, Free State, Kroonstad, maize (white), 2020, C.M. Visagie	–	ON807788	ON807925	ON808218	ON808086	ON808358
	CMW-IA 31 = CMW 58633 = CN 096-A1	South Africa, Mpumalanga, Bethal, soybean, 2020, S. Bezuidenhout	–	ON807787	ON807924	ON808217	ON808085	ON808357
	CMW-IA 27 = CMW 58629 = CN 089-A2	South Africa, Gauteng, Afrikaskop, soybean, 2020, S. Bezuidenhout	–	ON807786	ON807923	ON808216	ON808084	ON808356
	CMW-IA 33 = CMW 58635 = CN 116-D2	South Africa, Free State, Heuningspruit, sunflower, 2020, C.M. Visagie	–	ON807785	ON807922	ON808215	ON808083	ON808355
	DTO 319-F2 = IBT 28293	Denmark, Fano, seawater, 2014, E.K. Lynne	–	ON807784	ON807921	ON808214	ON808082	ON808354
	DTO 319-D2 = IBT 14828	United Kingdom, wheat, 2014, M. Hetmanski	–	ON807783	ON807920	ON808213	ON808081	ON808353
	DTO 268-C6	Uruguay, Montevideo, house dust, 2008, Z. Torrano	–	ON807782	ON807919	ON808212	ON808080	ON808352
	S 384	Spain, Nerja Cave, cave sediment, 2012, A. Nováková	–	ON807781	ON807918	ON808211	ON808079	ON808351
	CMW-IA 25 = CMW 58627 = CN 088-I9	South Africa, Gauteng, Afrikaskop, soybean, 2020, S. Bezuidenhout	–	ON807780	ON807917	ON808210	ON808078	ON808350
	CMW-IA 28 = CMW 58630 = CN 089-A3	South Africa, Gauteng, Afrikaskop, soybean, 2020, S. Bezuidenhout	–	ON807779	ON807916	–	ON808077	ON808349
	CMW-IA 26 = CMW 58628 = CN 089-A1	South Africa, Gauteng, Afrikaskop, soybean, 2020, S. Bezuidenhout	–	ON807778	ON807915	ON808209	ON808076	ON808348
	NRRL 13150 = CBS 145752 = DTO 225-F5 = IBT 32283 (ex-type of *A. tennesseensis*)	USA, TN, toxic dairy cattle feed, 1984, B.W. Horn	JQ301895	JN853976	JN854017	JN853806	JN854113	JN853872

Table 1. (Continued).

Species	Strain No.[1]	Provenance (locality, substrate, year of isolation, isolator/ollector)	GenBank/ENA/DDBJ accession Nos.					
			ITS	*benA*	*CaM*	*RPB2*	*Mcm7*	*Tsr1*
	CCF 5066	Spain, Nerja Cave, cave air, 2011, A. Nováková	–	OP762558	ON807914	OP762578	OP762564	OP762572
	CMW-IA 24 = CMW 58636 = CN 116-D4	South Africa, Free State, Heuningspruit, sunflower, 2020, C.M. Visagie	–	ON807776	ON807913	ON808207	ON808074	ON808346
	CMW-IA 23 = CMW 58625 = CN 066-E9	South Africa, Gauteng, Afrikaskop, soybean, 2020, S. Bezuidenhout	–	ON807775	ON807912	ON808206	ON808073	ON808345
	NRRL 229	Unknown, 1917, R. Thaxter	–	JN853972	JN854022	JN853811	–	JN853870
	DTO 178-C5 = KAS 3787	South Africa, house dust, 2010, C.M. Visagie	–	ON807774	ON807911	ON808205	ON808072	ON808344
	DTO 019-A6 = CBS 556.90	Japan, dried *Lentinus edodes*, 1990, J.C. Frisvad	–	ON807773	ON807910	ON808204	ON808071	ON808343
	CGMCC 3.05345	China, moon cake, 1999	–	ON807772	ON807909	ON808203	ON808070	ON808342
	CGMCC 3.05331	China, moldy oil, 1999	–	ON807771	ON807908	ON808202	ON808069	ON808341
	DTO 321-F4	Netherlands, cystic fibrosis patient material, between 2011–2013	–	ON807770	ON807907	ON808201	ON808068	ON808340
	S 475	Spain, Nerja Cave, cave air, 2012, A. Nováková	–	ON807769	ON807906	ON808200	ON808067	ON808339
	S 139	Romania, Limanu Cave, cave air, 2012, A. Nováková	–	ON807768	ON807905	ON808199	ON808066	ON808338
	S 309	Slovakia, Ardovská Cave, cave air, 2009, A. Nováková	–	ON807767	ON807904	ON808198	ON808065	ON808337
	UTHSCSA 10-71 = FMR 14200	USA, CT, bronchoalveolar lavage, 2010, D.A. Sutton	LN898703	LN898857	LN898780	LN898934	ON808064	ON808336
	UTHSCSA 09-425 = FMR 14234	USA, UT, human nail, 2009, D.A. Sutton	LN898704	LN898858	LN898781	LN898935	ON808063	ON808335
	S 371	Spain, Cueva del Tesoro, cave sediment, 2012, A. Nováková	–	ON807766	ON807903	ON808197	ON808062	ON808334
	DTO 319-F6 = IBT 31894	Japan, Noto, Peninsula, Mediterranean mussel (*Mytilus galloprovinciales*) 2014, M. Tzukamoto	–	ON807765	ON807902	ON808196	ON808061	ON808333
	NRRL 58671	USA, PA, indoor air, 2009, Ž. Jurjević	–	JN854008	JN854054	JN853843	JN854104	JN853864
	NRRL 58600 (ex-type of *A. jensenii*)	USA, MT, indoor air, 2008, Ž. Jurjević	JQ301892	JN854007	JN854046	JN853835	JN854103	JN853863
	EMSL 4720	USA, MA, Cohasset, air, apartment, 2018, Ž. Jurjević	–	ON807764	ON807901	–	ON808060	ON808332
	DTO 303-H3	Netherlands, Leerdam, surface of archive material, 2014, M. Meijer	–	ON807763	ON807900	–	ON808059	ON808331
	CMW-IA 39 = CMW 58641 = CN 138-G5	Canada, Nova Scotia, Little Lepreau, house dust, 2015, C.M. Visagie	–	ON807762	ON807899	–	ON808058	ON808330
	S 315	Slovakia, Ochtinská Aragonitová Cave, cave air, 2010, A. Nováková	–	ON807761	ON807898	–	ON808057	ON808329
	UTHSCSA 10-327 = FMR 14152	USA, PA, sputum, 2010, D.A. Sutton	LN898700	LN898854	LN898777	LN898931	–	ON808328
	CGMCC 3.05297	China, moldy shoe, 1999, collector unknown	–	ON807760	ON807897	ON808195	ON808056	ON808327
	S 317	Slovakia, Krásnohorská Cave, cave air, 2006, A. Nováková	–	ON807759	ON807896	ON808194	ON808055	ON808326
	DTO 138-B3	Germany, indoor air, 2010, collector unknown	–	–	ON807895	ON808193	ON808054	ON808325
	EMSL 4825	USA, OH, Pepper Pike, bedroom, settle plates, 2018, Ž. Jurjević	–	ON807758	ON807894	ON808192	ON808053	ON808324
	S 447	Spain, Cueva del Tesoro, cave sediment, 2012, A. Nováková	–	ON807757	ON807893	ON808191	ON808052	ON808323
	EMSL 4785	USA, NJ, Cherry Hill, office - indoor air, 2018, Ž. Jurjević	–	ON807756	ON807892	ON808190	ON808051	ON808322
	NRRL 240	USA, NY, rhizosphere of pepper plants, 1911, C.N. Jensen	–	JN854002	JN854030	JN853819	JN854102	JN853862
	NRRL 235	United Kingdom, London, paraffin, 1930, H. Raistrick	–	JN854001	JN854027	JN853816	JN854101	JN853860

Table 1. (Continued).

Species	Strain No.[1]	Provenance (locality, substrate, year of isolation, isolator/ollector)	GenBank/ENA/DDBJ accession Nos.					
			ITS	*benA*	*CaM*	*RPB2*	*Mcm7*	*Tsr1*
	NRRL 225	United Kingdom, substrate unknown, 1913, collector unknown	–	JN854000	JN854020	JN853809	JN854100	JN853858
	DTO 319-D8 = IBT 23103	Slovenia, soil salterns, 2014, N. Gunde-Cimerman	–	ON807755	ON807891	ON808189	ON808050	ON808321
	UTHSCSA 05-3600 = FMR 14136	USA, MN, sputum, 2005, D.A. Sutton	LN898698	LN898852	LN898775	LN898929	ON808049	–
	S 207	Romania, Meziad Cave, Capela, bat guano, 2010, A. Nováková	–	ON807754	ON807890	ON808188	ON808048	ON808320
A. subversicolor	**NRRL 58999^{T} = CBS 145751^{T} = DTO 225-G9^{T}**	India, Karnataka, coffee berry, 1970, B. Muthappa	JQ301894	JN853970	JN854010	JN853799	JN854069	JN853857
	DTO 353-D8 = URM 7878	Brazil, Recife, Honey of *Melipona scutellaris*, 2014, R. Barbosa	–	ON807753	ON807889	–	ON808047	ON808319
	DTO 353-A7 = URM 7877	Brazil, Recife, Honey of *Melipona scutellaris*, 2014, R. Barbosa	–	ON807752	ON807888	–	ON808046	ON808318
A. sydowii	**NRRL 254^{T} = CBS 593.65^{T} = IMI 211384^{T} = NRRL 250^{T} = ATCC 16844^{T}**	USA, GA, clinical material, isolation date unknown, M.M. Harris	EF652451	LC589353	LC589325	EF652187	–	JN853897
	CMW-IA 46 = CMW 58648 = CN 164B6 = DN 86	Botswana, Gcwihaba Cave, guano-contaminated cave sediment, 2019, G. Modise & D. Nkwe	–	ON807751	ON807887	ON808187	ON808045	ON808317
	CMW-IA 44 = CMW 58646 = CN 164B4 = DN 47	Botswana, Gcwihaba Cave, guano-contaminated cave sediment, 2019, G. Modise & D. Nkwe	–	ON807750	ON807886	ON808186	ON808044	ON808316
	CMW-IA 42 = CMW 58644 = CN 164B2 = DN 30	Botswana, Gcwihaba Cave, guano-contaminated cave sediment, 2019, G. Modise & D. Nkwe	–	ON807749	ON807885	ON808185	ON808043	ON808315
	CMW-IA 41 = CMW 58643 = CN 164B1 = DN 6	Botswana, Gcwihaba Cave, guano-contaminated cave sediment, 2019, G. Modise & D. Nkwe	–	ON807748	ON807884	ON808184	ON808042	ON808314
	S 41	Spain, near Castañar de Ibor Cave, outdoor air, 2009, A. Nováková	–	ON807747	ON807883	ON808183	ON808041	ON808313
	S 15	Spain, Cueva del Tesoro, Sala de Marco Craso, cave air, 2010, A. Nováková	–	ON807746	ON807882	ON808182	ON808040	ON808312
	UTHSCSA 06-2780 = FMR 14185	USA, MN, bronchus, 2006, D.A. Sutton	LN898721	LN898875	LN898798	LN898952	ON808039	–
	S 23	Czech Republic, Moravian Karst, New Amateur Cave, „Dóm Ráztoka“ Dome, cave sediment, 2009, A. Nováková	–	ON807745	ON807881	ON808181	ON808038	ON808311
	DTO 145-G7	Egypt, tomb of dogs, 2010, M. Meijer	–	ON807744	ON807880	ON808180	ON808037	ON808310
	DTO 268-C2	Uruguay, Montevideo, house dust, 2008, Z. Torrano	–	ON807743	ON807879	ON808179	ON808036	ON808309
	CGMCC 3.06723	China, fermented crop, 2004, collector unknown	–	ON807742	ON807878	ON808178	ON808035	ON808308
	UTHSCSA 09-1708 = FMR 14338	USA, UT, lung tissue, 2009, D.A. Sutton	LN898732	LN898886	LN898809	LN898963	ON808034	ON808307
	CMW-IA 35 = CMW 58637 = CN 117-C2	South Africa, Viljoenskroon, sunflower, 2020, C.M. Visagie & N. Yilmaz	–	ON807741	ON807877	ON808177	ON808033	ON808306
	UTHSCSA 12-934 = FMR 14210	USA, MN, bronchoalveolar lavage, 2012, D.A. Sutton	LN898725	LN898879	LN898802	LN898956	ON808032	ON808305
	UTHSCSA 11-204 = FMR 14155	USA, PA, clinical sample - eye, 2011, D.A. Sutton	LN898717	LN898871	LN898794	LN898948	ON808031	ON808304
	CGMCC 3.13937	China, shoe, 2009, collector unknown	–	ON807740	ON807876	ON808176	ON808030	ON808303
	UTHSCSA 13-2518 = FMR 14164	USA, UT, clinical sample - eye, 2013, D.A. Sutton	LN898718	LN898872	LN898795	LN898949	ON808029	ON808302

Table 1. (Continued).

Species	Strain No.[1]	Provenance (locality, substrate, year of isolation, isolator/ollector)	GenBank/ENA/DDBJ accession Nos.					
			ITS	*benA*	*CaM*	*RPB2*	*Mcm7*	*Tsr1*
	CCF 3621	Czech Republic, Olomouc, endotracheal secret of man, 2003, P. Hamal	–	FR775355	ON807875	OP762580	OP762566	OP762574
	DTO 002-H3 = CBS 117771	South Korea, Yeongi, hot pepper from pepper field, 2003, S.B. Hong	–	ON807738	ON807874	ON808174	ON808027	ON808300
	DTO 266-H9	Federated States of Micronesia, Malem, house dust, 2009, W. Law	–	ON807737	ON807873	ON808173	ON808026	–
	CCF 5063	Spain, Cueva del Tesoro, cave sediment, 2011, A. Nováková	–	FR775337	ON807872	OP762581	OP762567	OP762575
	DTO 004-G1 = CBS 118475	Netherlands, tattoo paint, isolate date and collector unknown	–	ON807735	ON807871	–	ON808024	ON808298
A. versicolor	**NRRL 238^{T} = CBS 583.65^{T} = ATCC 9577^{T} = IFO 33027^{T} = IMI 229970^{T} = JCM 10258^{T} = UAMH 4956^{T} = UAMH 9314^{T}**	USA, unknown substrate and year of isolation, V.K. Charles	EF652442	LC589363	EF652354	EF652178	JN854079	JN853911
	CMW-IA 22 = CMW 58624 = CN 054-B5	South Africa, North West Province, Ottosdal, maize (white), 2020, C.M. Visagie & N. Yilmaz	–	ON807734	ON807870	–	ON808023	ON808297
	UTHSCSA 03-3679 = FMR 14181	USA, FL, bronchoalveolar lavage, 2003, D.A. Sutton	LN898740	LN898894	LN898817	LN898971	ON808022	ON808295
	DTO 241-I4	Indonesia, surface in medical rehabilitation room, 2012, A. Sidar	–	ON807733	ON807869	ON808171	ON808021	–
	DTO 270-D1	Mexico, Sayulita, house dust, 2009, A. Amend	–	ON807732	ON807868	ON808170	ON808020	ON808296
	DTO 174-H9	Imported from Madagascar, vanilla sticks, 2012, J. Houbraken	–	ON807731	ON807867	ON808169	ON808019	ON808294
	DTO 319-E9 = IBT 28029 = ATCC 32662	USA, TX, soil, 2014, H.W. Schroeder	–	ON807730	ON807866	ON808168	ON808018	ON808293
	NRRL 13144 = NRRL A-27273	USA, TN, toxic dairy cattle feed, 1984, B.W. Horn	–	JN853949	JN854011	JN853800	JN854081	JN853915
	NRRL 3505 = CBS 602.74 = ATCC 18990 (ex-type of *A. protuberus*)	former Yugoslavia, rubber coated electrical cables, before 1968, M. Muntañola-Cvetkovic	EF652460	EF652284	EF652372	EF652196	JN854088	LC004923
	CCF 5055	Spain, Nerja Cave, cave sediment, 2011, A. Nováková	–	OP762562	OP650540	OP762584	OP762570	–
	DTO 019-D4 = CBS 601.74 = IMI 278378	former Yugoslavia, rubber coated electrical cables, before 1968, M. Muntañola-Cvetkovic	–	ON807728	ON807864	ON808166	ON808016	–
	EMSL 4703	USA, CA, Lawndale, framing below balcony, swab, 2018, Ž. Jurjević	–	ON807727	ON807863	ON808165	ON808015	–
	UTHSCSA 11-269 = FMR 14156	USA, IL, bronchoalveolar lavage, 2011, D.A. Sutton	LN898707	LN898861	LN898784	LN898938	ON808014	ON808292
	S 49	Spain, Nerja Cave, cave sediment, 2011, A. Nováková	–	ON807726	ON807862	ON808164	ON808013	ON808291
	UTHSCSA 06-2837 = FMR 14328	USA, bronchoalveolar lavage, 2006, D.A. Sutton	LN898713	LN898867	LN898790	LN898944	ON808012	–
	S 450	Spain, Cueva del Tesoro, cave sediment, 2012, A. Nováková	–	ON807725	ON807861	ON808163	ON808011	ON808290
	CCF 5370	Romania, Movile Cave, cave air, 2013, A. Nováková	–	OP762563	OP650500	OP762585	OP762571	–
	EMSL 4753	USA, FL, Jacksonville, bedroom, settle plates, 2018, Ž. Jurjević	–	ON807723	ON807859	–	ON808009	–
	UTHSCSA 09-246 = FMR 14148	USA, CT, animal clinical specimen, 2009, D.A. Sutton	LN898706	LN898860	LN898783	LN898937	ON808008	ON808289
	S 445	Spain, Cueva del Tesoro, cave sediment, 2012, A. Nováková	–	ON807722	ON807858	ON808161	ON808007	ON808288
	EMSL 4846	USA, NJ, Trenton, office building - indoor air, 2018, Ž. Jurjević	–	ON807721	ON807857	ON808160	ON808006	–
	UTHSCSA 11-2175 = FMR 14205	USA, AL, Ohio, sputum, 2011, D.A. Sutton	LN898710	LN898864	LN898787	LN898941	ON808005	ON808287

Table 1. (Continued).

Species	Strain No.[1]	Provenance (locality, substrate, year of isolation, isolator/ollector)	GenBank/ENA/DDBJ accession Nos.					
			ITS	*benA*	*CaM*	*RPB2*	*Mcm7*	*Tsr1*
	S 39	Spain, Cueva del Tesoro, cave air, 2010, A. Nováková	–	ON807720	ON807856	ON808159	ON808004	ON808286
	DTO 247-E7	Mexico, Sayulita, house dust, 2009, A. Amend	–	ON807719	ON807855	ON808158	ON808003	–
	DTO 019-D6	Montenegro, Ulcinj, seawater, isolation year unknown, M. Muntañola-Cvetkovic	–	ON807718	ON807854	ON808157	ON808002	–
	UTHSCSA 08-1574 = FMR 14336	USA, CO, bronchoalveolar lavage, 2008, D.A. Sutton	LN898714	LN898868	LN898791	LN898945	ON808001	–
	UTHSCSA 06-4104 = FMR 14140	USA, MD, bronchoalveolar lavage, 2006, D.A. Sutton	LN898705	LN898859	LN898782	LN898936	ON808000	ON808285
	NRRL 233 = CBS 145748 = DTO 225-D8 (ex-type of *A. austroafricanus*)	South Africa, Cape Town, 1922, V.A. Putterill	JQ301891	JN853963	JN854025	JN853814	JN854086	JN853916
	DTO 268-A1	Thailand, Songkla, house dust, 2009, P. Noonim	–	ON807717	ON807853	ON808156	ON807999	ON808284
	DTO 237-D1	Indonesia, Yogyakarta, food and nutrient library, 2012, R. Rahmawati	–	ON807716	ON807852	ON808155	ON807998	OP688454
	CBS 145671 = HKU49 = NBRC 110693 = NCPF 7870 = BCRC FU30360 = DTO 351-C3 (ex-type of *A. hongkongensis*)	Hong Kong, human toenail, 2013	NR_138262	LC000552	LC000565	LC000578	LC000583	LC000584
	S 627	Spain, Cueva del Tesoro, cave air, 2012, A. Nováková	–	ON807715	ON807851	ON808154	ON807997	ON808283
	DTO 267-G2	South Africa, Stellenbosch, house dust, 2009, K. Jacobs	–	ON807714	ON807850	ON808153	ON807996	ON808282
	CMW-IA 45 = CMW 58647 = CN 164B5 = DN 52	Botswana, Gcwihaba Cave, guano-contaminated cave sediment, 2019, G. Modise & D. Nkwe	–	ON807713	ON807849	ON808152	ON807995	ON808281
	NRRL 4838 = NRRL 236 = CBS 111.32 = CBS 600.65 = DTO 019-A4 = IMI 211400 = ATCC 16845 (ex-type of *A. amoenus*)	Germany, Münster, botanical garden, fruit of *Berberis* sp., 1930, M. Roberg	EF652480	EF652304	EF652392	EF652216	JN854074	JN853907
	DTO 246-D6	South Africa, *Gonatophragmium* sp., 2013, J. Houbraken	–	ON807712	ON807848	ON808151	ON807994	ON808280
	DTO 268-I7	Federated States of Micronesia, Lelu, house dust, 2008, W. Law	–	ON807711	ON807847	ON808150	ON807993	ON808279
	EMSL 4790	USA, MD, Aberdeen, bathroom wall, swab, 2018, Ž. Jurjević	–	ON807710	ON807846	ON808149	ON807992	ON808278
	DTO 319-D5 = IBT 21121 = CCRC 32142	Taiwan, Hwalien City, stored sesame seeds, 2014, S.S. Tzean	–	ON807709	ON807845	ON808148	ON807991	–
	UTHSCSA 09-2582 = FMR 14368	USA, MA, lung tissue, 2009, D.A. Sutton	LN898677	LN898831	LN898754	LN898908	ON807990	ON808277
	DTO 319-E2 = NRRL 35600 = IBT 29647	USA, HI, Kapuka Pauula, basidiomata of *Ganoderma australe*, 2014, D.T. Wicklow	–	JN853952	JN854033	JN853822	JN854073	JN853908
	DTO 267-F7	Federated States of Micronesia, Lelu, house dust, 2008, W. Law	–	–	ON807844	ON808147	ON807989	–
	DTO 269-A7	Federated States of Micronesia, Lelu, house dust, 2008, W. Law	–	ON807708	ON807843	ON808146	ON807988	ON808276
	DTO 319-D3 = IBT 16439 = IMI 096225	United Kingdom, hay, 2014, M.E. Lacey	–	ON807707	ON807842	ON808145	ON807987	ON808275
	S 333	Romania, Fânaţe Cave, bat guano, 2010, A. Nováková	–	ON807706	ON807841	ON808144	ON807986	–
	EMSL 4779	USA, TX, Tyler, bedroom, vent - swab, 2018, Ž. Jurjević	–	ON807705	ON807840	ON808143	ON807985	ON808274
	DTO 248-D1	Mexico, Sayulita, house dust, 2009, A. Amend	–	ON807704	ON807839	ON808142	ON807984	ON808273
	UTHSCSA 06-4284 = FMR 14188	USA, South Carolina, bronchoalveolar lavage, 2006, D.A. Sutton	LN898672	LN898826	LN898749	LN898903	ON807983	–

Table 1. (Continued).

Species	Strain No.[1]	Provenance (locality, substrate, year of isolation, isolator/ollector)	GenBank/ENA/DDBJ accession Nos.					
			ITS	*benA*	*CaM*	*RPB2*	*Mcm7*	*Tsr1*
	S 310	Spain, Cueva del Tesoro, cave sediment, 2010, A. Nováková	–	ON807703	ON807838	ON807982	ON808141	ON808272
	S 459	Spain, Cueva del Tesoro, cave sediment, 2012, A. Nováková	–	ON807702	ON807837	ON808140	ON807981	ON808271
	CCF 5038	Spain, Nerja Cave, cave air, 2011, A. Nováková	–	OP762561	OP650489	OP762583	OP762569	OP762577
	UTHSCSA 09-125 = FMR 14198	USA, MD, bronchoalveolar lavage, 2009, D.A. Sutton	LN898673	LN898827	LN898750	LN898904	ON807979	ON808270
	CMW-IA 38 = CMW 58640 = CN 137-I5	South Africa, animal feed, 2021, C.M. Visagie & N. Yilmaz	–	ON807700	ON807835	–	ON807978	–
	NRRL 239 = CBS 584.65 ATCC 16856 = IMI 211385 (ex-type of *A. fructus*)	USA, CA, date fruit (*Phoenix dactylifera*), 1939, D.E. Bliss	EF652449	EF652273	EF652361	EF652185	JN854076	JN853917
	FMR 15740	Argentina, soil, 2016, A.M. Stchigel	LT903690	LT903681	LT903684	LT903687	–	ON808269
	CMW-IA 32 = CMW 58634 = CN 116-D1	South Africa, Heuningspruit, sunflower, 2020, C.M. Visagie & N. Yilmaz	–	ON807699	ON807834	ON808138	ON807977	ON808268
	DTO 319-D4	USA, WY, Farson, dungy soil under *Artemisia tridentata*, 2014, J.C. Frisvad	–	ON807698	ON807833	ON808137	ON807976	ON808267
	CMW-IA 40 = CMW 58642 = CN 164A9 = DN 2	Botswana, Gcwihaba Cave, guano-contaminated cave sediment, 2019, G. Modise & D. Nkwe	–	ON807697	ON807832	ON808136	ON807975	ON808266
	NRRL 241	Unknown, pomegranate fruit, 1916, L. McCulloch	–	JN853943	JN854031	JN853820	JN854087	JN853918
	DTO 267-G8	South Africa, Stellenbosch, house dust, 2009, K. Jacobs	–	ON807696	ON807831	ON808135	ON807974	ON808265
	S 434	Spain, near Nerja Cave, soil, 2012, A. Nováková	–	ON807695	ON807830	ON808134	ON807973	ON808264
	UTHSCSA 12-3194 = FMR 14162	USA, CA, pericardium, 2012, D.A. Sutton	LN898696	LN898850	LN898773	LN898927	ON807972	ON808263
	DTO 019-A2	USA, CA, fruit of *Phoenix dactylifera,* isolation date and collector unknown	–	ON807694	ON807829	ON808133	ON807971	ON808262
	CBS 142028 = MFBF AV11051B IX = SZMC 22333 (ex-type of *A. pepii*)	Croatia, Zagreb, grain mill - indoor air, 2012, D. Jakšić Despot	KU613368	KU613371	KU613365	–	–	–
	DTO 243-G4	Indonesia, polyclinic for children, 2012, A. Sidar	–	ON807693	OP650454	ON808132	ON807970	ON808261
	CBS 138191 = DTO 267-D8 (ex-type of *A. griseoaurantiacus*)	Federated States of Micronesia, Yela of Kosrae Island, house dust, 2010, E. Whitfield & K. Mwange	KJ775553	KJ775086	KJ775357	KU866988	–	–
	CMW-IA 43 = CMW 58645 = CN 164B3 = DN 40	Botswana, Gcwihaba Cave, guano-contaminated cave sediment, 2019, G. Modise & D. Nkwe	–	ON807692	ON807828	ON808131	ON807969	ON808260
	S 465	Spain, near Nerja Cave, cave air, 2012, A. Nováková	–	ON807691	ON807827	ON808130	ON807968	–
	DTO 276-F9	Iran, bronchoalveolar lavage, 2013, J. Najafzadeh	–	ON807690	ON807826	ON808129	ON807967	ON808259
	DTO 138-A3	Germany, airconditioning system, 2010, collector unknown	–	ON807689	ON807825	ON808128	ON807966	ON808258
	S 334	Romania, Zidita Cave, bat guano, 2009, A. Nováková	–	ON807688	ON807824	ON808127	ON807965	ON808257
	S 215	Romania, Zidita Cave, bat guano, 2009, A. Nováková	–	ON807687	ON807823	ON808126	ON807964	ON808256
	CMW-IA 36 = CMW 58638 = CN 131-G9	South Africa, animal feed, 2021, C.M. Visagie & N. Yilmaz	–	ON807686	ON807822	–	ON807963	ON808255
	DTO 245-F5 = CBS 138189	Mexico, Sayulita, house dust, 2009, A. Amend	–	ON807685	ON807821	ON808125	ON807962	ON808254
	CMW-IA 37 = CMW 58639 = CN 132-C9	South Africa, animal feed, 2021, C.M. Visagie & N. Yilmaz	–	ON807684	ON807820	ON808124	ON807961	ON808253

Table 1. (Continued).

Species	Strain No.[1]	Provenance (locality, substrate, year of isolation, isolator/ollector)	GenBank/ENA/DDBJ accession Nos.					
			ITS	*benA*	*CaM*	*RPB2*	*Mcm7*	*Tsr1*
	EMSL 4723	USA, NJ, Morris Plains, bathroom wall, swab, 2018, Ž. Jurjević	–	ON807683	ON807819	ON808123	ON807960	ON808252
	DTO 337-C3	Germany, school material, 2015, U. Hack	–	ON807682	ON807818	ON808122	ON807959	ON808251
	DTO 267-D2 = CBS 138190	Federated States of Micronesia, Lelu, house dust, 2009, W. Law	–	ON807681	ON807817	ON808121	ON807958	ON808250
	NRRL 4791 = CBS 122718 = IFO 4098 (ex-type of *A. tabacinus*)	Unknown, tobacco, before 1934, Y. Nakazawa	EF652478	EF652302	EF652390	EF652214	JN854084	JN853922
	DTO 337-B9	Germany, wallpaper, 2015, U. Hack	–	ON807680	ON807816	ON808120	ON807957	ON808249
	EMSL 4820	USA, NY, New York, bedroom, swab, 2018, Ž. Jurjević	–	ON807679	ON807815	ON808119	ON807956	ON808248
	UTHSCSA 07-2427 = FMR 14190	USA, bronchoalveolar lavage, 2007, D.A. Sutton	LN898737	LN898891	LN898814	LN898968	ON807955	ON808247
	DTO 319-E6 = IBT 26806	India, Kerala, green coffee beans, 2014, M. Franck	–	ON807678	ON807814	ON808118	ON807954	ON808246
	ANV 16-4K	Czech Republic, Prague, book in library, 2018, Nováková	–	ON807677	ON807813	ON808117	ON807953	ON808245
	CCF 3690	Czech Republic, Liberec, toenail of woman, 2006, J. Doležalová	–	OP762560	FR751430	OP762582	OP762568	OP762576
	NRRL 5031 (ex-type of *A. versicolor* var. *magnus*)	Unknown country and source, before 1962, Y. Sasaki	–	JN853947	JN854036	JN853825	–	JN853920
	DTO 019-D2	South Korea, Daejeon, soil from pepper field, 2003, S.B. Hong	–	ON807675	ON807811	ON808115	ON807951	ON808243
	UTHSCSA 03-1197 = FMR 14179	USA, FL, sputum, 2003, D.A. Sutton	LN898736	LN898890	LN898813	LN898967	ON807950	ON808242
	UTHSCSA 08-2898 = FMR 14232	USA, bronchoalveolar lavage, 2008, D.A. Sutton	LN898739	LN898893	LN898816	LN898970	ON807949	–
	CGMCC 3.05288	China, moldy broom, 1999, collector unknown	–	ON807674	ON807810	ON808114	ON807948	ON808241
	DTO 319-E3	Thailand, Hua Hin, soil under bush, 2014, J.C. Frisvad	–	OP82096	OP650458	OP820970	OP820969	–

[1] Acronyms of culture collections in alphabetic order: ATCC, American Type Culture Collection, Manassas, Virginia; BCRC, Bioresource Collection and Research Center, Hsinchu, Taiwan; CBS, Westerdijk Fungal Biodiversity Institute (formerly Centraalbureau voor Schimmelcultures), Utrecht, the Netherlands; CCF, Culture Collection of Fungi, Department of Botany of Charles University, Prague, Czech Republic; CGMCC, China General Microbiological Culture Collection Center, China; CMW, CMW-IA & CN, working and formal culture collections housed at FABI (Forestry and Agricultural Biotechnology Institute) and Innovation Africa, University of Pretoria, South Africa; DN, working collection of David Nkwe, housed at the Department of Biological Sciences and Biotechnology, Botswana International University of Science and Technology, Palapye, Botswana; DTO, Internal Culture Collection of the Department of Applied and Industrial Mycology of the CBS-KNAW Fungal Biodiversity Centre, Utrecht, The Netherlands; EMSL, EMSL Analytical Inc., New Jersey, USA; FMR, Facultat de Medicina i Ciències de la Salut, Reus, Spain; HKU,The University of Hong Kong Mycological Herbarium, Hong Kong; IBT, Culture Collection at the Department of Biotechnology and Biomedicine, Lyngby, Denmark; IFO, Institute for Fermentation, Osaka, Japan (IFO strains were transferred to the NBRC NITE collection); IMI, CABI's collection of fungi and bacteria, Wallingford, UK; JCM, Japan Collection of Microorganisms, Tsukuba, Japan; KAS, fungal collection of Keith A. Seifert, internal working culture collection at DAOMC (Culture collection of the National Mycological Collections, Agriculture & Agri-Food Canada), Ottawa, Canada; MFBF, collection of the Department of Microbiology, Faculty of Pharmacy and Biochemistry, University of Zagreb, Croatia; NBRC (NITE), National Institute of Technology and Evaluation, Biological Resource Center, Department of Biotechnology, Kisarazu, Chiba, Japan; NCPF, The National Collection of Pathogenic Fungi, Bristol, UK; NRRL, Agricultural Research Service Culture Collection, Peoria, Illinois, USA; SZMC, Szeged Microbiological Collection at the Department of Microbiology, Faculty of Science and Informatics, University of Szeged, Hungary; UAMH, UAMH Centre for Global Microfungal Biodiversity (formerly University of Alberta Microfungus collection and Herbarium), Gage Research Institute, University of Toronto, Toronto, Canada; URM, culture collection at the Federal University of Pernambuco, Recife, Brazil; UTHSCSA, Collection of Fungus Testing Laboratory, University of Texas, Health Science Center, San Antonio, USA. Other: ANV, S, personal designation of strains isolated by A. Nováková (no permanent preservation of cultures).

Molecular studies

Total genomic DNA was isolated from 7-d-old cultures with the NucleoSpin® Soil (Macherey–Nagel, Düren, Germany) DNA isolation kit and its quality was verified using a NanoDrop 1 000 Spectrophotometer.

Sequences of the ITS region of rDNA were not obtained for the majority of strains because the variability of this locus within series *Versicolores* is low (Jurjević *et al.* 2012). A part of the β-tubulin gene (*benA*) was amplified using forward primers Bt2a (Glass & Donaldson 1995) or T10 (O'Donnell & Cigelnik 1997) and reverse primer Bt2b (Glass & Donaldson 1995). A part of the calmodulin gene (*CaM*) was amplified using forward primers CF1L, CF1M (Peterson 2008) or cmd5 (Hong *et al.* 2006) and reverse primers CF4 (Peterson 2008) or cmd6 (Hong *et al.* 2006). A part of the *Mcm7* gene encoding the minichromosome maintenance factor 7 was amplified using either universal primers Mcm7-709for and Mcm7-1348rev (Schmitt *et al.* 2009) or newly developed primers specific for the series *Versicolores*, namely Mcm7-Aver710for (5'-CACGAGTATCAGATGTTAAACCG-3') and Mcm7-Aver1354rev (5'- GATTTGGCAACACCAGGGTC -3'). A part of the RNA polymerase II second largest subunit gene (*RPB2*) was amplified using forward primer fRPB2-5F and reverse primer fRPB2-7CR (Liu *et al.* 1999). Finally, a part of the *Tsr1* gene encoding the ribosome biogenesis protein was amplified with primers Tsr1-1453for and Tsr1-2308rev (Schmitt *et al.* 2009).

The PCR was performed with standard or touchdown protocol and the PCR products were purified with ethanol and sodium acetate. All procedures and amplification conditions are described in detail by Sklenář *et al.* (2021).

The resulting DNA sequences were assembled in BioEdit v. 7.0.5 (Hall 1999) and deposited in GenBank. Obtained accession numbers are listed in Table 1. The sequences were aligned in MAFFT v. 7 (Katoh & Standley 2013) using the G-INS-I strategy. The best fitting model of evolution for every alignment was determined in jModelTest v. 2.1.7 (Posada 2008) using Bayesian information criterion with the following results. For the alignment of *benA s*equences, K80+G was selected as the best fitting model; TrNef+G for the alignment of *CaM* sequences; K80+G for the alignment of *Mcm7* sequences; TrNef+G for the alignment of *RPB2* sequences; and TrN+I for the alignment of *Tsr1* sequences. The TrNef+I+G model was chosen as the best fitting model for the alignment of 518 *CaM* sequences, and the TrNef model for the alignment of 48 ITS rDNA sequences. All alignments (together with input data for phylogenetic methods) were deposited into the Dryad Digital Repository (https://doi.org/10.5061/dryad.63xsj3v5q).

Phylogenetic analysis and species delimitation

We first assembled *CaM* sequences of 518 strains belonging to series *Versicolores* and calculated a Maximum Likelihood (ML) tree in IQ-TREE v. 2.1.2 (Minh *et al.* 2020). The branch support was determined by 1 000 standard bootstrap replicates. The graphical output was prepared in iTOL v. 6.5.6 (Letunic & Bork 2016) with colour strips next to the phylogenetic tree representing the geographic origin and substrate/environment. The provenance of strains used in the analysis is listed in Supplementary Table S1.

Based on the results of this *CaM p*hylogenetic tree, we selected 213 strains to be used for further analyses and thus obtained additional sequences from four loci for them. The ML analysis based on a concatenated dataset was then calculated in IQ-TREE v. 2.1.2. Each locus was set up as a separate partition and the branch support was determined by 1 000 standard bootstrap replicates.

To further demonstrate the relationships between currently accepted species in series *Versicolores*, we calculated the species tree in starBEAST v. 2.0 (Drummond *et al.* 2012). The strains were assigned to 17 species according to the best scoring ML tree calculated from the concatenated dataset. The length of the mcmc chain was 1×10^9 generations, the molecular clock model was set to strict clock, and the *species tree* prior was set to the Coalescent constant population model. To present the results of this analysis we employed the program Densitree v. 2.2.7 (Bouckaert & Heled 2014).

To investigate the stability and robustness of identification across the currently accepted 17 species and different DNA loci, we performed BLAST (basic local alignment search tool) searches with all available sequences from all species against the local BLAST database consisting of only ex-type strains sequences. To demonstrate the results, we prepared colour strips in iTOL and plotted them on the ML tree.

Five single-locus species delimitation methods (GMYC, bGMYC, PTP, bPTP, ABGD) were performed with alignments reduced to unique sequences. The reduction was carried out in R v. 4.1.2 (R Core Team 2015) using the *haplotype* function from the package PEGAS (Paradis 2010). The GMYC method was performed in R v. 4.1.2 with the package SPLITS (Fujisawa & Barraclough 2013) based on the phylogenetic tree calculated in BEAST v. 2.6.7 (Bouckaert *et al.* 2019) with the chain length of 1×10^7 generations, strict molecular clock, and tree prior set to Yule model. The same source material was used for the bGMYC method, but instead of using one consensus tree, we used 100 randomly selected trees after discarding the initial 25 % of trees as burn-in. The analysis was performed in R v. 3.4.1 using the package BGMYC (Reid & Carstens 2012). PTP and bPTP utilized one thousand ML standard bootstrap trees calculated in IQ-TREE v. 2.1.2. Both PTP and bPTP analyses were performed in Python v. 3 (van Rossum & Drake 2019) with the package PTP (Zhang *et al.* 2013). The ABGD (Automatic Barcode Gap Discovery) (Puillandre *et al.* 2012) was performed on the ABGD web server (available online: http://wwwabi.snv.jussieu.fr/public/abgd/abgdweb.html). Alignments of unique sequences were used as input and the distance matrix was calculated on the server with the K2P model of evolution. The default value of parameter X (1.5) resulted in all strains delimited as one species, so a lower value (1.2) was used. Since ABGD analysis results in a number of different delimitation schemes, the decision on which result to consider was based on the recommendation of Puillandre *et al.* (2012) and Kekkonen & Hebert (2014) and therefore we chose the results of the initial partition which was closest to P = 0.01.

To prepare input for the multilocus method STACEY, we first merged all single-locus alignments into one, then we reduced this alignment to unique sequences using the *haplotype* function (the number of strains was reduced from 214 to 195), and finally we split the concatenated dataset back into separate single-locus alignments. The analysis was performed in BEAST v. 2.6.7 with the STACEY v. 1.2.5 add-on (Jones 2017). The following settings were selected: the length of mcmc chain was 1×10^9 generations, the molecular clock model was set to strict clock, the *species tree* prior was set to the Yule model, *growth rate* prior was set to lognormal distribution (M = 5, S = 2), *clock rate* priors for all loci were set to lognormal distribution (M = 0, S = 1), *PopPriorScale* prior was set to lognormal distribution (M = -7, S = 2) and *relativeDeathRate* prior was set to beta distribution (α = 1, β = 1 000). The output was processed with SpeciesDelimitationAnalyzer (Jones 2017). The results of STACEY are presented in two ways. Firstly, we

created a plot to show how the number of delimited species and the probability of the most probable and the second most probable scenario change in relation to the value of *collapseheight* parameter (the input data and the R script written for the production of this plot can be found in the Dryad Digital Repository: https://doi.org/10.5061/dryad.63xsj3v5q). Secondly, we created similarity matrices using code from Jones *et al.* (2015) with three different values of *collapseheight* parameter (0.005, 0.007 and 0.009) chosen from the plot.

Finally, we formulated six hypotheses about species boundaries based on the current taxonomy of the series and the results of the species delimitation methods, and we tested them with DELINEATE software (Sukumaran *et al.* 2021). The dataset was split into hypothetical populations with "A10" analysis in BPP v. 4.3 (Yang 2015) and the species tree of these populations was created in starBEAST v. 2.0 (Drummond *et al.* 2012) implemented in BEAST v. 2.6.7. Then we set up six scenarios, lumping some populations into defined species and leaving others to be delimited as either part of those defined species or separate species. The analysis was run in Python v. 3 with the package DELINEATE (Sukumaran *et al.* 2021).

Morphology

The macromorphological characters of colonies were observed on eight cultivation media, namely malt extract agar (MEA; Oxoid, Melbourne, Australia), Czapek yeast autolysate agar (CYA; Fluka, Buchs, Switzerland), Czapek-Dox agar (CZA), yeast extract Sucrose agar (YES), dichloran 18 % glycerol agar (DG18), oatmeal agar (OA; Difco, La Ponte de Claix, France), CYA supplemented with 20 % sucrose (CY20S), and creatine sucrose agar (CREA) (Samson *et al.* 2014). The strains were inoculated at three equidistant points on 90 mm Petri dishes and incubated at 25 °C in darkness. For the description of colony colours, we used the hexadecimal colour codes and the names were assigned according to website https://coolors.co/. After 14 d incubation, the plates were photographed, and strains incubated for a further one wk to check Hülle cells production. The strains were also grown on MEA for 14 d at 10, 15, 20, 25, 30, 35, 37, and 40 °C, in darkness, to determine cardinal temperatures.

Micromorphological characters were observed from 14-d-old colonies grown on MEA. Every character (conidia length and width, stipe length and width, vesicle diameter, length of phialides and metulae) was measured at least 35 times for each strain. Lactic acid (60 %) was used as the mounting medium. Photographs were taken on an Olympus BX51 microscope equipped with an Olympus DP72 camera. Based on the measurements, we created boxplots using R v. 4.1.2 and the package GGPLOT2 (Wickham 2016). The statistical differences in phenotypic characters between species were calculated using one-way ANOVA followed by Tukey's honest significant difference (HSD) test in R v. 4.1.2 and displayed using the package GGSIGNIF (Ahlmann-Eltze & Patil 2021). The linear discriminant analysis based on the measurements of the above-mentioned micromorphological features was performed in R v. 4.1.2 with the packages MASS (Venables & Ripley 2002) and GGORD (Beck 2017).

Physiology

To test the osmotic tolerance of strains/species, we cultivated strains at 25 °C on MEA supplemented with 0 %, 5 %, 10 %, and 15 % NaCl. The growth increment was measured each day for ten days. Based on these measurements, we created primary growth curves for every strain and NaCl concentration. Then we extracted the slope values from these curves and used them to create secondary growth curves which represent the growth rate of the strains in relation to the NaCl concentration. The secondary growth curves were calculated using the *loess* function in R v. 4.1.2 with the package GGPLOT2.

RESULTS

Phylogeny and ecology

A Maximum Likelihood (ML) phylogenetic tree based on *CaM* from 518 strains is presented in Fig. 1, with geographic origin and substrate (if known) plotted on the tree using the colour strips. The phylogenetic reconstruction shows full support for four large clades, but then the support is lost towards the terminal branches. There was no clear pattern in the distribution of localities or substrates of isolation. The two most common combinations overrepresented throughout the tree included, *i.e.*, North America / indoor environment and Europe / cave, but this condition is caused by sampling bias and is not limited to particular species or group of species.

Figure 2 shows the ML reconstruction based on a concatenated alignment of five loci from the representative dataset of 213 strains covering genetic and ecological variability (mostly selected based on *CaM* genotype, locality and substrate). There are still four main fully supported lineages in the tree corresponding to those in the *CaM* tree. For practical reasons, we named these lineages based on the priority rules as follows: *A. subversicolor* lineage and *A. sydowii* lineage contain only single species, while the *A. versicolor* lineage contains nine species (*A. amoenus*, *A. austroafricanus*, *A. fructus*, *A. griseoaurantiacus*, *A. hongkongensis*, *A. pepii*, *A. protuberus*, *A. tabacinus*, and *A. versicolor*), and the *A. creber* lineage contains six species (*A. creber*, *A. cvjetkovicii*, *A. jensenii*, *A. puulaauensis*, *A. tennesseensis*, and *A. venenatus*). The bootstrap support values in the combined tree are high on many branches even for the small terminal clades. It is however well-known that bootstrap values in the concatenated trees are often falsely high (Kubatko & Degnan 2007, Seo 2008). If only the monophyly and statistical support of branches in this tree would be considered, all currently recognized species could be accepted. To retain monophyly, however, several new species would have to be described in the *A. versicolor* lineage, especially in the proximity of *A. austroafricanus*/*A. hongkongensis*/*A. amoenus* and also in the clade containing *A. griseoaurantiacus* and *A. tabacinus*. The geography and substrate of isolation showed no clear patterns that could be associated with particular species similarly to *CaM* tree.

A species tree calculated in starBEAST (Drummond *et al.* 2012) is shown in Fig. 3 with strains assigned to species based on the current taxonomy. The visualization by Densitree (Bouckaert & Heled 2014) demonstrates the incongruences in the dataset, which are apparent in both the *A. versicolor* lineage (within the clade containing *A. pepii*, *A. fructus*, and *A. versicolor*, and within the clade containing the remaining species) and the *A. creber* lineage (between all species except *A. venenatus*).

Incongruences between single gene datasets: evidence from species tree and BLAST searches

To show practical consequences of incongruences between single-gene datasets, we created a local BLAST database containing

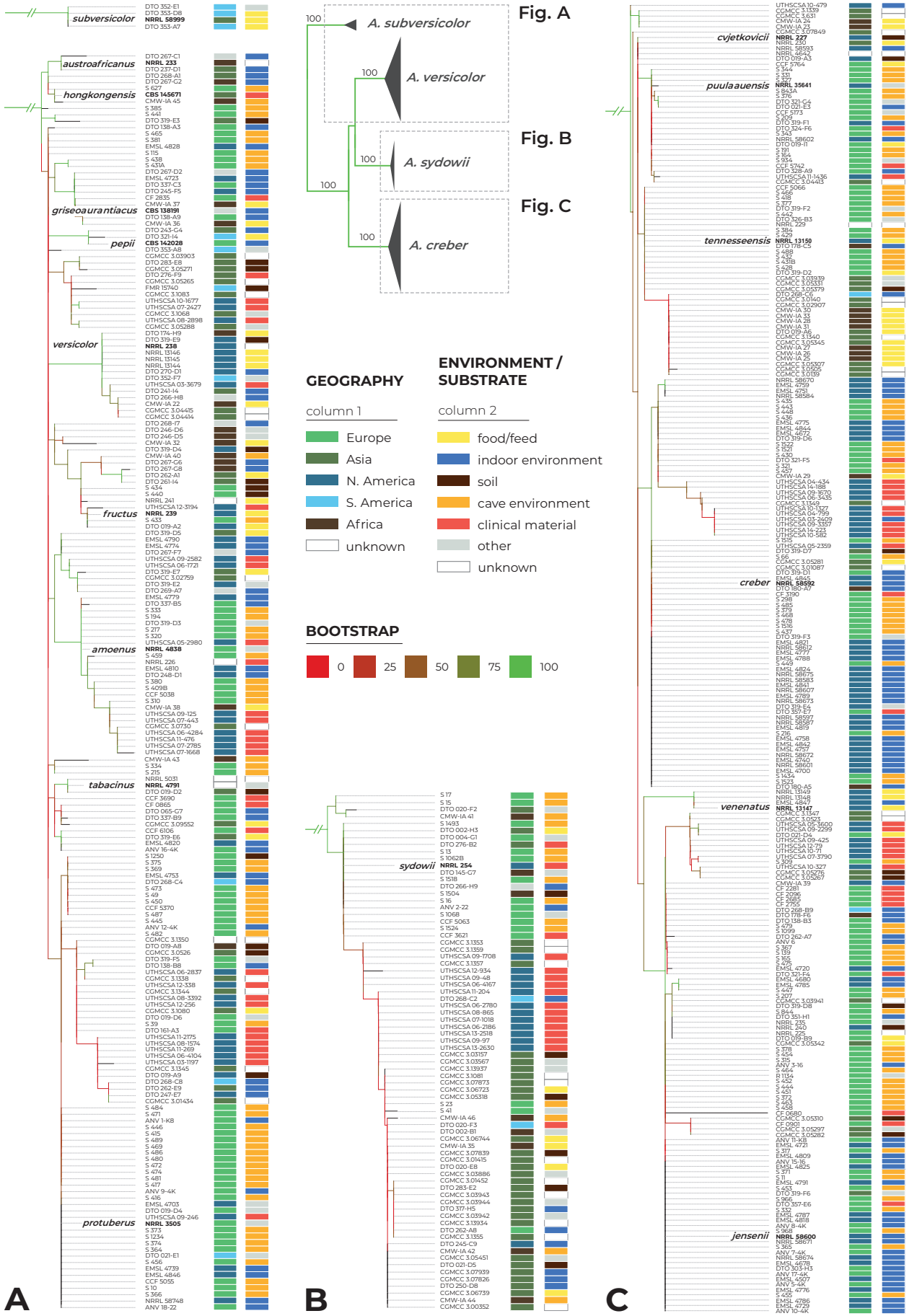

Fig. 1. Phylogenetic tree of 518 series *Versicolores* strains based on *CaM*. The tree was calculated in IQ-TREE with 1 000 standard bootstrap replicates. The tree is split into three parts for better readability: **A.** *Aspergillus versicolor* lineage and *A. subversicolor*. **B.** *A. sydowii*, and **C.** *A. creber* lineage. Coloured stripes placed to the right of the strain codes represent the geographic origin of strains (continent) and source of isolation (substrate or environment). Tree branches are coloured according to their bootstrap supports, red colour representing bootstrap value of 0 and green colour bootstrap value of 100. Ex-type isolates are highlighted with bold font.

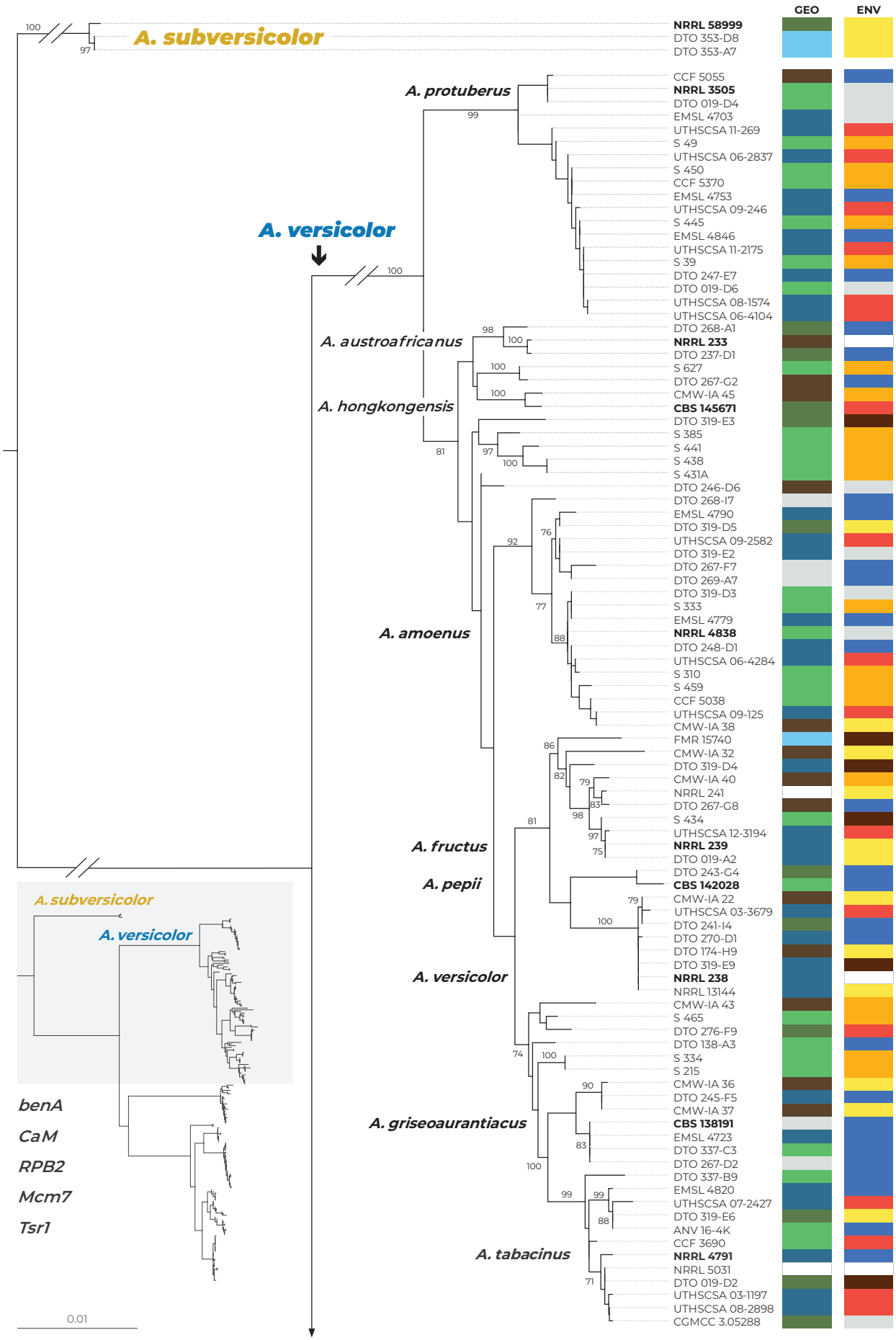

Fig. 2. Multilocus phylogeny of *Aspergillus* series *Versicolores* based on five loci (*benA*, *CaM*, *RPB2*, *Mcm7*, *Tsr1*) and comprising 213 strains. The displayed tree was calculated employing a Maximum likelihood method in IQ-TREE using partitioned analysis. The support was assessed by 1 000 standard bootstrap replicates, only values higher than 70 % are displayed. Coloured stripes next to strain codes represent the geographic origin of strains (continent) and the source of isolation (substrate or environment). Ex-type isolates are highlighted with bold font.

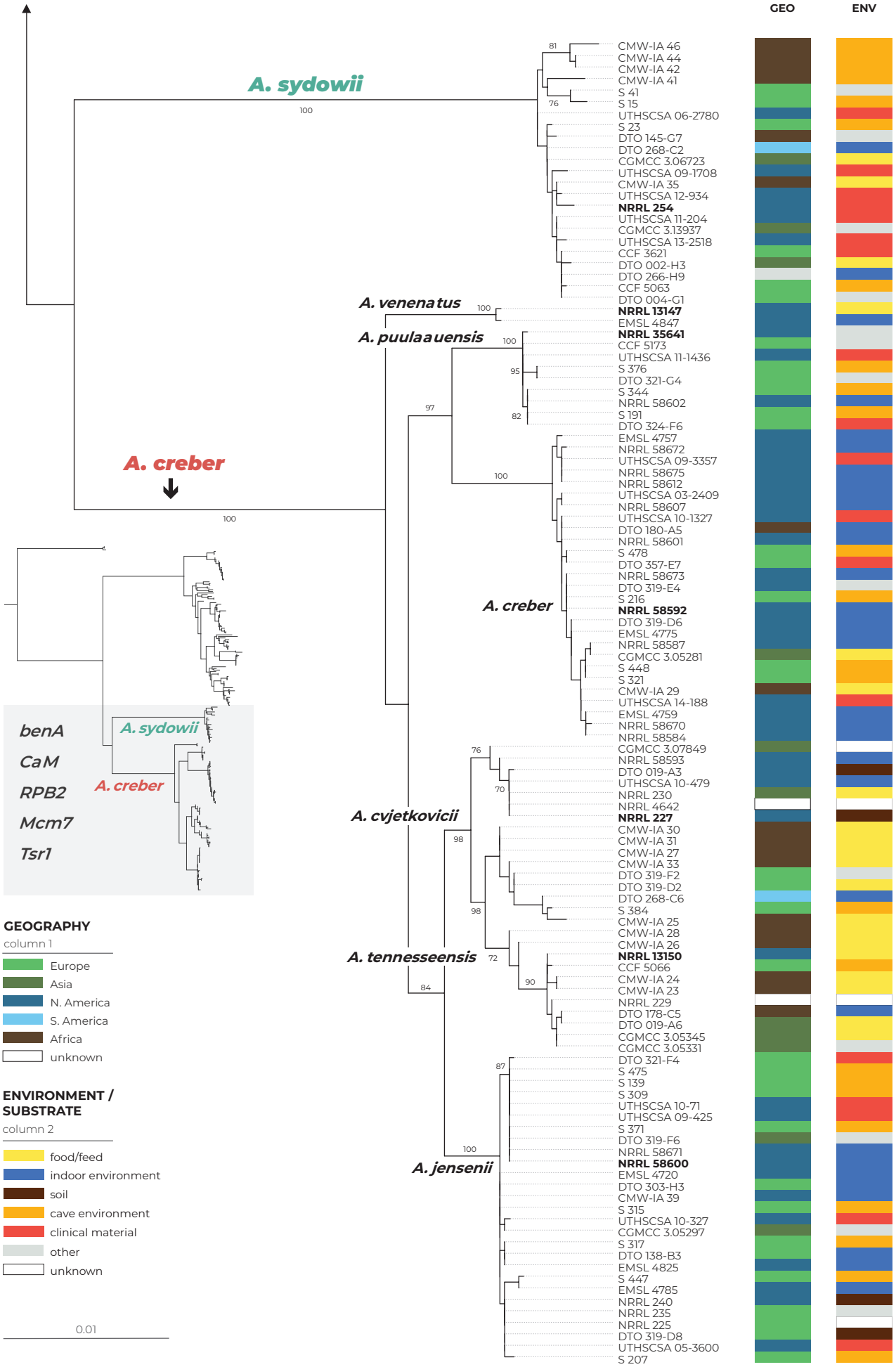

Fig. 2. (Continued).

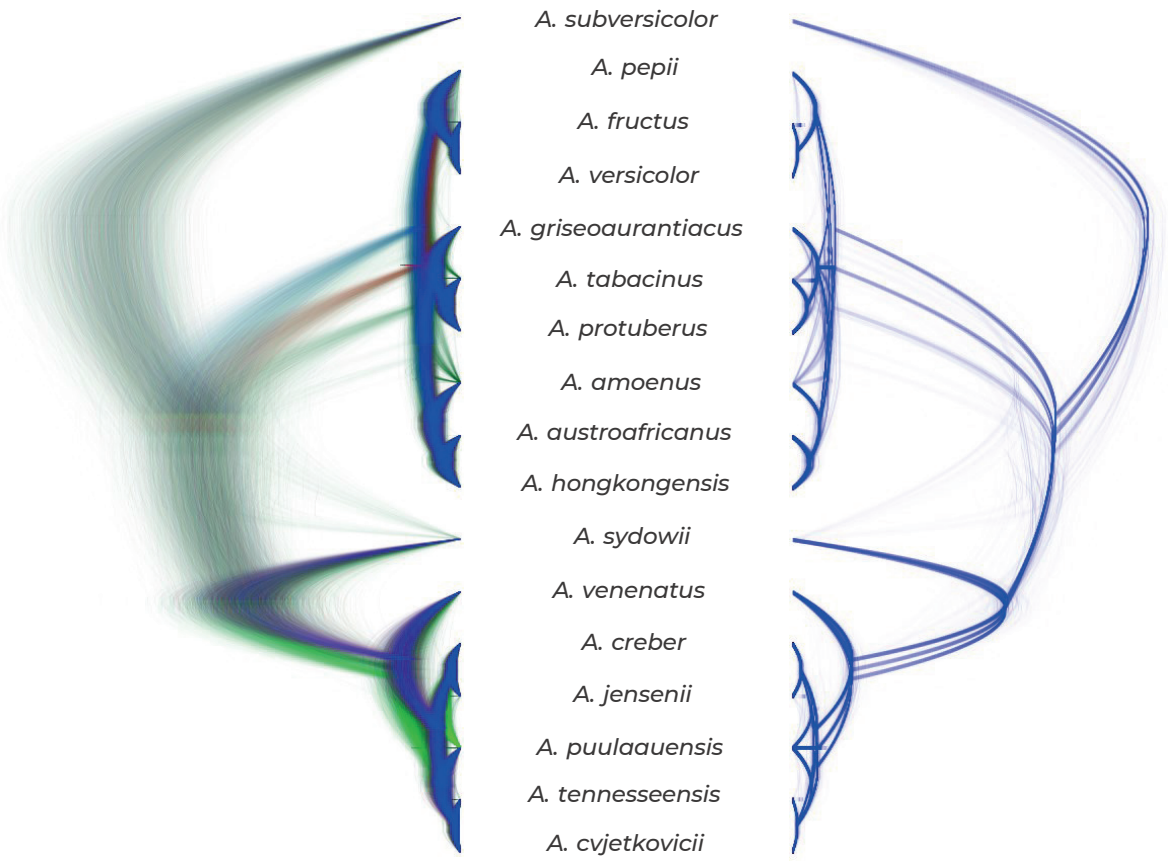

Fig. 3. Species tree inferred with starBEAST and visualized in DensiTree. All trees created in the analysis with the exception of the first 25 % (burn-in) are displayed on the left side. Trees with the most common topology are depicted by blue lines, trees with the second most common topology by red, trees with the third most common topology by light green, and all other trees by dark green. The consensus trees of the three most common topologies are displayed on the right side.

sequences from five genes of all 17 ex-type strains. Then we performed BLAST searches for all sequences from five loci we gathered for 213 isolates against this database. The results of BLAST searches and the closest similarities to the ex-type strains are presented in Fig. 4. We can see that sequences of different genes from the same strain frequently resulted in closest sequence similarities with ex-type strains of different species and this results in different species identifications. This phenomenon does not involve *A. subversicolor* and *A. sydowii.* In the *A. creber* lineage, the switching between different accepted species is present in *A. cvjetkovicii* and *A. tennesseensis*, while in the *A. versicolor* lineage, the unstable identification is very prevalent and present among all species except *A. pepii* and *A. versicolor*. At first glance, *A. protuberus* seems to be isolated from other species and well-defined phylogenetically in the combined ML tree, but there are conflicts in identification of some strains as well, suggesting the ongoing recombination with other representatives of the *A. versicolor* lineage. This is apparent for strains S 627 and DTO 267-G2, identified as *A. austroafricanus* and *A. hongkongensis* using *benA*, *CaM*, *and RPB2*, which had closest hits to *A. protuberus* using *Tsr1*. Similarly, strains S 465, S 334, and S 214, which belong to the clade containing ex-type strains of *A. griseoaurantiacus* and *A. tabacinus*, were identified as *A. protuberus* using *CaM*. The most extreme situation is present in the intermediate clade located between *A. austroafricanus*/*A. hongkongensis* and *A. amoenus* comprising strains DTO 319-E3, S 385, S 441, S 438, and S 431A. BLAST searches of almost every locus in this clade resulted in the closest hit to different species. This clearly demonstrates that there are no barcode gaps between many species and that there are phylogenetic conflicts between individual loci.

There are also 13 cases of *benA* sequences with equal similarity to three or more ex-type strains. This number is high in comparison with other loci (2 cases in *CaM*, no cases in any other locus), but it is most likely caused by shorter length of *benA* sequences and thus also their lower discriminatory power compared to the other loci.

Species delimitation

The results of various species delimitation methods, mostly based on the MSC model, are displayed in Fig. 5. The majority of methods and their various settings (19 out of 28) support the delimitation of four species in series *Versicolores*, *i.e.*, *A. subversicolor*, *A. sydowii*, *A. versicolor* (lineage containing nine species names), and *A. creber* (lineage with six species names). Two out of 28 analyses delimited less than four species, and seven delimited more than four species. The highest number of delimited species by any method was seven. The GMYC and ABGD methods based on *RPB2* sequences delimited only *A. subversicolor* and lumped all the remaining strains into one hypothetical species. Few methods delimited more than one species within the *A. versicolor* and *A. creber* lineages. Namely, STACEY delimited three species in the *A. creber* lineage with *collapseheight* value 0.005 and two species in the *A. creber* lineage with *collapseheight* value 0.007; GMYC and bGMYC based on *benA* sequences delimited two species in the *A. creber* lineage and three species in the *A. versicolor* lineage; bPTP based on *RPB2* sequences delimited two species in the *A. versicolor* lineage; bGMYC based on *Mcm7* sequences delimited two species in the *A. creber* lineage and two species in *A. versicolor*

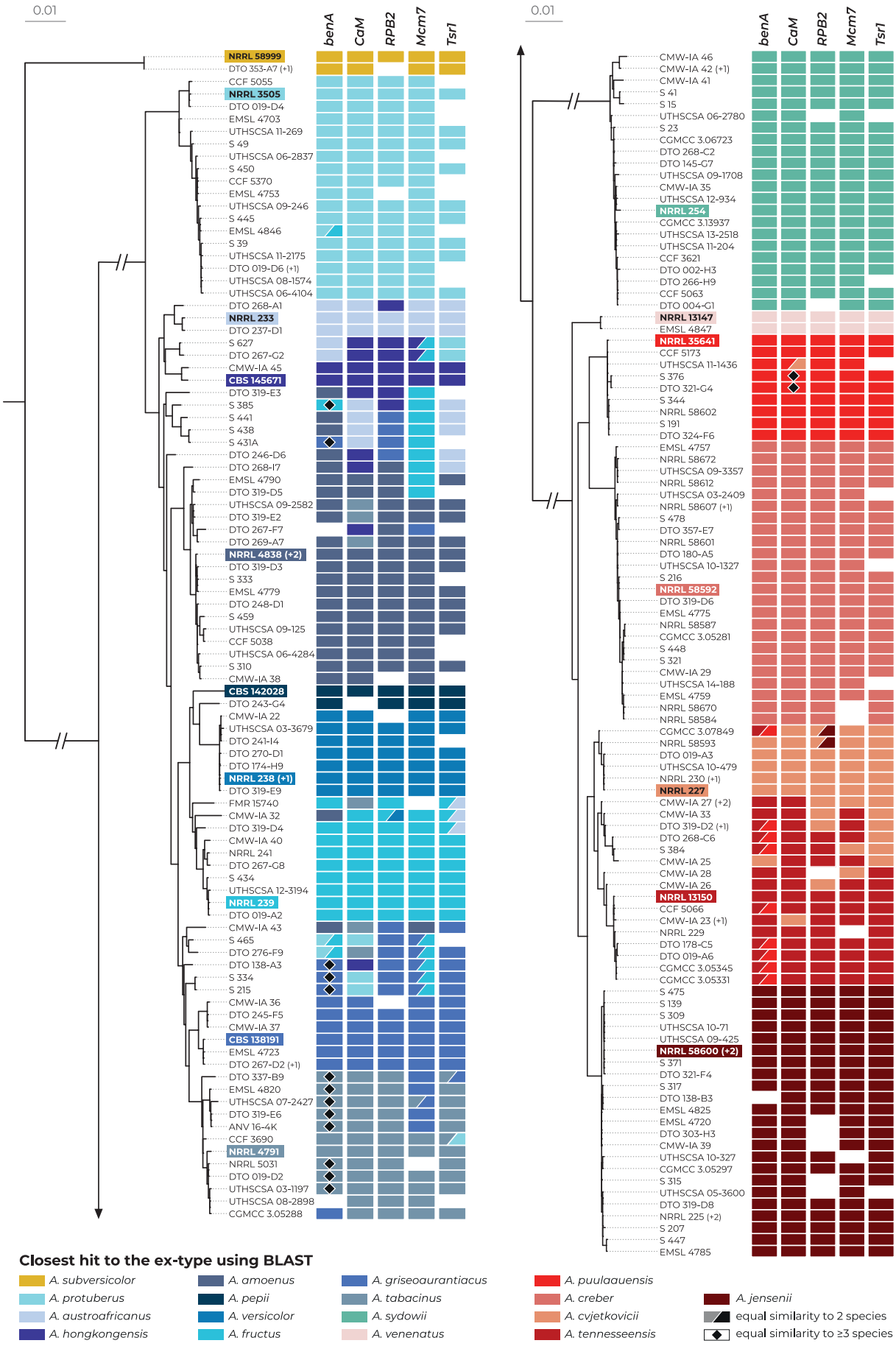

Fig. 4. The results of BLAST similarity searches of five unlinked loci (*benA*, *CaM*, *RPB2*, *Mcm7* and *Tsr1*) derived from 195 strains (only unique multilocus haplotypes were used) across the genetic diversity of series *Versicolores*. Coloured rectangles represent the closest hits to one of the 17 ex-type strains (every species has unique colour). If there was an identical similarity to two or more ex-type strains, the rectangles were diagonally divided or marked with a rhombus, respectively. Blank spaces represent missing sequences. Ex-type isolates are marked with bold font and coloured background. The phylogenetic tree was calculated in IQ-TREE using partitioned analysis and 1 000 ultrafast bootstrap replicates.

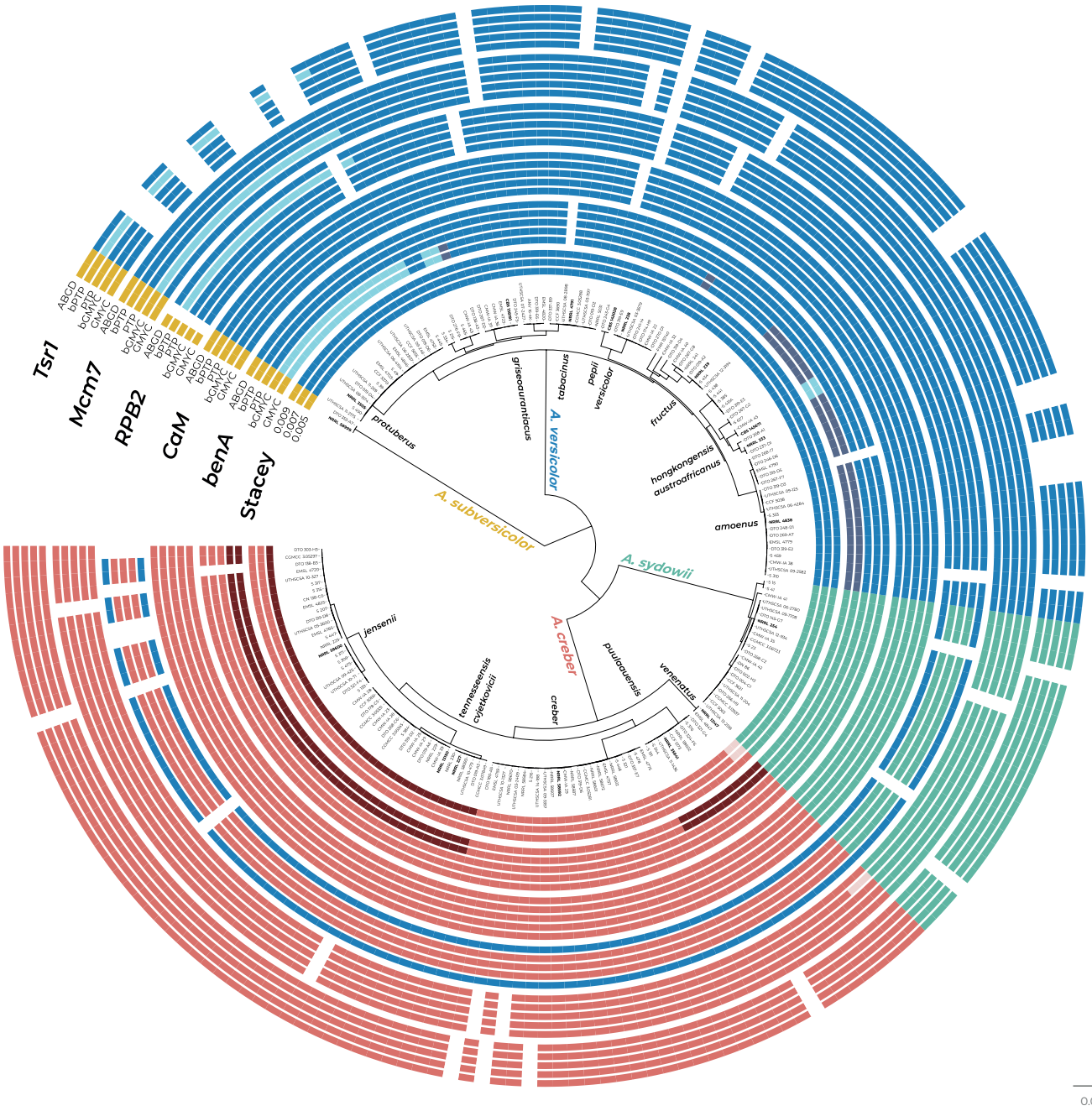

Fig. 5. Schematic representation of results of species delimitation methods in the series *Versicolores*. One multilocus method (STACEY) and five single-locus methods (ABGD, bPTP, PTP, bGMYC and GMYC) were applied on a dataset consisting of five loci (*benA*, *CaM*, *RPB2*, *Mcm7* and *Tsr1*). The dataset was reduced to strains with unique multilocus haplotypes. The results are depicted by coloured circles (blank spaces are missing sequence data for specific isolates) with different colours indicating tentative species delimited by each method. All ex-type isolates are highlighted with a bold font and the species are epithets written with black colour. The results of STACEY are presented with three different values of *collapseheight* parameter (0.005, 0.007 and 0.009). The phylogenetic tree was calculated during the STACEY analysis and is used solely for the comprehensive presentation of the results from different methods.

lineage; bPTP based on *Tsr1* sequences delimited two species in the *A. versicolor* lineage. Among the seven methods/settings which supported more than four species in series *Versicolores*, there was only very low agreement on the arrangement of these species. Most commonly, *A. protuberus* and *A. venenatus* gained support as additional species (3/28 methods).

The results of the multilocus method STACEY are presented in Fig. 6. Subfigure A illustrates the effect of *collapseheight* parameter value on the number of delimited species. This parameter is plotted on the x-axis, while on the y-axis on the left side, there is the number of delimited species with the given *collapseheight* value (black line). The support for the most probable scenario (red line), and the support for the second most probable scenario (turquoise line) are shown; other less supported scenarios were omitted. When the *collapseheight* value is low (0.001–0.005), the number of delimited species is high, but the probability for each delimitation is very low (the probabilities are plotted on the y-axis on the right side; the sum of probabilities of all scenarios at each *collapseheight* value is equal to one). The scenario with six species (three species in *A. creber* lineage) only received support slightly higher than 0.25, with several other scenarios receiving similar support at the respective *collapseheight* value. The scenario with five species (*A. venenatus* separated from *A. creber* lineage) is the first scenario with a relatively high support separating itself from the other scenarios at

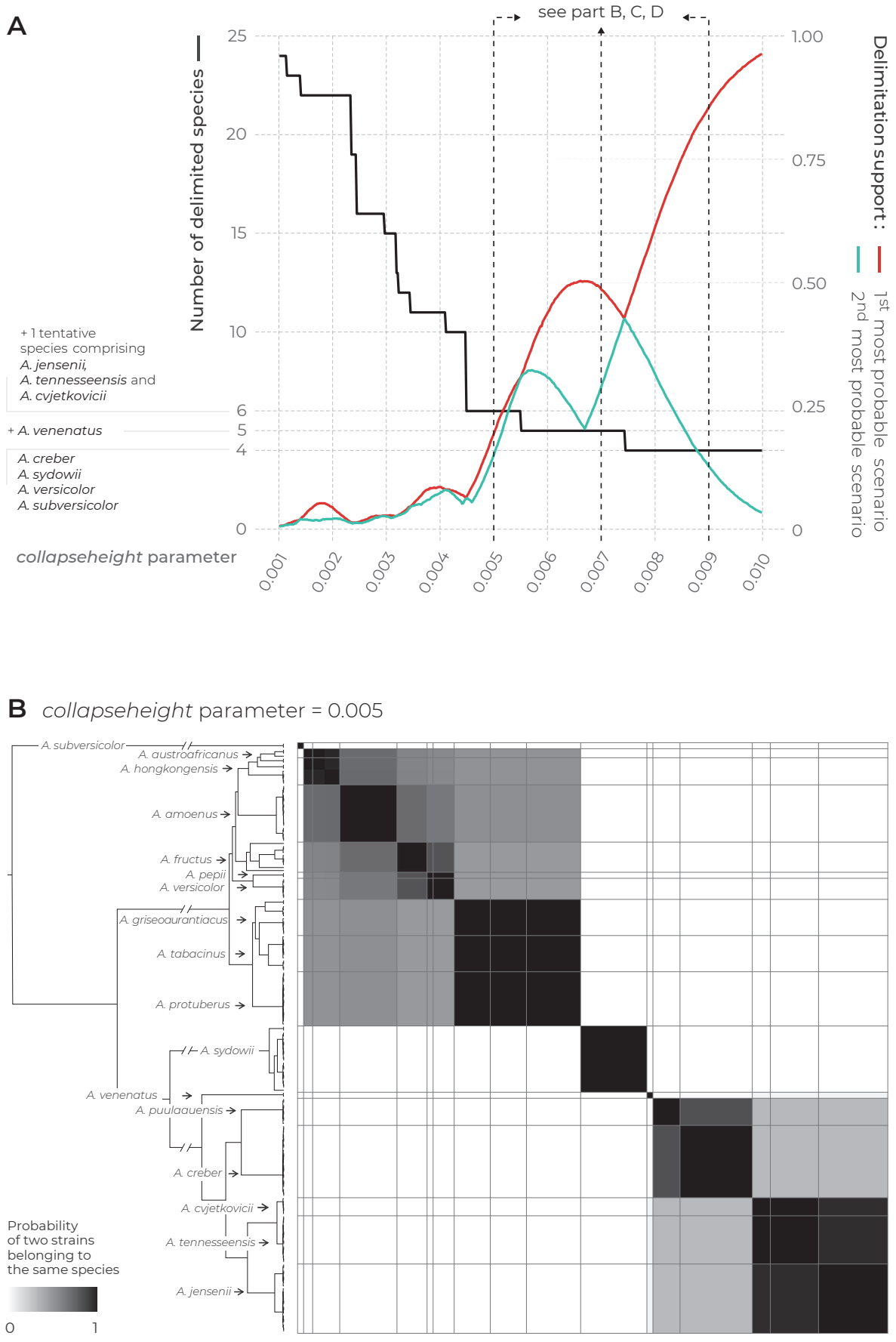

Fig. 6. The results of species delimitation by STACEY. **A.** Dependence of delimitation results on *collapseheight* parameter. The black solid line represents the number of delimited species (left y-axis) depending on the changing value of *collapseheight* parameter (x-axis). The red line represents the probability (right y-axis; range from 0 to 1) of the most probable scenario at specific *collapseheight* value. The turquoise line represents the probability of the second most probable scenario at specific *collapseheight* value. Dashed vertical lines mark three values (0.005, 0.007 and 0.009) of *collapseheight* parameter whose results are shown in detail by similarity matrices (**B**, **C**, **D**). The similarity matrices give the posterior probability of every two isolates belonging to the same multi-species coalescent cluster (tentative species). Black colour corresponds to a posterior probability of 1, while the white colour is equal to 0. Thicker horizontal and vertical lines in the similarity matrices depict the approximate boundaries of species in their narrow concept.

C *collapseheight* parameter = 0.007

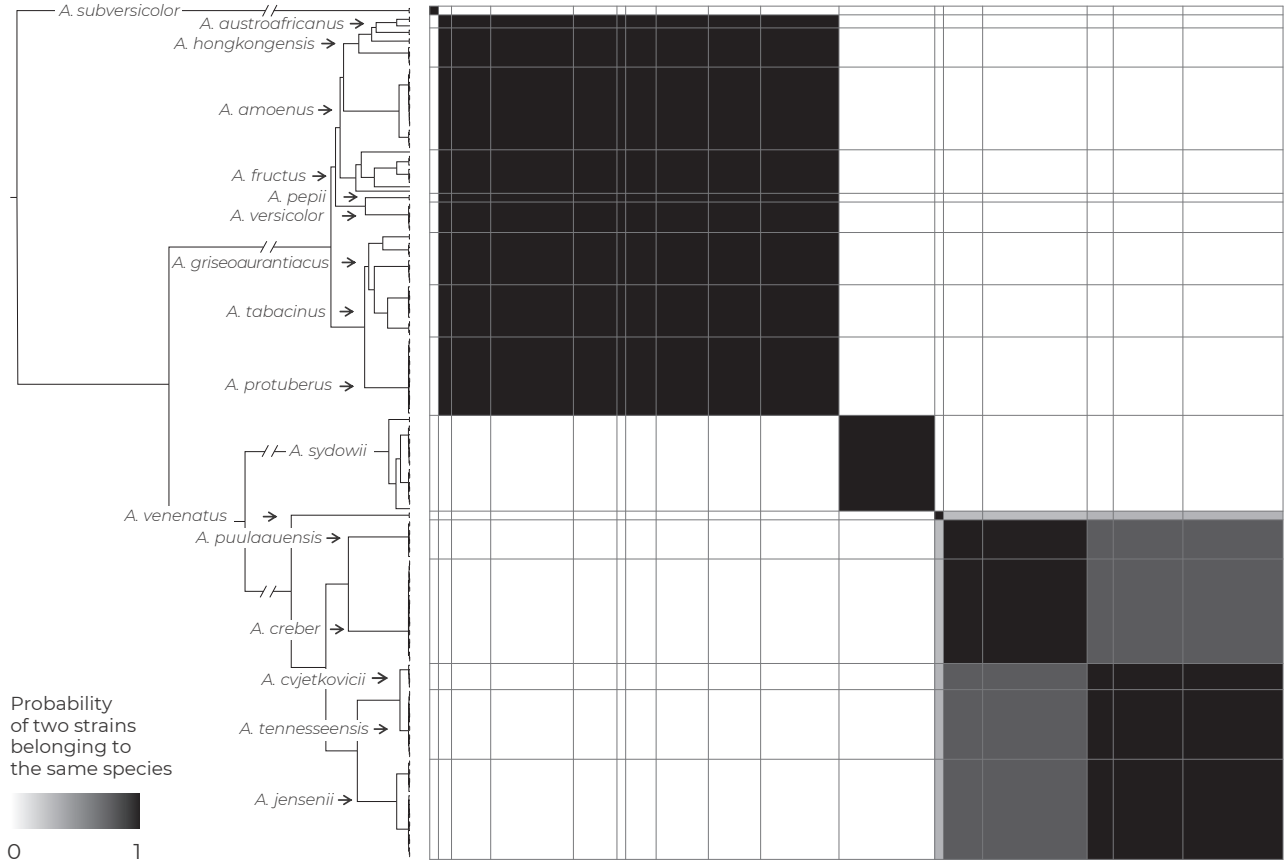

D *collapseheight* parameter = 0.009

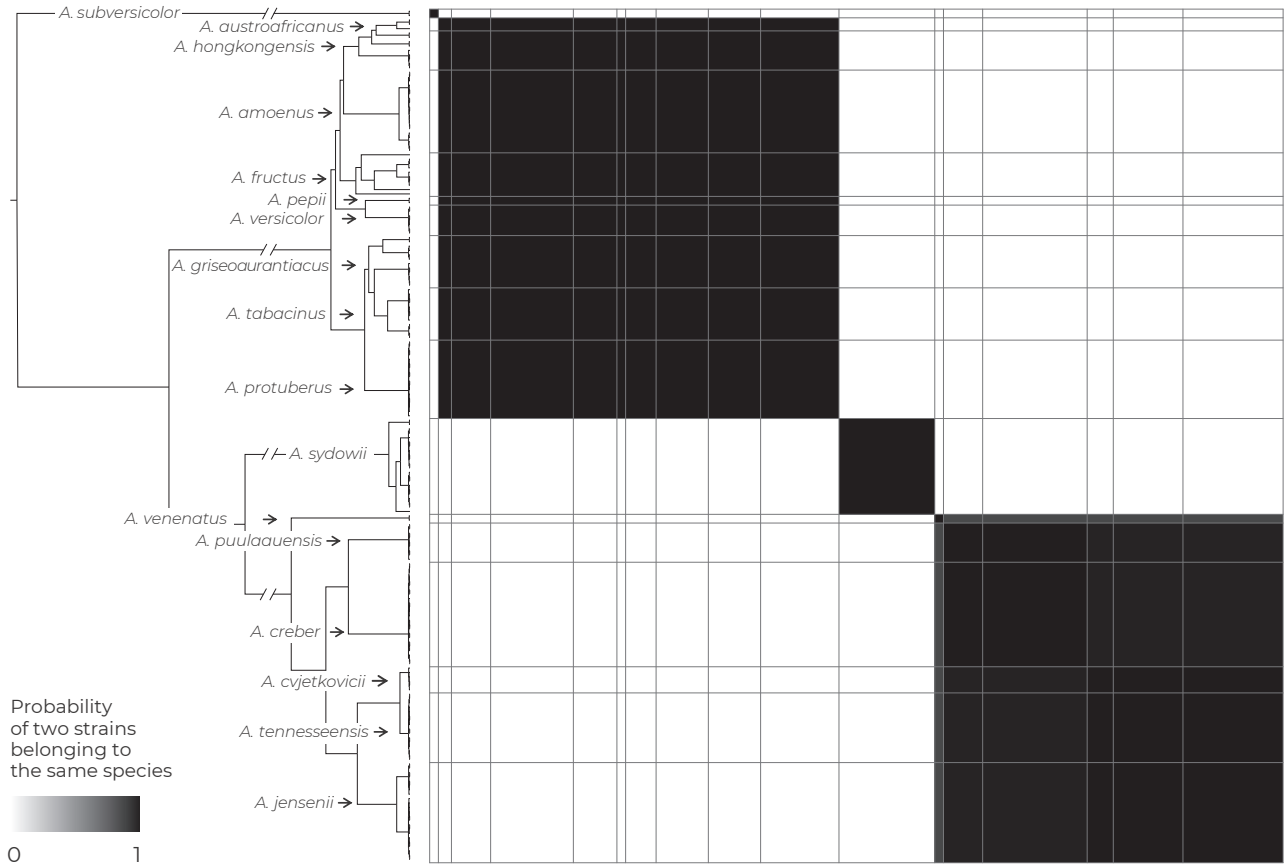

Fig. 6. (Continued).

collapseheight parameter around 0.006. At the *collapseheight* value of 0.0075, the delimitation of four species (*A. creber*, *A. sydowii*, *A. versicolor*, *A. subversicolor*) becomes the most supported scenario and its probability rises to almost 1.0 with increasing *collapseheight* value. The vertical dashed lines in Fig. 6A represent the scenarios illustrated in detail in subfigures B, C, and D in the form of similarity matrices. At the *collapseheight* of 0.005 (Fig. 6B), there are three species in the *A. creber* lineage (*A. venenatus*; *A. puulaauensis* + *A. creber*; *A. cvjetkovicii* + *A. tennesseensis* + *A. jensenii*) and there is also some visible structure in the *A. versicolor* lineage (*A. austroafricanus* + *A. hongkongensis* + *A. amoenus* + *A. fructus* + *A. pepii* + *A. versicolor*; *A. griseoaurantiacus* + *A. tabacinus* + *A. protuberus*). At *collapseheight* of 0.007 (Fig. 6C), the structure within *A. versicolor* and *A. creber* lineages disappears except for the strains of *A. venenatus* which remain separate from the *A. creber* lineage. At *collapseheight* of 0.009 (Fig. 6D), *A. venenatus* becomes part of the broad *A. creber* species.

The species hypotheses were independently tested with DELINEATE (Sukumaran *et al.* 2021) and the results are summarized in Fig. 7. We set up six models with *A. subversicolor* and *A. sydowii* always fixed as separate species and various parts of the *A. versicolor* and *A. creber* lineages left to be delimited. All populations from the *A. creber* lineage were left unassigned in models 1 and 2. In the first model, we assigned all populations from the *A. versicolor* lineage to one species, and in the second model, we split the *A. versicolor* lineage into three hypothetical species based

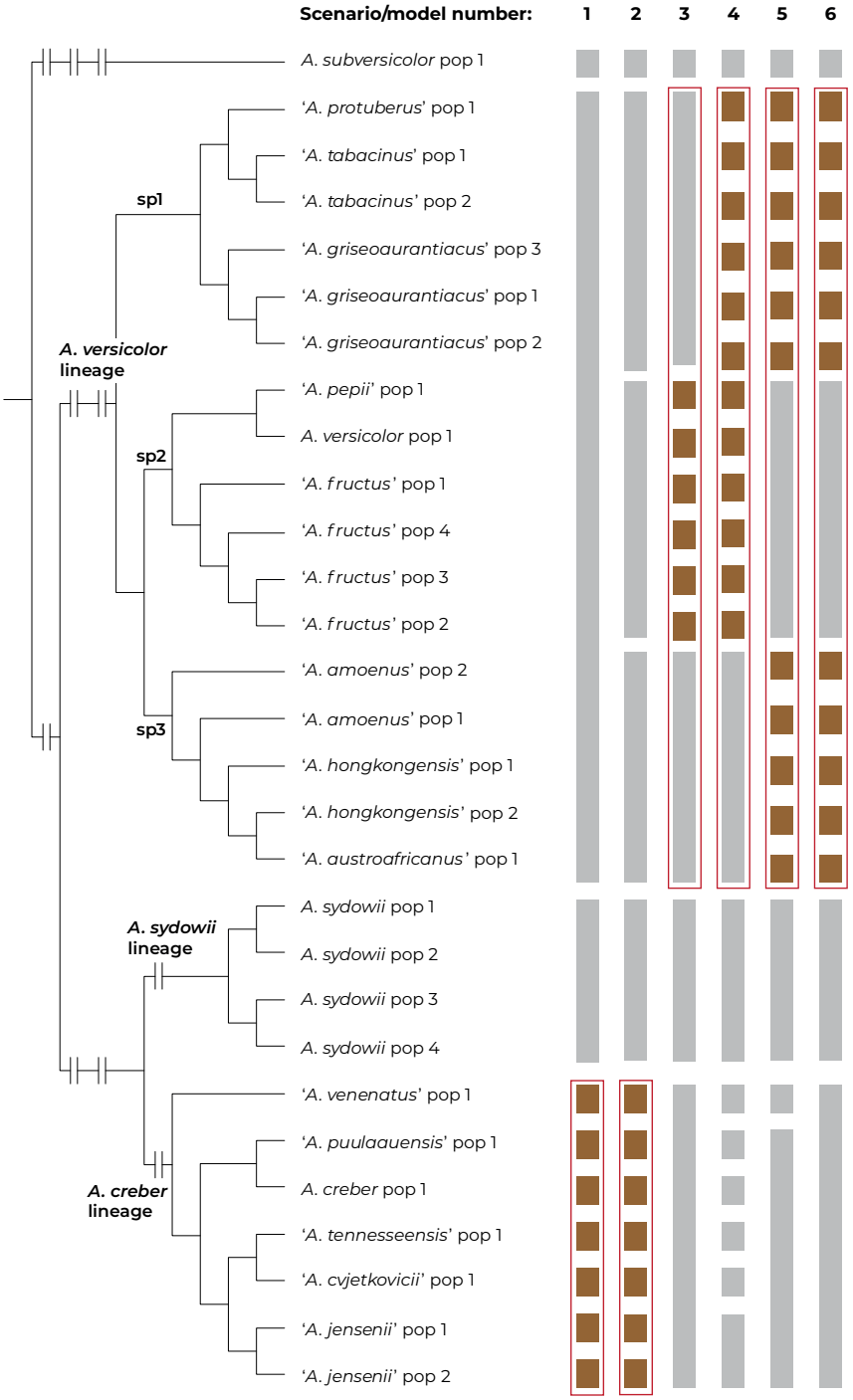

Fig. 7. Overview of species delimitation by DELINEATE. The populations were delimited with BPP and the species tree was calculated in starBEAST. The bars depict the setting and result of every scenario/model (numbered 1 to 6). The grey bars represent the predefined species (locked in the specific model), the brown bars represent unassigned populations, which were left free to be delimited. The red rectangles represent the species boundaries proposed by DELINEATE.

on the tree from starBEAST (Fig. 3) and the results of STACEY with a low *collapseheight* parameter of 0.005 (Fig. 6B): "versicolor sp1" (*A. protuberus*, *A. tabacinus*, and *A. griseoaurantiacus*) "versicolor sp2" (*A. pepii*, *A. versicolor*, and *A. fructus*) and "versicolor sp3" (*A. amoenus*, *A. hongkongensis*, and *A. austroafricanus*) (Fig. 7). Both models 1 and 2 resulted in delimitation of a single wide species in *A. creber* lineage.

Models 3-6 focused on *A. versicolor* lineage. In model 3, there were three fixed species: the whole *A. creber* lineage, clade "versicolor sp1", and clade "versicolor sp3", while the populations of "versicolor sp2" were left unassigned. In model 4, *A. creber* lineage was split into six currently accepted species, clade "versicolor sp3" was fixed as one species and all other populations in *A. versicolor* lineage were left to be delimited. In models 5 and 6, clade "versicolor sp2" was fixed as one species and all populations of clades "versicolor sp1" and "versicolor sp3" were left unassigned. The difference between models 5 and 6 was in the setting of *A. creber* lineage, where *A. venenatus* was set as separate species in model 5 and lumped together with the rest of the lineage in model 6. Models 3–6 resulted in lumping all the populations in *A. versicolor* lineage into a single wide species.

Morphology

Figures 8 and 9 and Supplementary Table S2 demonstrate the macromorphological variability within the series *Versicolores*. The conclusion we can draw from this comparison is that the strains in this series are extremely variable in terms of colony obverse and reverse colour and colony dimensions, and it is extremely hard to differentiate the phylogenetically defined clades/species from this series based on macromorphology. Even *A. sydowii*, a species usually considered as morphologically and physiologically well-defined can produce colonies with very different colours and texture on some media, *e.g.*, CYA, CZA, OA, CREA (Figs 8, 9). On the other hand, its typical blue-green colonies seem to be almost always present on MEA with exception of several strains examined by us, isolated from clinical material and caves which constantly produced light pink colonies on MEA (not shown). *Aspergillus subversicolor* generally produced smaller colonies than other species, but not exclusively and it could be in some cases misidentified as a member of the *A. creber* lineage based solely on macromorphological characters. Even phylogenetically very closely related strains of the same species frequently produce dissimilar colonies under the same conditions and vice versa, phylogenetically distant strains sometimes produce similar pattern of colonies (Figs 8, 9). Some differences, *e.g.*, the lack of sporulation, can be attributed to the long-term preservation of some strains (NRRL 238 or NRRL 227). On the other hand, in some other recently isolated strains, the lack of sporulation on some media seems to be rather random than specific to media. The production of Hülle cells is also rather random and not limited to some clades or media (Supplementary Table S3). The strain NRRL 239 was the only examined strain which produced Hülle cells regularly on all media except CREA. In conclusion, it is difficult to find macromorphological patterns specific for the narrow species or even for the main lineages. The variability within the two main lineages of *A. versicolor* and *A. creber* is extreme and largely overlapping between themselves.

Figures 10 and 11 display an overview of the dimensions of micromorphological characters separately for each strain and for the four main lineages. The plot showing the results of Linear Discriminant Analysis in Fig. 10 suggests that it is possible to differentiate the *A. versicolor* lineage, *A. sydowii* and *A. subversicolor* based on micromorphological measurements, but that the *A. creber* lineage interferes with all other lineages. The characters most useful for the discrimination were the length and width of conidia. Although the differences in measurements between the main lineages were mostly small, they were often evaluated as significant even using Tukey's HSD test, probably due to a large number of measurements. The variability of micromorphological characters between individual strains showed sometimes large differences even between phylogenetically closely related strains. The length and width of conidia were the most stable characters throughout the main lineages (smaller conidia in *A. versicolor* lineage compared to other lineages). The degree of stability within species/lineage is much lower in measurements of phialides and metulae, and completely lost in vesicle diameters and stipe lengths. The stipe width is rather similar throughout the whole series.

Physiology

The growth rates at variable temperatures and in osmotic gradient were measured for the same set of strains that were characterized macromophologically (Supplementary Tables S2, S3). The ability to grow at different temperatures differentiates *A. sydowii* and *A. subversicolor* from the remaining species/lineages (Fig. 12). Only some isolates of *A. sydowii* are capable of growing at 37 °C and this species grows moderately at 35 °C. *Aspergillus subversicolor* differs from all species by its inability of growing at 10 °C. It grows at 35 °C in contrast to strains from *A. creber* and *A. versicolor* lineages. All tested isolates of the *A. versicolor* and *A. creber* lineages grew restrictedly at 10 °C and none of them grew at 35 °C. There are very small differences between the *A. versicolor* and *A. creber* lineages in colony dimensions at 10, 15 and 30 °C. The strains of the *A. versicolor* lineage attained on average slightly larger colony diameters (in mm) after 14 d at 30 °C than *A. creber* lineage strains (minimum–average–maximum; *A. versicolor*: 18–30–43; *A. creber*: 10–20–32), and slightly smaller colony diameter at 10 °C (*A. versicolor*: 2–4.5–7; *A. creber*: 7–8.5–10) and 15 °C (*A. versicolor*: 10–13–17; *A. creber*: 15–17–19). The temperature optimum of the *A. versicolor* lineage is therefore higher than the optimum of the *A. creber* lineage.

The growth pattern in an osmotic gradient (Fig. 13) was similar to the growth rates at different temperatures, *i.e.*, *A. sydowii* and *A. subversicolor* being clearly different from other species, while *A. versicolor* and *A. creber* lineages expressed a similar growth profile (Fig. 13B). The biggest differences between the strains can be observed at 5 % NaCl concentration. *Aspergillus sydowii* grows much faster at this concentration than other species, while *A. subversicolor* is on the other side of the spectrum. Similar results but with less pronounced differences can be seen on MEA without NaCl and on MEA with 10 % NaCl. All tested strains grew very restrictedly at 15 % NaCl concentration. Figure 13A displays the variable growth rate within the *A. versicolor* and *A. creber* lineages. The differences between representatives of different clades/species are more distinct within the *A. versicolor* lineage with *A. hongkongensis* growing the fastest at 5 % and 10 % NaCl and *A. tabacinus* and *A. fructus* growing at the slowest rate. The fastest growing species in the *A. creber* lineage at 5 % and 10 % NaCl were *A. cvjetkovicii* and *A. tennesseensis* but the differences from other species were very small.

Fig. 8. Overview of macromorphological characters (obverse side of Petri dishes) within series *Versicolores* on eight cultivation media (MEA, CYA, CZA, YES, DG18, OA, CY20S, CREA) grown for 14 d at 25 °C.

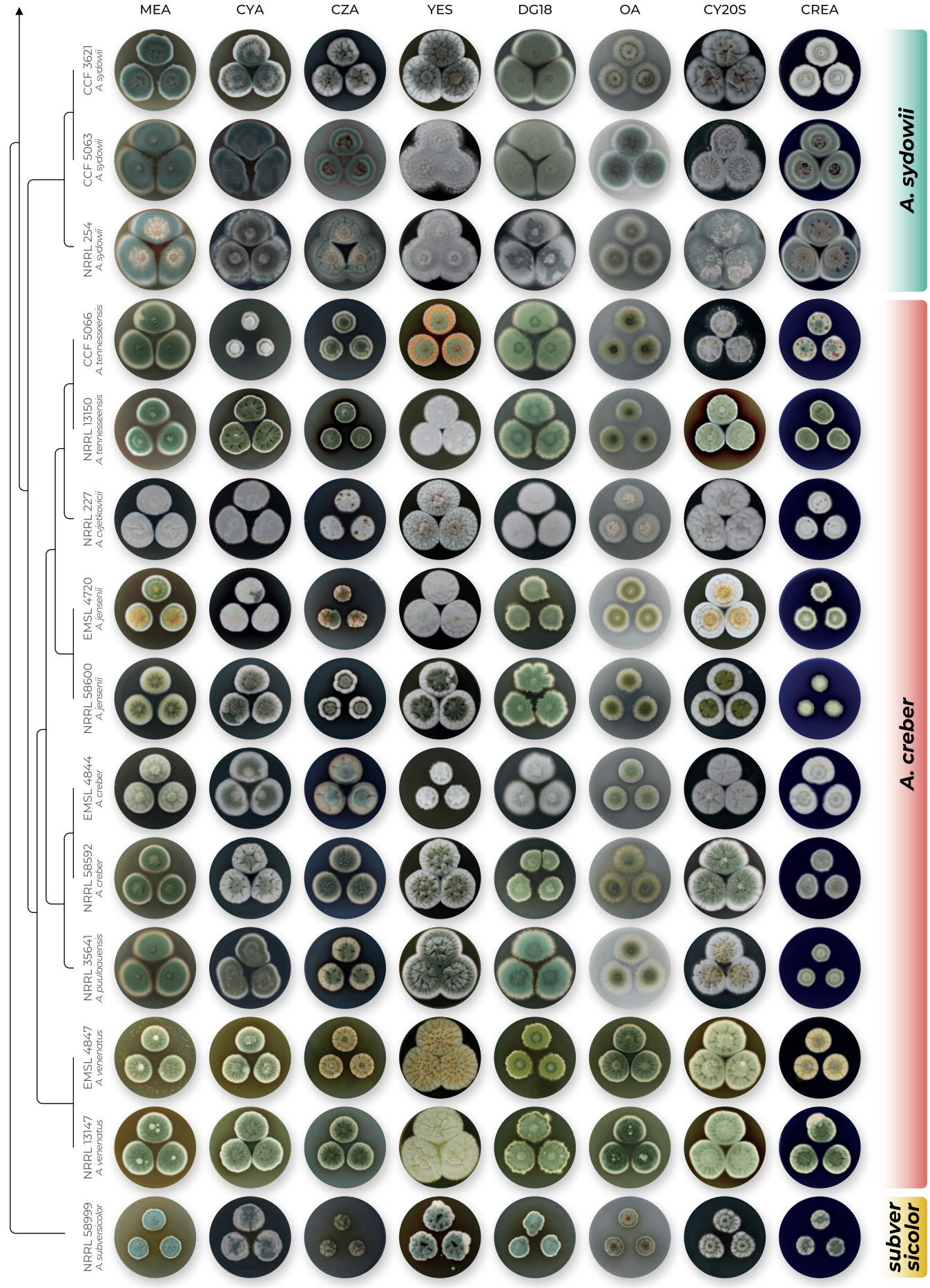

Fig. 8. (Continued).

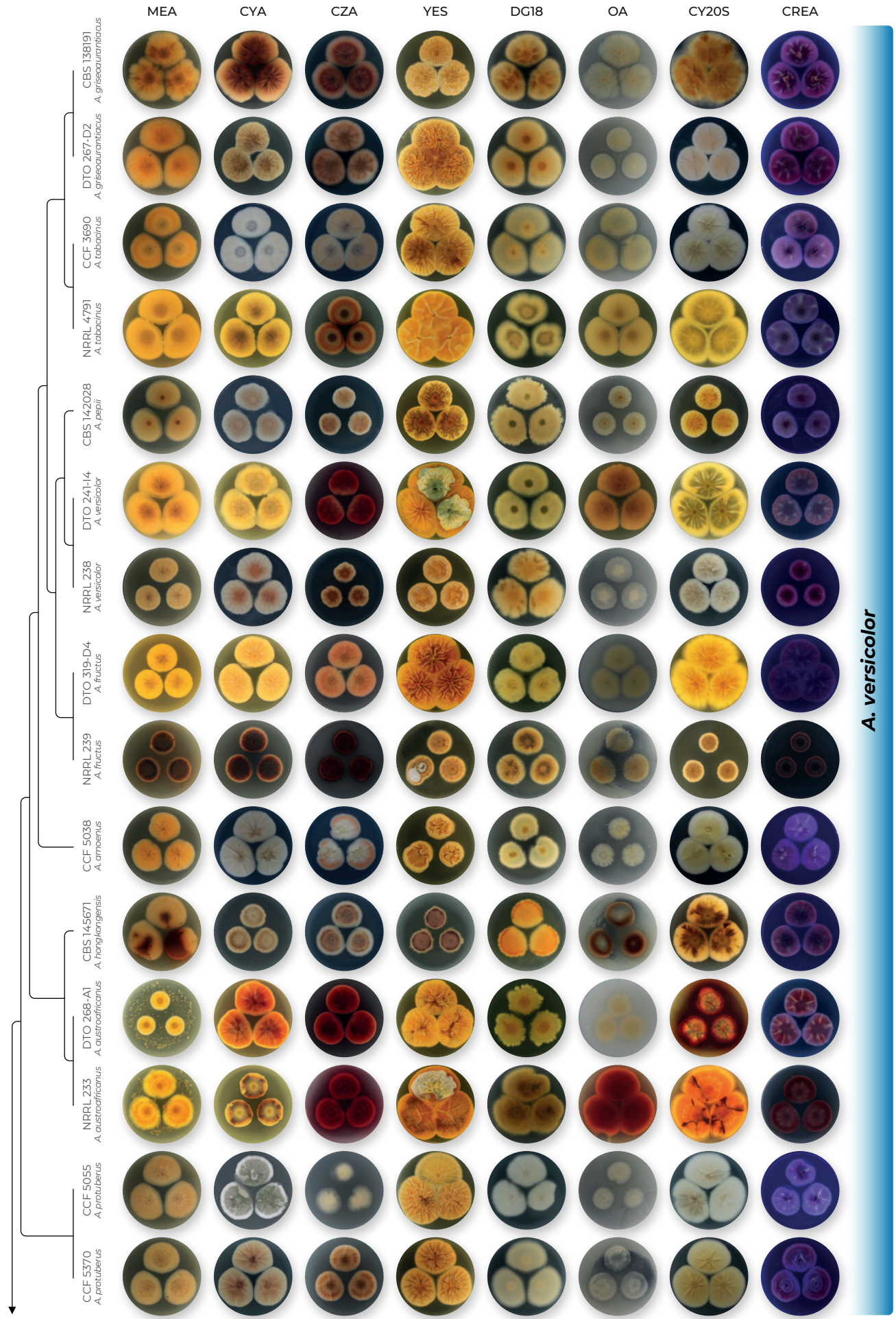

Fig. 9. Overview of macromorphological characters (reverse side of Petri dishes) within series *Versicolores* on eight cultivation media (MEA, CYA, CZA, YES, DG18, OA, CY20S, CREA) grown for 14 d at 25 °C.

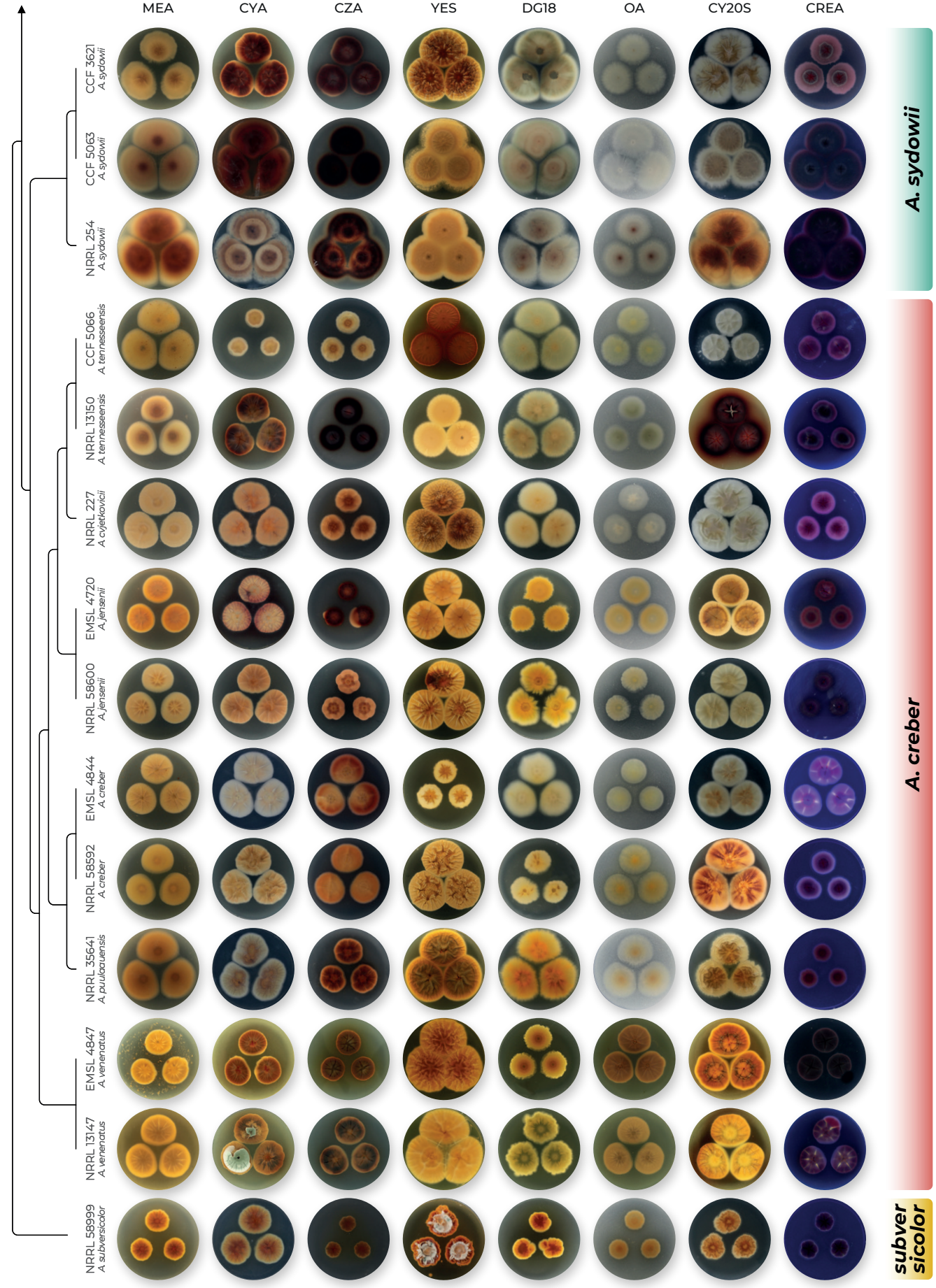

Fig. 9. (Continued).

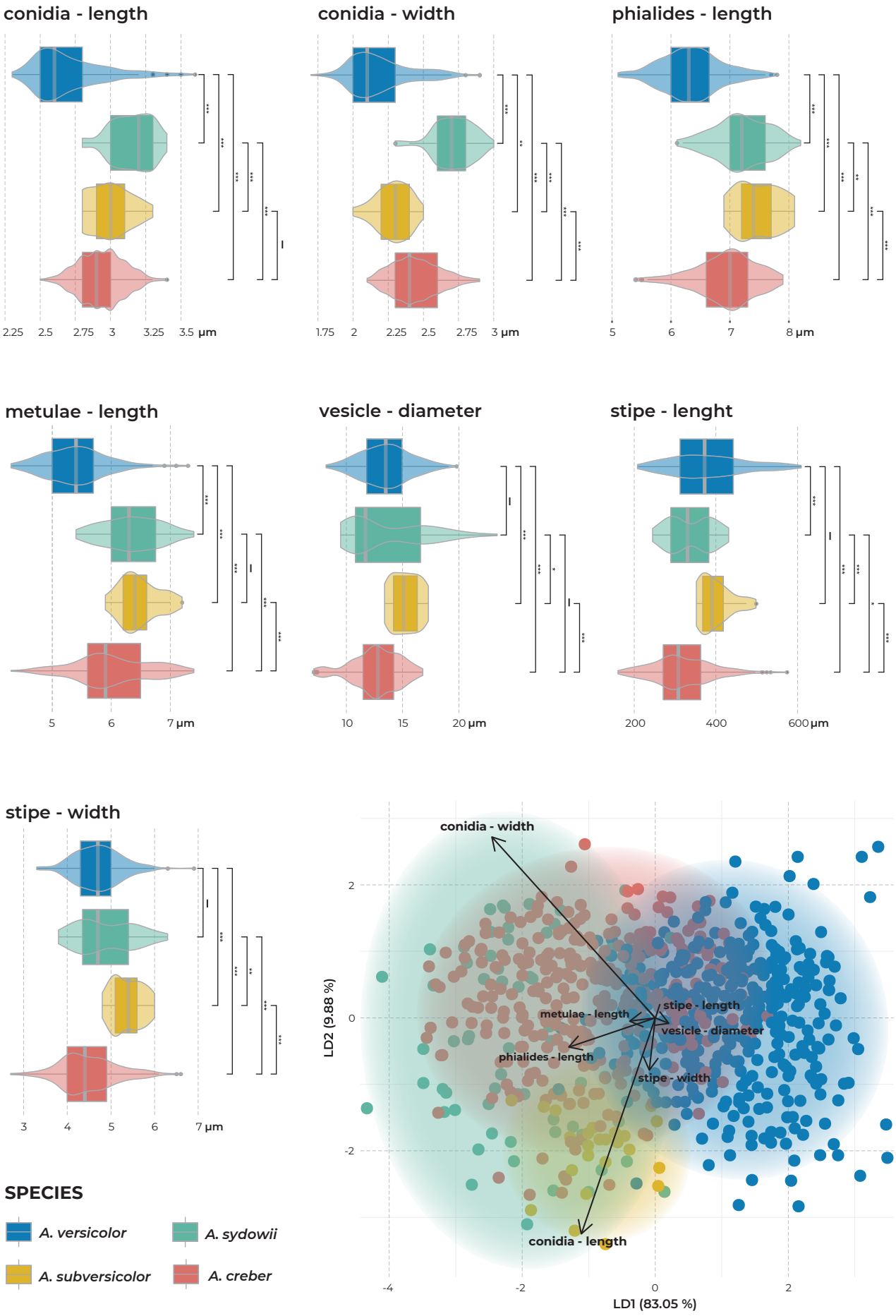

Fig. 10. Overview of dimensions of seven micromorphological characters. Box plots and violin plots of measurements distributed into four broadly defined species. Box plots show interquartile range, values within ± 1.5 of interquartile range (whiskers) and outliers. Asterisks on the right side of each plot express the statistical significance of pairwise comparisons using the Tukey's HSD test (* < 0.05; ** < 0.01; *** < 0.001). The lower right subfigure shows the results of linear discriminant analysis based on micromorphological measurements distributed into four broadly defined species.

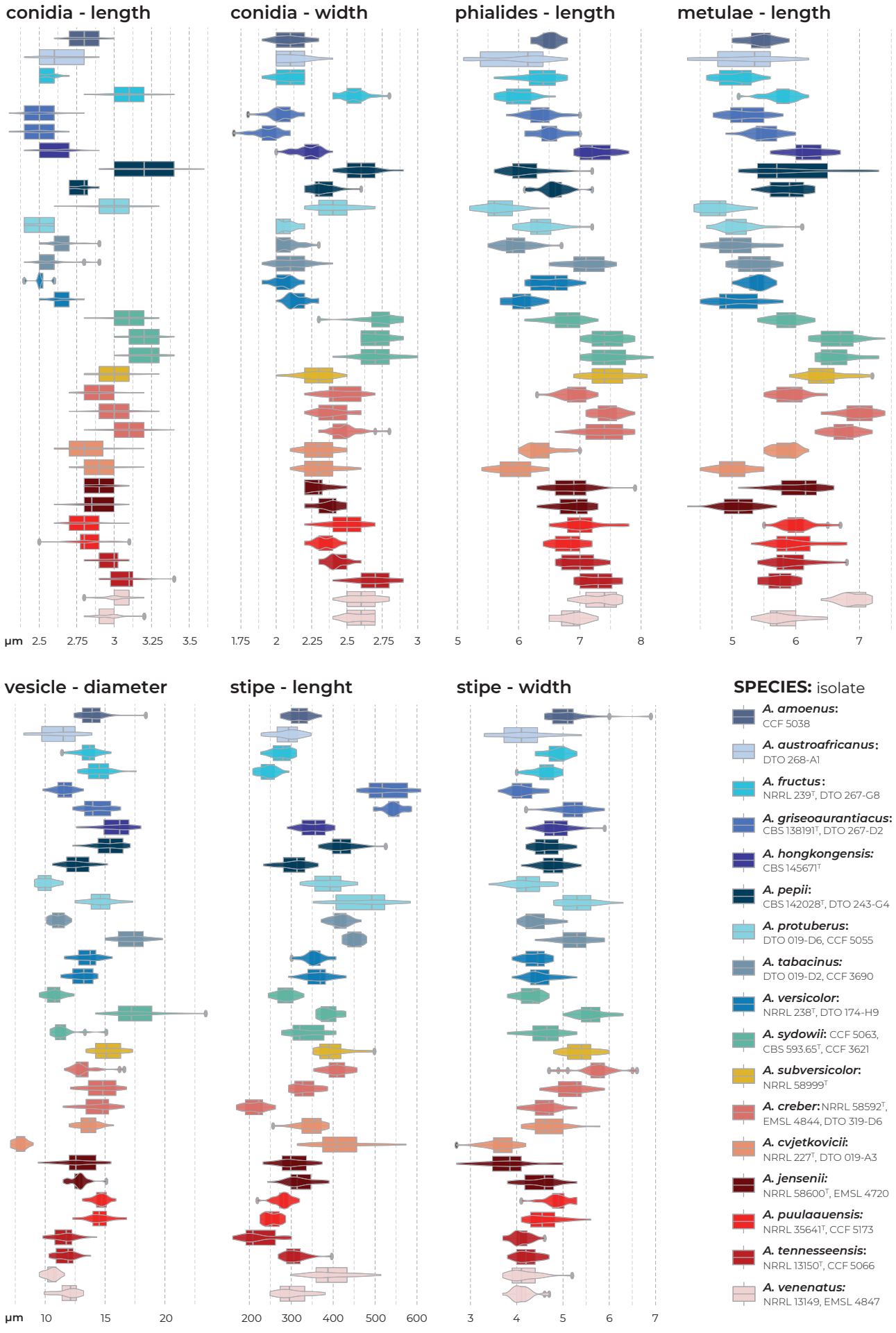

Fig. 11. Dimensions of seven micromorphological characters across isolates of narrowly defined species in the series *Versicolores* shown in the form of box plots and violin plots. Box plots show interquartile range, values within ± 1.5 of interquartile range (whiskers) and outliers.

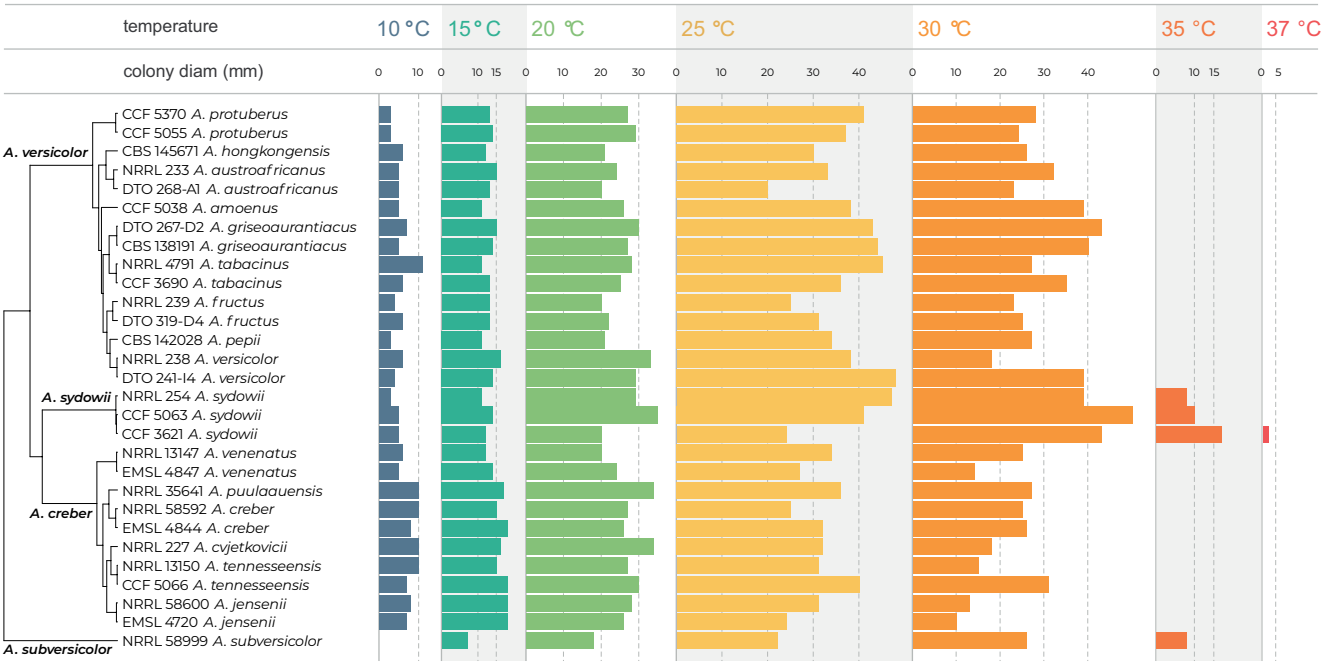

Fig. 12. Comparison of growth rates on MEA at temperatures ranging from 10 °C to 37 °C after 14 d of cultivation. Phylogenetic tree is based on the *CaM* sequences of selected strains and calculated in IQ-TREE; bar plots representing the colony size at specific temperature are displayed on the right.

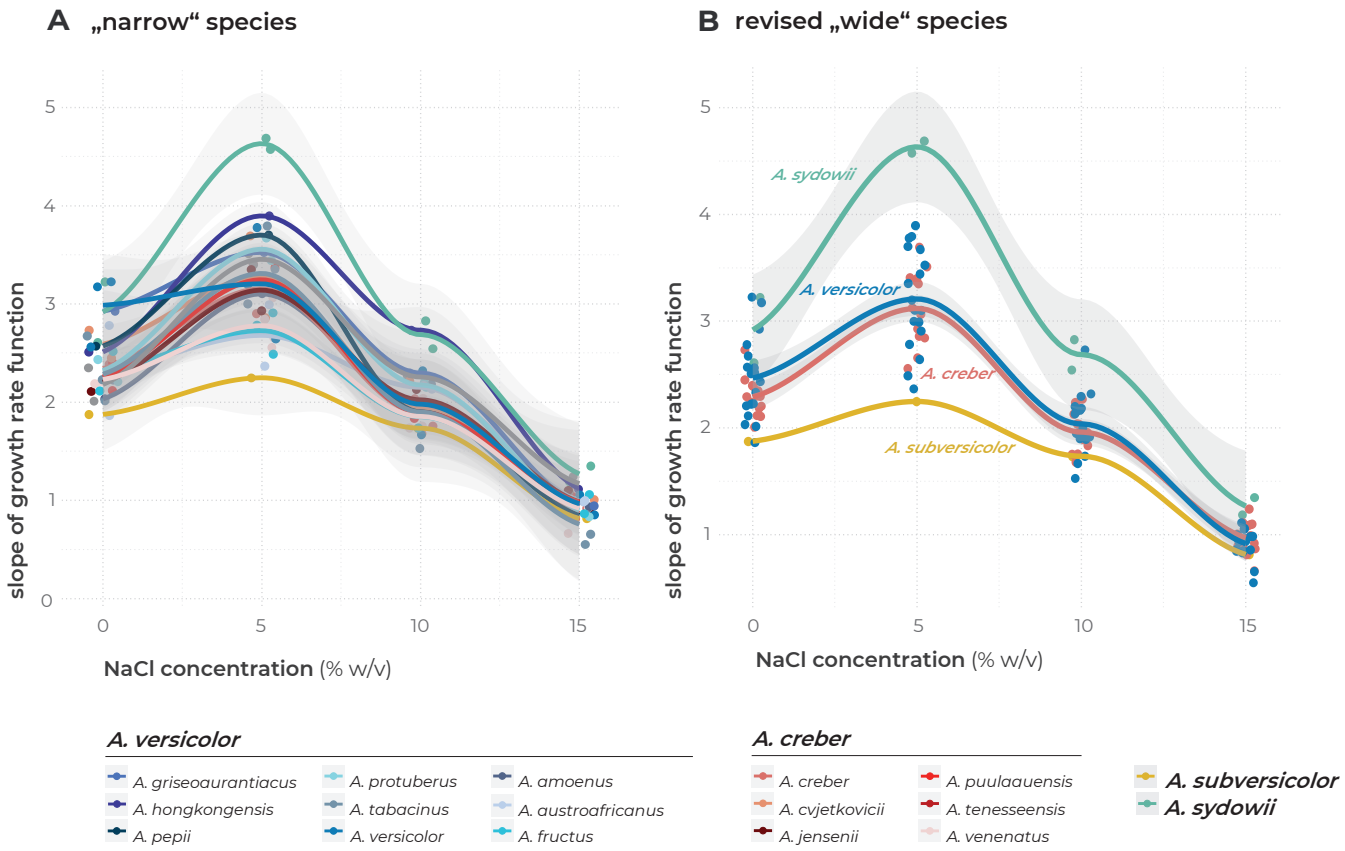

Fig. 13. Growth rates of species in osmotic (NaCl) gradient. Each point represents the slope value of the linear trendline from the growth curve of strains and NaCl concentration (0, 5, 10, 15 % w/v). The curve was created using the LOESS function in R package ggplot2, grey zones represent 95 % confidence intervals. **A.** Strains distributed into 17 narrow species. **B.** Strains distributed into four main lineages.

TAXONOMY

Aspergillus creber Jurjević, S.W. Peterson & B.W. Horn, IMA Fungus 3: 69. 2012. MycoBank MB 800598. Fig. 14.
= *Aspergillus cvjetkovicii* Jurjević, S.W. Peterson & B.W. Horn, IMA Fungus 3: 69. 2012. MycoBank MB 800599.
= *Aspergillus jensenii* Jurjević, S.W. Peterson & B.W. Horn, IMA Fungus 3: 70. 2012. MycoBank MB 800601.
= *Aspergillus puulaauensis* Jurjević, S.W. Peterson & B.W. Horn, IMA Fungus 3: 71. 2012. MycoBank MB 800602.
= *Aspergillus tennesseensis* Jurjević, S.W. Peterson & B.W. Horn, IMA Fungus 3: 73. 2012. MycoBank MB 800604.
= *Aspergillus venenatus* Jurjević, S.W. Peterson & B.W. Horn, IMA Fungus 3: 73. 2012. MycoBank MB 800605.

Typus: BPI 800912. Culture ex-type: CBS 145749 = NRRL 58592 = DTO 225-G7 = IBT 32277.

Colony diam, *25 °C (if not otherwise stated)*, *14 d (mm)*: MEA: 25–40; CYA: 18–38; CZA: 21–30; YES: 23–52; DG18: 25–51; OA: 22–36; CY20S: 26–47; CREA: 22–31. MEA 10 °C: 7–10; MEA 15 °C: 15–19; MEA 20 °C: 26–34; MEA 30 °C: 10–32; MEA 35 °C: 0.

Culture characteristics, *25 °C*, *14 d*: MEA: Colonies centrally raised, in some strains radially wrinkled; texture velutinous, floccose in the centre; margins entire to delicately filiform; mycelial areas white (#ffffff); sporulation bottle green (#006a4e) or viridian green (#40826d), at first white; orange yellow crayola patches with Hülle cells occasionally present; reverse centrally windsor tan (#a75502) to maximum yellow red (#f2ba49) in margins. CYA: Colonies centrally raised, radially wrinkled in some strains; texture velutinous; margins undulate; mycelial areas white to wheat (#f5deb3); sporulation at first white to wheat (#f5deb3), xanadu (#738678) or fern green (#4d744d); reverse centrally ochre (#cc7722) to gold crayola (#e6be8a) in margins, saddle brown (#964b00) when sporulation is dense. CZA: Colonies centrally raised, radially wrinkled in some strains; texture velutinous to floccose; margins undulate; exudate in the form of clear droplets present in some strains; bistre (#3d2b1f) soluble pigment present in some strains; mycelial areas jasmine (#f8de7e) or white; sporulation middle green (#4d8c57) or viridian (#40826d); reverse centrally seal brown (#59260b) or maximum yellow red (#f2ba49), in margins alloy orange (#c46210) or bistre (#3d2b1f) when soluble pigment is present. YES: Colonies centrally raised, significantly, irregularly wrinkled; texture floccose; margins entire, delicately undulate in some strains; mycelial areas white, in some strains bright yellow crayola (#ffaa1d); sporulation russian green (#679267), asparagus (#87a96b) or ash gray (#b2beb5); reverse centrally saddle brown (#964b00) or sepia (#704214) to naples yellow (#fada5e) in margins. DG18: Colonies flat or umbonate; texture velutinous; margins undulate to filiform; mycelial areas white; sporulation at first white, dark sea green (#8fbc8f) or green sheen (#6eaea1); reverse alloy orange (#c46210) to orange yellow crayola (#f8d568), in margins flax (#eedc82). OA: Colonies centrally raised; texture floccose to granular; margins entire, irregular in some strains; sporulation brunswick green (#1b4d3e) to yellow green crayola (#c5e384), in margins white; reverse orange peel (#ff9f00) to flax (#eedc82) in margins. CY20S: Colonies centrally raised, radially wrinkled; texture velutinous to floccose; margins entire to filiform; bistre (#3d2b1f) soluble pigment present in some strains; mycelial areas white in margins, maize crayola (#f2c649) in central areas; sporulation russian green (#679267), asparagus (#87a96b), ash gray (#b2beb5) or white; reverse centrally alloy orange (#c46210) or golden brown (#996515), in margins maize crayola (#f2c649) or medium champagne (#f3e5ab). CREA: Colonies centrally raised; texture velutinous to floccose; margins entire to delicately filiform; exudate in the form of clear droplets present in some strains; bistre (#3d2b1f) soluble pigment present in some strains; mycelial areas white; sporulation dark sea green (#8fbc8f) or cambridge blue (#a3c1ad); reverse dark purple (#301934), fuchsia crayola (#c154c1) or bistre (#3d2b1f); no acid production.

Micromorphology: *Ascomata* absent. *Hülle cells* present in some strains, most commonly on MEA or CZA (Supplementary Table S3), hyaline, subglobose, usually 18–21 × 16–19 µm. *Conidial heads* radiate, remaining compact, *conidiophores* biseriate. *Stipes* smooth, hyaline or light brown, (200–)250–350(–400) × 4–6 µm; *vesicles* hyaline, pyriform to subglobose, (10–)12–16 µm diam; *metulae* hyaline, cylindrical to barrel-shaped, 5–7 µm long, covering three quarters of the vesicle; *phialides* hyaline, flask-shaped, 6.5–7.5 µm long. *Conidia* globose to subglobose, verrucose, hyaline 2.5–3 (2.9 ± 0.2) × 2–2.5 (2.4 ± 0.2) µm.

Cardinal temperatures: *Aspergillus creber* grows at 10 °C, and the optimum growth temperature is between 20 and 25 °C. This species is able to grow well at 30 °C but does not grow at 35 °C.

Distinguishing characters: *Aspergillus creber* and *A. versicolor* are two species that possess huge genetic and phenotypic variability. It is impossible to distinguish these two species, because all morphological and physiological characters measured in this study largely overlap. The conidia of *A. versicolor* tend to be the smallest among the series members (*A. versicolor* 2.6 ± 0.2 × 2.1 ± 0.1 µm *vs A. creber* 2.9 ± 0.2 × 2.4 ± 0.2 µm). The strains of *A. versicolor* are usually growing slightly faster than those of *A. creber* on MEA supplied with 5 % NaCl (Fig. 13). The temperature optimum of these two species is also slightly different: *A. versicolor* strains grows faster at 30 °C and strains of *A. creber* grows faster at 10 and 15 °C. (Fig. 12) For distinguishing characters from *A. subversicolor* and *A. sydowii*, see the respective paragraphs below.

Aspergillus subversicolor Jurjević, S.W.Peterson & B.W. Horn, IMA Fungus 3: 69. 2012. MycoBank MB 800603. Fig. 15.

Typus: BPI 880918. Culture ex-type: CBS 145751 = NRRL 58999 = DTO 225-G9.

Colony diam, *25 °C (if not otherwise stated)*, *14 d (mm)*: MEA: 22; CYA: 31; CZA: 12; YES: 29; DG18: 22; OA: 19; CY20S: 25; CREA: 17. MEA 10 °C: 0; MEA 15 °C: 7; MEA 20 °C*:* 18; MEA 30 °C: 26; MEA 35 °C: 8.

Culture characteristics, *25 °C*, *14 d*: MEA: Colonies centrally raised, moderately wrinkled; texture velutinous; margins undulate; mycelial areas white (#ffffff); sporulation verdigris (#43b3ae); reverse centrally alloy orange (#c46210) to jasmine (#f8de7e) in margins. CYA: Colonies centrally raised, moderately wrinkled; texture floccose; margins undulate; mycelial areas white; sporulation polished pine (#5da493); reverse centrally burnt orange (#cc5500) to flax (#eedc82) in margins. CZA: Colonies crateriform (raised with central depression), significantly wrinkled; texture floccose; margins undulate; exudate present in the form of clear droplets; mycelial areas white; sporulation pine green (#01796f) to olivine (#9ab973); reverse saddle brown (#964b00) with medium champagne

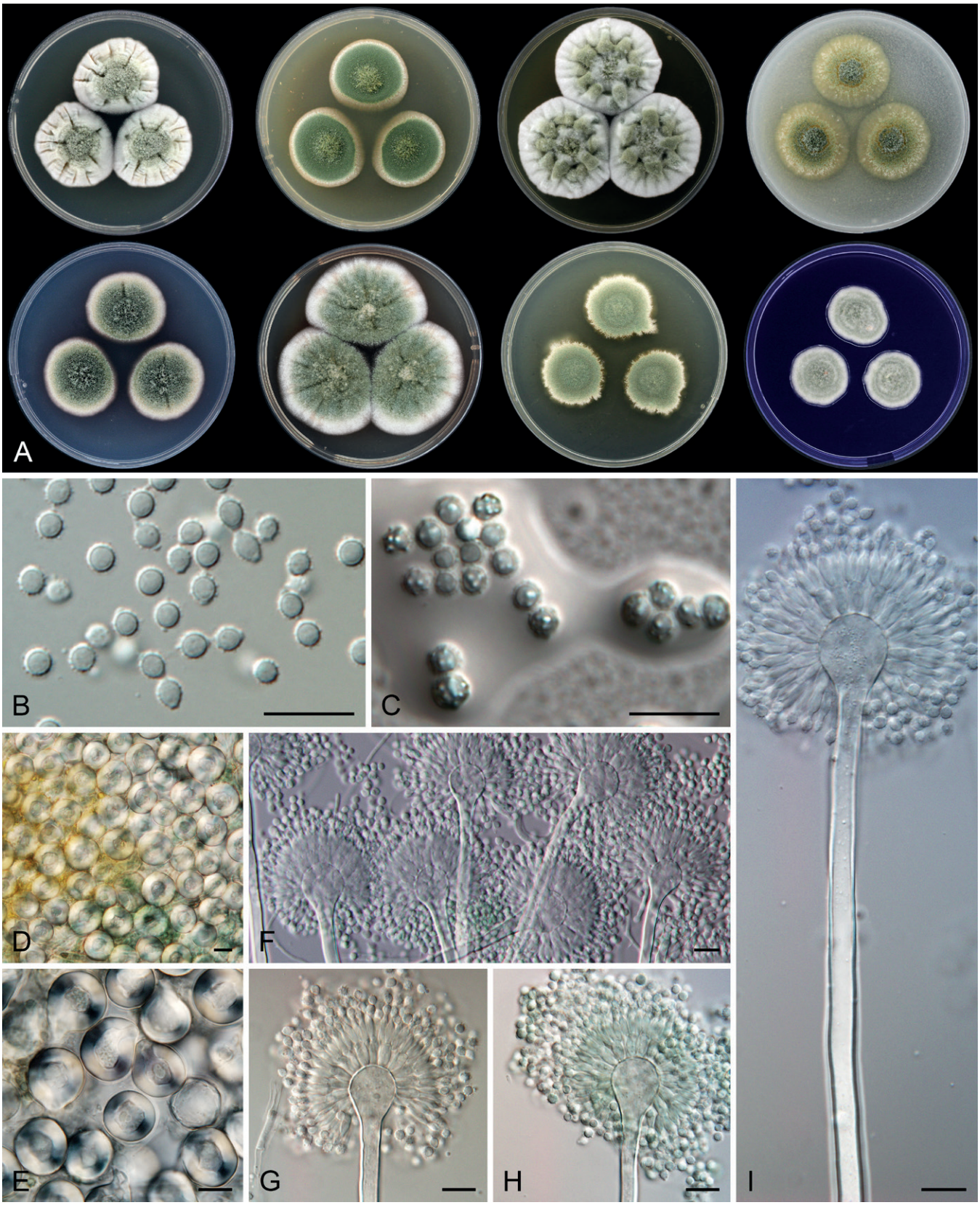

Fig. 14. Macromorphology and micromorphology of *Aspergillus creber*. **A.** Top row left to right: colonies on CYA, MEA, YES and OA after 14 d at 25 °C; bottom row left to right: colonies on CZA, CY20S, DG18 and CREA after 14 d at 25 °C (all colonies from strain NRRL 58592). **B.** Conidia. **C.** Conidia in air bubble. **D, E.** Hülle cells. **F–I.** Conidiophores. Scale bars = 10 µm.

(#f3e5ab) margins. YES: Colonies crateriform (raised with central depression), significantly wrinkled; texture velutinous to floccose; margins undulate to lobate; mycelial areas white to linen (#faf0e6); sporulation dark sea green (#8fbc8f) to green sheen (#6eaea1); reverse centrally earth yellow (#e1a95f) to black bean (#3d0c02), in margins alloy orange (#c46210). DG18: Colonies centrally raised, moderately radially wrinkled; texture velutinous; margins undulate to lobate; mycelial areas hyaline; sporulation green sheen (#6eaea1); reverse saddle brown (#964b00) to alloy orange (#c46210) to naples yellow (#fada5e) in margins. OA: Colonies centrally raised; texture irregularly floccose; margins delicately undulate; mycelial areas hyaline; sporulation deep jungle green (#004b49); reverse

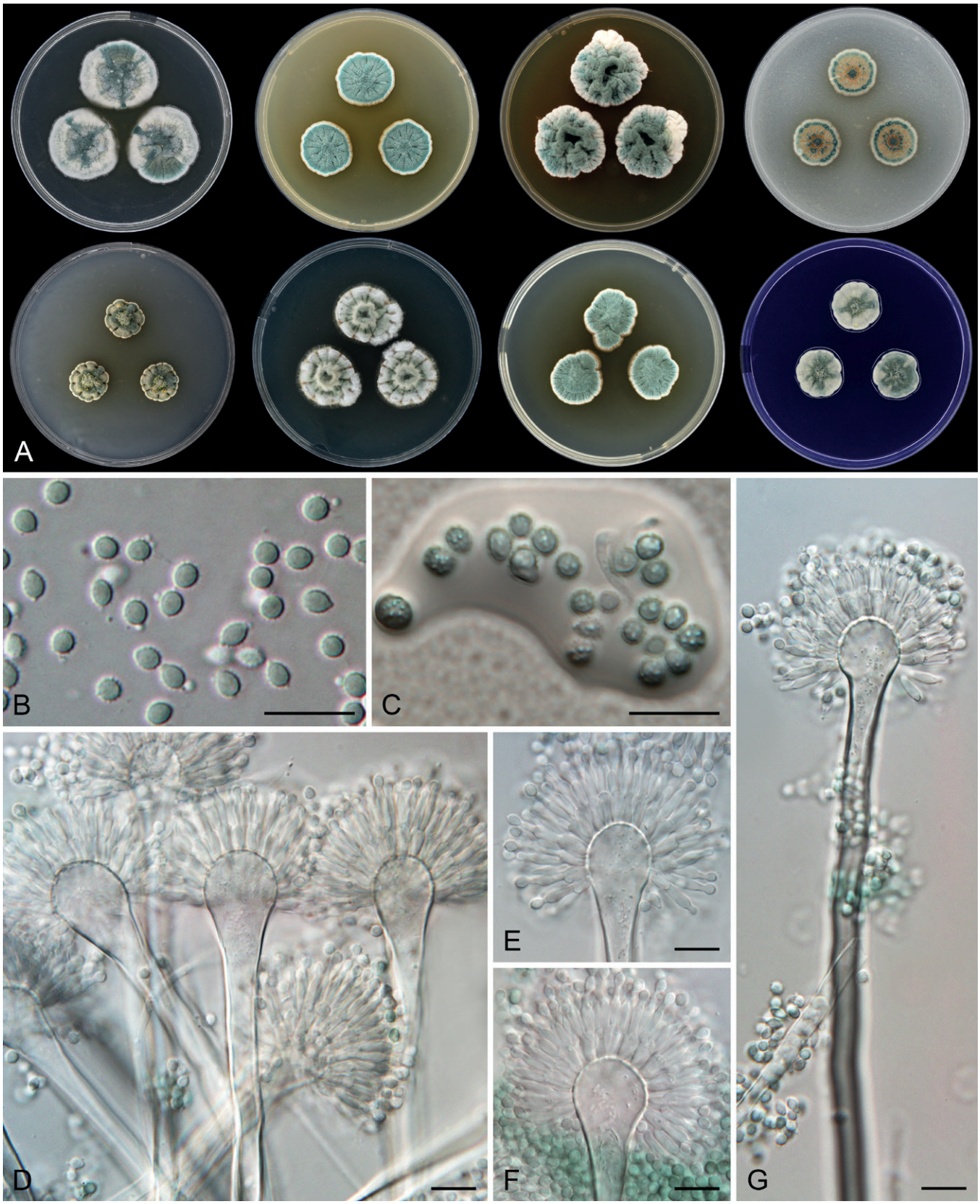

Fig. 15. Macromorphology and micromorphology of *Aspergillus subversicolor*. **A.** Top row left to right: colonies on CYA, MEA, YES and OA after 14 d at 25 °C; bottom row left to right: colonies on CZA, CY20S, DG18 and CREA after 14 d at 25 °C (all colonies from strain NRRL 58999). **B.** Conidia. **C.** Conidia in air bubble. **D–G.** Conidiophores. Scale bars = 10 µm.

centrally alloy orange (#c46210) to medium champagne (#f3e5ab) in margins. CY20S: Colonies crateriform (raised with central depression), radially wrinkled; texture floccose; margins undulate to delicately filiform; mycelial areas white; sporulation dark sea green (#8fbc8f); reverse centrally alloy orange (#c46210) to sunray (#e3ab57), in margins jasmine (#f8de7e). CREA: Colonies centrally raised; texture floccose; margins undulate; exudate present in the form of clear droplets; mycelial areas white to beige (#f5f5dc); sporulation viridian (#40826d) to russian green (#679267); reverse raisin black (#242124), pink lavender (#d8b2d1) in margins; no acid production.

Micromorphology: *Ascomata* absent. *Hülle cells* absent. *Conidial heads* radiate, remaining compact, *conidiophores* biseriate. *Stipes* smooth, hyaline or light brown, 350–450 × 5–6 µm; *vesicles* hyaline, pyriform to spatulate, 14–17 µm diam; *metulae* hyaline, cylindrical to obovate, 6–7 µm long, covering three quarters of the vesicle; *phialides* hyaline, flask-shaped, 7–8 µm long. *Conidia* subglobose to ovoid, verrucose, hyaline 3 (3 ± 0.1) × 2–2.5 (2.3 ± 0.1) µm.

Cardinal temperatures: *Aspergillus subversicolor* does not grow at 10 °C, but grows at 15 °C, and its optimum growth temperature is 30 °C. This species is able to grow restrictedly at 35 °C but not at 37 °C.

Notes: *Aspergillus subversicolor* is phylogenetically distant from other species in the series *Versicolores*, but clearly belongs to the series (Houbraken *et al.* 2020). It is easily distinguishable from other members of the series by its slower growth on almost all cultivation media and on MEA supplied with 5 % NaCl (Fig. 13). Unlike other species, it is unable to grow at 10 °C, but contrary to *A. creber* and *A. versicolor*, it grows restrictedly at 35 °C (Fig. 12).

Aspergillus sydowii (Bainier & Sartory) Thom & Church, Aspergilli: 147. 1926. MycoBank MB 279636. Fig. 16.

Typus: IMI 211384. Culture ex-type: CBS 593.65 = NRRL 250 = IMI 211384 = NRRL 254 = ATCC 16844.

Colony diam, *25 °C (if not otherwise stated)*, *14 d (mm)*: MEA: 34–48; CYA: 36–50; CZA: 32–40; YES: 45–48; DG18: 49–54; OA: 28–39; CY20S: 38–61; CREA: 38–43. MEA 10 °C: 3–5; MEA 15 °C: 11–13; MEA 20 °C: 20–35; MEA 30 °C: 39–50; MEA 35 °C: 10–17; MEA 37 °C: 0–5.

Culture characteristics, *25 °C*, *14 d*: MEA: Colonies centrally raised, moderately radially wrinkled; texture velutinous; margins undulate; mycelial areas white (#ffffff); sporulation celadon green (#2f847c) to dark cyan (#008b8b); reverse centrally dark brown (#654321) to medium champagne (#f3e5ab) in margins or centrally rust (#b7410e) to yellow crayola (#fce883) in margins. CYA: Colonies centrally raised, moderately radially wrinkled in some strains; texture velutinous; margins entire to delicately filiform; exudate present in some strains in the form of clear droplets; mycelial areas white; sporulation centrally deep space sparkle (#4a646c), dark cyan in margins (#008b8b); reverse centrally seal brown (#59260b), in margins windsor tan (#a75502) or banana mania (#fae7b5). CZA: Colonies centrally raised, wrinkled in some strains; texture floccose; margins undulate to delicately filiform; exudate present in the form of clear droplets; bistre (#3d2b1f) soluble pigment present in some strains; mycelial areas white to linen (#faf0e6); sporulation brunswick green (#1b4d3e) to celadon green (#2f847c); reverse centrally bistre (#3d2b1f) or seal brown (#59260b) to banana mania (#fae7b5) in margins. YES: Colonies raised, moderately wrinkled; texture floccose, cottony in margins; margins undulate to irregular; mycelial areas white; sporulation ash gray (#b2beb5) or celadon green (#2f847c); reverse copper (#b87333) to jasmine (#f8de7e). DG18: Colonies centrally raised; texture velutinous; margins entire to delicately filiform; mycelial areas white; sporulation deep jungle green (#004b49) to ash gray (#b2beb5); reverse centrally camel (#c19a6b) to beige (#f5f5dc) in margins. OA: Colonies centrally raised, moderately wrinkled in some strains; texture velutinous to floccose; margins undulate to irregular; mycelial areas white or hyaline; sporulation centrally deep jungle green (#004b49) or russian green (#679267) to ash grey in margins (#b2beb5); reverse centrally saddle brown (#964b00) to medium champagne (#f3e5ab) in margins. CY20S: Colonies centrally raised or crateriform (raised with central depression), radially or irregularly wrinkled; texture centrally floccose to cottony in margins; margins undulate to delicately filiform; mycelial areas white to linen (#faf0e6); sporulation celadon green (#2f847c) or ash gray (#b2beb5); reverse centrally French bistre (#856d4d) to beige (#f5f5dc) in margins. CREA: Colonies centrally raised; texture velutinous to floccose; margins entire to delicately filiform; exudate present in the form of clear droplets; mycelial areas white to tan (#d2b48c); sporulation dark cyan (#008b8b) to middle blue green (#8dd9cc); reverse centrally raisin black (#242124) to charcoal (#36454f), in margins pink lavender (#d8b2d1); no acid production.

Micromorphology: *Ascomata* absent. *Hülle cells* absent. *Conidial heads* radiate, remaining compact, *conidiophores* biseriate. *Stipes* smooth, hyaline or light brown 250–400 × 4–6 µm; *vesicles* hyaline, spatulate to clavate, 10–17(–25) µm diam; *metulae* hyaline, cylindrical to barrel-shaped, 6–7 µm long, covering three quarters of the vesicle; *phialides* hyaline, flask-shaped, 6.5–8 µm long. *Conidia* subglobose to ovate, verrucose, hyaline 3–3.5 (3.1 ± 0.1) × 2.5–3 (2.7 ± 0.1) µm.

Cardinal temperatures: *Aspergillus sydowii* grows restrictedly at 10 °C, and the optimum growth temperature is 30 °C. Some strains of this species are able to grow restrictedly at 37 °C but not at 40 °C.

Distinguishing characters: *Aspergillus sydowii* exhibits some genetic variability, however it was never split into more species and the concept of this species remains the same since its original description in 1926 (Thom & Church). It can be distinguished from other species in series *Versicolores* by its typically blue-green to turquoise colony colours on MEA, CYA, and CZA. Additionally, this species is more osmotolerant than other members of the series as it grows the fastest on media supplied with 5 and 10 % of NaCl (Fig. 13). It is also the only species of the series with some strains capable of growing at 37 °C (Fig. 12).

Aspergillus versicolor (Vuill.) Tirab., Ann. Bot., Roma 7: 9. 1908. MycoBank MB 172159. Fig. 17.
= *Aspergillus amoenus* M. Roberg, Hedwigia 70: 138. 1931. MycoBank MB 250654.
= *Aspergillus austroafricanus* Jurjević, S.W. Peterson & B.W. Horn, IMA Fungus 3: 67. 2012. MycoBank MB 800597.
= *Aspergillus fructus* Jurjević, S.W. Peterson & B.W. Horn, IMA Fungus 3: 70. 2012. MycoBank MB 800600.
= *Aspergillus griseoaurantiacus* Visagie, Hirooka & Samson, Stud. Mycol. 78: 112. 2014. MycoBank MB 809197.
= *Aspergillus hongkongensis* C.C. Tsang *et al.*, Diagn. Microbiol. Infect. Dis. 84: 130. 2016. MycoBank MB 810279.
= *Aspergillus pepii* Despot *et al.*, Mycol. Prog. 16: 67. 2017. MycoBank MB 817073.
= *Aspergillus protuberus* Munt.-Cvetk., Mikrobiologiya 5: 119. 1968. MycoBank MB 326650.
= *Aspergillus tabacinus* Nakaz. *et al.*, J. Agric. Chem. Soc. Japan 10: 177. 1934. MycoBank MB 539544.

Typus: CBS 583.65. Culture ex-type: CBS 583.65 = NRRL 238 = ATCC 9577 = IFO 33027 = IMI 229970 = JCM 10258 = UAMH 4956 = QM 7478 = Thom 5519.57 = WB 238.

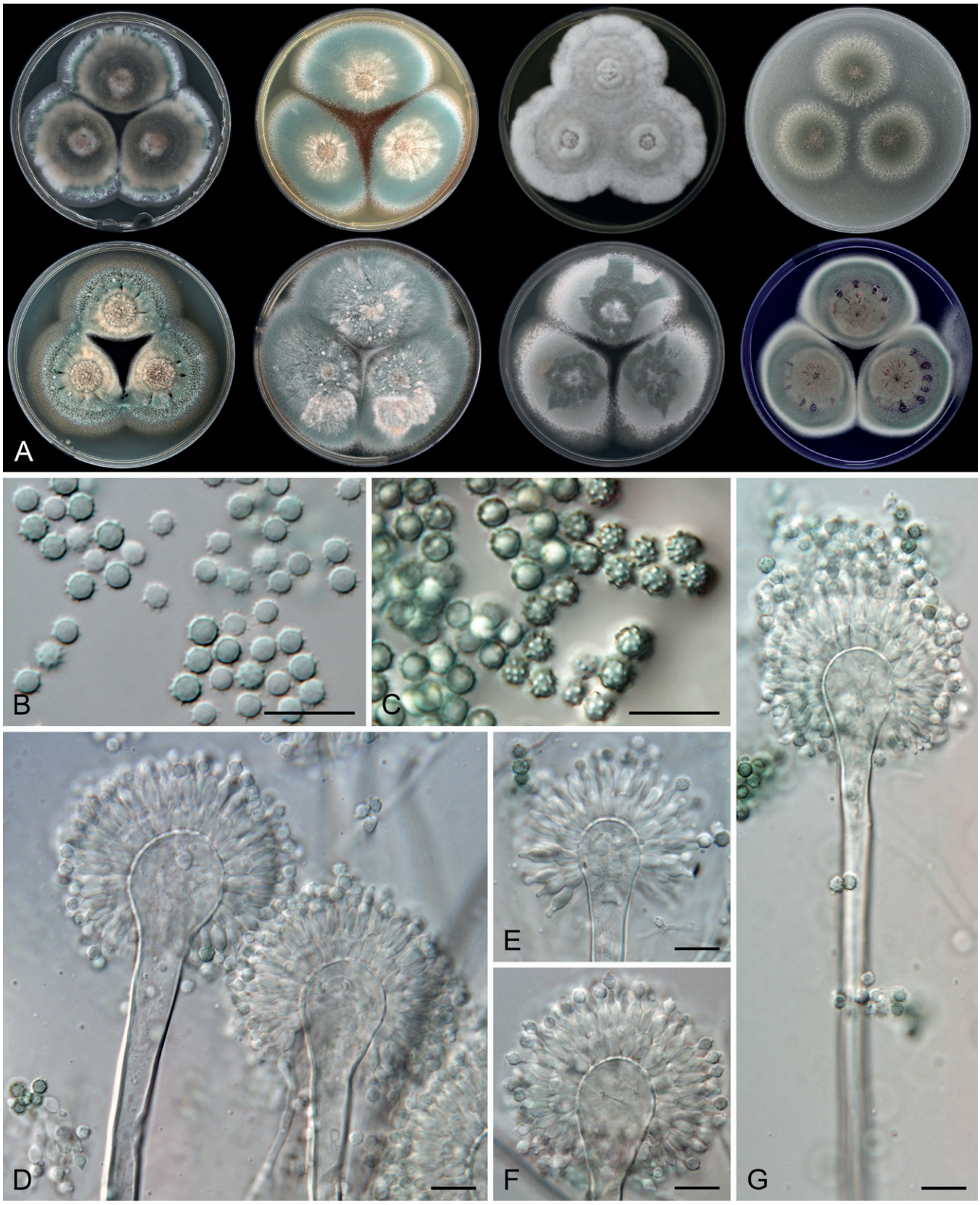

Fig. 16. Macromorphology and micromorphology of *Aspergillus sydowii*. **A.** Top row left to right: colonies on CYA, MEA, YES and OA after 14 d at 25 °C; bottom row left to right: CZA, CY20S, DG18 and CREA after 14 d at 25 °C (all colonies from strain NRRL 254). **B.** Conidia. **C.** Conidia in air bubble. **D–G.** Conidiophores. Scale bars = 10 µm.

Colony diam, *25 °C (if not otherwise stated)*, *14 d (mm)*: MEA: 20–48; CYA: 26–46; CZA: 22–38; YES: 25–60; DG18: 30–49; OA: 22–49; CY20S: 26–60; CREA: 22–45. MEA 10 °C: 2–7; MEA 15 °C: 10–17; MEA 20 °C: 20–32; MEA 30 °C: 18–43; MEA 35 °C: 0.

Culture characteristics, *25 °C*, *14 d*: MEA: Colonies centrally raised, in some strains radially wrinkled; texture velutinous, floccose in the centre; margins entire to delicately filiform; exudate present in the form of clear droplets; mycelial areas white (#ffffff); sporulation forest green crayola (#5fa777), russian green (#679267), viridian (#40826d) or myrtle green (#317873); flax (#eedc82) patches with

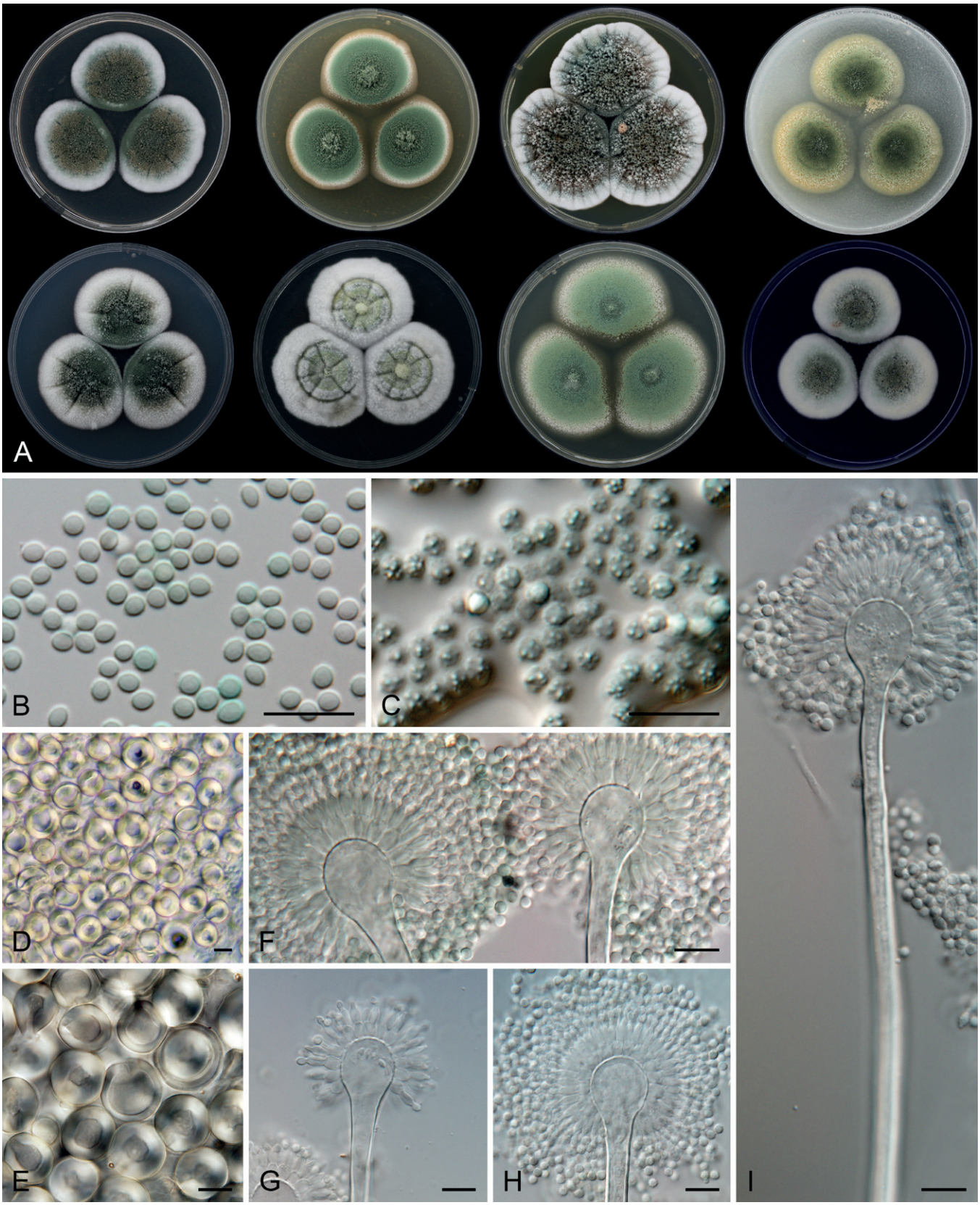

Fig. 17. Macromorphology and micromorphology of *Aspergillus versicolor*. **A.** Top row left to right: colonies on CYA, MEA, YES and OA after 14 d at 25 °C; bottom row left to right: CZA, CY20S, DG18 and CREA after 14 d at 25 °C (all colonies from strain CCF 3690). **B.** Conidia. **C.** Conidia in air bubble. **D, E.** Hülle cells. **F–I.** Conidiophores. Scale bars = 10 µm.

Hülle cells present in some strains; reverse centrally alloy orange (#c46210) or dark brown (#654321) to flax (#eedc82) in margins. CYA: Colonies centrally raised, radially wrinkled; texture velutinous to floccose, with cottony centre in some strains; margins entire, less commonly undulate; exudate present in the form of clear droplets; mycelial areas white; sporulation bottle green (#006a4e), pine green (#01796f) or fern green (#4d744d); reverse centrally bistre brown (#967117) or copper (#b87333) to beige (#f5f5dc) in margins. CZA: Colonies centrally raised, radially (in some strains also concentrically) wrinkled; texture velutinous to floccose; margins entire, seldom undulate; bistre (#3d2b1f) soluble pigment present in some strains; exudate present in the form of clear droplets; mycelial

areas white; sporulation brunswick green (#1b4d3e) or hunter green (#355e3b), seldom white to ash grey (#b2beb5); gold metallic (#d4af37) patches with Hülle cells present in some strains; reverse centrally saddle brown (#964b00) to windsor tan (#a75502) or black bean (#3d0c02) in strains producing soluble pigment, in margins wheat (#f5deb3). YES: Colonies centrally raised, significantly, irregularly wrinkled, texture velutinous to floccose; margins entire, seldom undulate or irregular; exudate present in some strains in the form of clear droplets; mycelial areas white; sporulation deep jungle green (#004b49) shiny shamrock (#5fa778) or cambridge blue (#a3c1ad), seldom white to ash gray (#b2beb5); yellow crayola (#fce883) patches with Hülle cells present in some strains; reverse centrally liver chestnut (#987456) to alloy orange (#c46210), in margins jasmine (#f8de7e). DG18: Colonies centrally raised; texture velutinous, in some strains cottony in the center; margins entire, in some strains irregular; mycelial areas white; sporulation illuminating emerald (#319177) or xanadu (#738678), seldom white to ash gray (#b2beb5); yellow crayola (#fce883) patches with Hülle cells present in some strains; reverse centrally saddle brown (#964b00) to alloy orange (#c46210), in margins straw (#e4d96f). OA: Colonies centrally raised; texture floccose; margins entire to irregular; rust (#b7410e) to ecru (#c2b280) soluble pigment present in some strains; mycelial areas white or hyaline; sporulation deep jungle green (#004b49), fern green (#4d744d) or green sheen (#6eaea1), in some strains with vegas gold (#c5b358) patches formed by conidiophores, not by Hülle cells; reverse centrally dark brown (#654321) to copper (#b87333) or rust (#b7410e) in strains producing soluble pigment, in margins flax (#eedc82). CY20S: Colonies centrally raised, radially wrinkled; texture floccose with cottony patches; margins entire to irregular; mycelial areas white; sporulation green sheen (#6eaea1), fern green (#4d744d) or ash grey (#b2beb5), in some strains with gold metallic (#d4af37) patches (formed by conidiophores, not Hülle cells); canary (#ffff9a) to yellow crayola (#fce883) patches with Hülle cells present in some strains; reverse centrally alloy orange (#c46210) to yellow crayola (#fce883) in margins or centrally olive green (#b5b35c) to beige (#f5f5dc) in margins. CREA: Colonies centrally raised, in some strains moderately wrinkled; texture velutinous to floccose; margins entire to delicately filiform; exudate present in some strains in the form of clear or fire opal (#e95c4b) droplets; mycelial areas white to medium champagne (#f3e5ab); sporulation cambridge blue (#a3c1ad), xanadu (#77897c) or fern green (#4d744d), in some strains ash grey (#b2beb5); reverse centrally dark purple (#301934) to fuchsia crayola (#c154c1) in margins, or centrally charcoal (#36454f) to tuscany (#c09999) in margins; no acid production.

Micromorphology: *Ascomata* absent. *Hülle cells* present in some strains, most commonly on MEA, YES or DG18 (Supplementary Table S3), hyaline, subglobose, usually 18–21 × 15–20 µm. *Conidial heads* radiate, remaining compact, *conidiophores* biseriate. *Stipes* smooth, hyaline or light brown, 300–600 × 4–6 µm; *vesicles* hyaline, pyriform to spatulate, (10–)12–16(–20) µm diam; *metulae* hyaline, cylindrical to barrel-shaped, 5–6 µm long, covering three quarters to the entire vesicle; *phialides* hyaline, flask-shaped, 6–7.5 µm long. *Conidia* subglobose to ovate, finely verrucose, hyaline 2.5–3 (2.6 ± 0.2) × 2–2.5 (2.1 ± 0.1) µm.

Cardinal temperatures: *Aspergillus versicolor* grows restrictedly at 10 °C, and the optimum growth temperature is between 25 and 30 °C. This species is able to grow well at 30 °C but does not grow at 35 °C.

Distinguishing characters: See respective paragraphs of the species above.

DISCUSSION

Larger amounts of molecular data led to a higher rate of description of new species, with phylogenetically defined/cryptic species becoming increasingly common (Struck *et al.* 2018). This is also the case in *Aspergillus*, where the number of accepted species was steadily rising for the last twenty years (Houbraken *et al.* 2020). Recently, studies employing the species delimitation methods often resulted in a reduction in the number of species (Hubka *et al.* 2018, Wang *et al.* 2018, Boluda *et al.* 2019, Li *et al.* 2019, Feng *et al.* 2021, Nguyen *et al.* 2021), even when phylogenomic approaches were used (Parker *et al.* 2022). These studies usually advocate for an integrative approach using as much data of different types as possible. Enough variability in the dataset is often a requirement from species delimitation methods (Mason *et al.* 2020, Burbrink & Ruane 2021, Cicero *et al.* 2021, Magoga *et al.* 2021). Unfortunately, this condition is frequently hard to follow in taxonomic studies because obtaining large numbers of genetically similar isolates from different localities is difficult to achieve especially in uncommon species. Such efforts are often hampered in practice by administrative (*e.g.*, Nagoya protocol), financial and other barriers. A logical outcome in practice is that the fungal species are frequently described based on a low number of isolates with a limited variability due to insufficient sampling. In such cases where intraspecific variability is low or not present at all, it is usually easy to find phenotypic features distinguishing small clusters of strains, or single strains representing different populations/species. True intraspecific variability is often uncovered much later when enough strains representing a broader species variability is collected. In the meantime, however, the species can already be fragmented into several newly described species, which are often cryptic and sometimes introduced only to preserve the monophyly of the other species in the phylogeny. Over time, the concept will become unsustainable until the next overhaul.

The taxonomy of *A. versicolor* and its relatives has been a subject of many taxonomic re-arrangements and repeated expansions followed by reductions in the number of species. Currently, the species number is again at one of the historical peaks and involves 17 species, most of which can be considered cryptic. Over time, the evidence began to accumulate that some isolates cannot be identified satisfactorily to the species level even with the help of molecular methods. Contradictory species identification results based on sequences of different genes were the initial signal that the species concept in series *Versicolores* is becoming unsustainable. To verify this assumption, we gathered a much larger collection of series *Versicolores* members compared to previous taxonomic studies. Most species delimitation methods have consistently suggested a significant reduction in the number of species as summarized below.

Phylogenetic support of species reduction

The species delimitation methods employed in this study broadly agreed on the distinction of four species (*A. creber*, *A. subversicolor*, *A. sydowii* and *A. versicolor*). Only seven out of 28 methods resulted in the delimitation of more than four species but without clear agreement on the arrangement of the additional species. Such conclusive results are probably caused by a sufficient sampling in the majority of subclades. In general, if there are only a few individuals with large genetic distances in the dataset, the species delimitation methods may overestimate the species number, but with a large set of individuals covering genetic diversity and closing the gaps between clades, the probability of methods to delimit species in

their correct boundaries increases (Pante *et al.* 2015, Chambers & Hillis 2020). The multilocus method STACEY gave similar support to the delimitation of four or five species with *A. venenatus* treated as separate species in the setting with a lower *collapseheight* parameter. The uncertainty about *A. venenatus* can probably be attributed to underrepresentation of isolates from this clade (only two strains from similar localities). Delimitation of *A. protuberus* as separate species from *A. versicolor* was also supported by several single-locus delimitation methods but with different arrangements. The incongruences and probable recombination were detected between *A. protuberus* and other species in *benA* and *Tsr1* loci (Fig. 4). Considering all results together with the inability to reliably distinguish these species morphologically, we suggest treating *A. venenatus* as a synonym of *A. creber* and *A. protuberus* as a synonym of *A. versicolor*.

For the independent testing of species hypotheses proposed by delimitation methods, we used a recently developed program DELINEATE (Sukumaran *et al.* 2021), which gives more relevant results compared to the program BPP as discussed previously (Sukumaran & Knowles 2017, Sklenář *et al.* 2021). The results of the analysis were stable, supporting the broad concept of the species in all scenarios (Fig. 7). The tendency to lump the populations into broad species was always present, even in less probable and meaningful scenarios which were tested by us and not shown in Fig. 7. DELINEATE needs some *a priori* defined species that are certainly correctly delimited in the dataset. This requirement is problematic in the series *Versicolores* since the only species that could be conclusively *a priori* defined were *A. sydowii* and *A. subversicolor*. We overcame this fact by setting up more scenarios with additionally defined delimitations in the *A. creber* and *A. versicolor* lineages (both lineages were divided into subgroups based on the species trees calculated by starBEAST - see Fig. 3). Another solution could be the inclusion of several well-defined species from other related series in section *Nidulantes*.

We also compared the amount of intraspecific variability between the broadly defined species and other accepted species from *Aspergillus* with described intraspecific variability. The resulting graph (Fig. 18) shows that the majority of examined species express the phylogenetic variability of up to 4 % (we can also see that there are only a few species of *Aspergillus* that possess intraspecific genetic variability and have the sequences of *Mcm7* and *Tsr1* genes available and some species gather a large amount of variability in the *benA* gene, which is caused by intronic sequences). The species from series *Versicolores* exhibit different amounts of variability with *A. sydowii* having approximately 1 % maximum phylogenetic distance between its strains, *A. creber* between 2 and 3 %, and *A. versicolor* accumulating more than 3 % of variability in all studied loci. However, even this amount of variability does not make *A. versicolor* an outlier among other *Aspergillus* species.

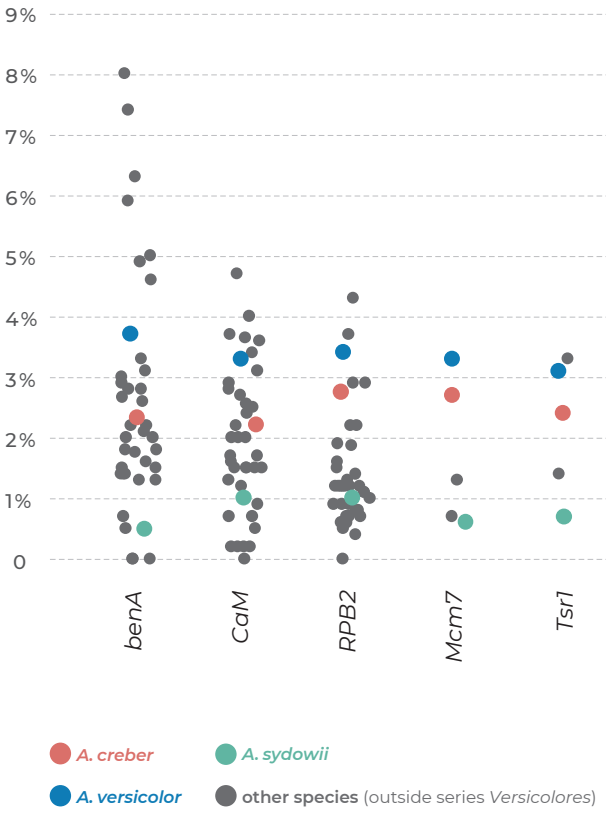

Fig. 18. Graphical representation (jitter plot) of maximum sequence dissimilarity between strains of series *Versicolores* (coloured points) and other *Aspergillus* species (grey points). The comparison includes only species with strains isolated at least from three countries to ensure the presence of representative intraspecific genetic variability. Basic data used for construction of the jitter plot are listed in the Supplementary Table S4.

Morphological and physiological aspects

High morphological variability has always been connected with *A. versicolor* and its relatives (Raper & Fennell 1965, Klich *et al.* 1993, Jurjević *et al.* 2012, Géry *et al.* 2021). This fact also contributed to many re-arrangements in this group before the molecular era. We demonstrated the high intraspecific variability of the series *Versicolores* in macromorphological and micromorphological characters (see Figs 8–11). It is clear from both the colony colours, texture, and dimensions, as well as from boxplots representing micromorphological features that even phylogenetically closely related isolates can exhibit very different phenotypic characteristics. These observations further support reducing the number of species accepted in the series. The linear discriminant analysis (Fig. 10) shows that it is almost impossible to distinguish *A. creber* and *A. versicolor* lineages based on micromorphological characters. The growth curves in the osmotic gradient displayed the same pattern (Fig. 13), *i.e.*, *A. sydowii* and *A. subversicolor* were easily distinguishable, but lineages of *A. creber* and *A. versicolor* grew similarly under changing conditions. From a practical point of view, this means that even after this drastic reduction in the number of species there are still two species that can be considered cryptic from the phenotypic point of view and can only be reliably identified using molecular methods.

Updated taxonomy of series *Versicolores*

Molecular analyses performed in this study indicated that the current species number is overestimated and not sustainable. With a high level of agreement, the majority of methods supported only *A. creber*, *A. subversicolor*, *A. sydowii*, and *A. versicolor* in the series. If we were to consider maintaining the current taxonomic scheme despite the results mentioned above, then we would have to describe at least one new species in the *A. creber* lineage and up to ten new species in the *A. versicolor* lineage (Figs 1, 2). Alternative solutions would be to synonymize some species and describe fewer new species. These solutions were not supported by phenotypic data and receive no or negligible support from phylogenetic methods.

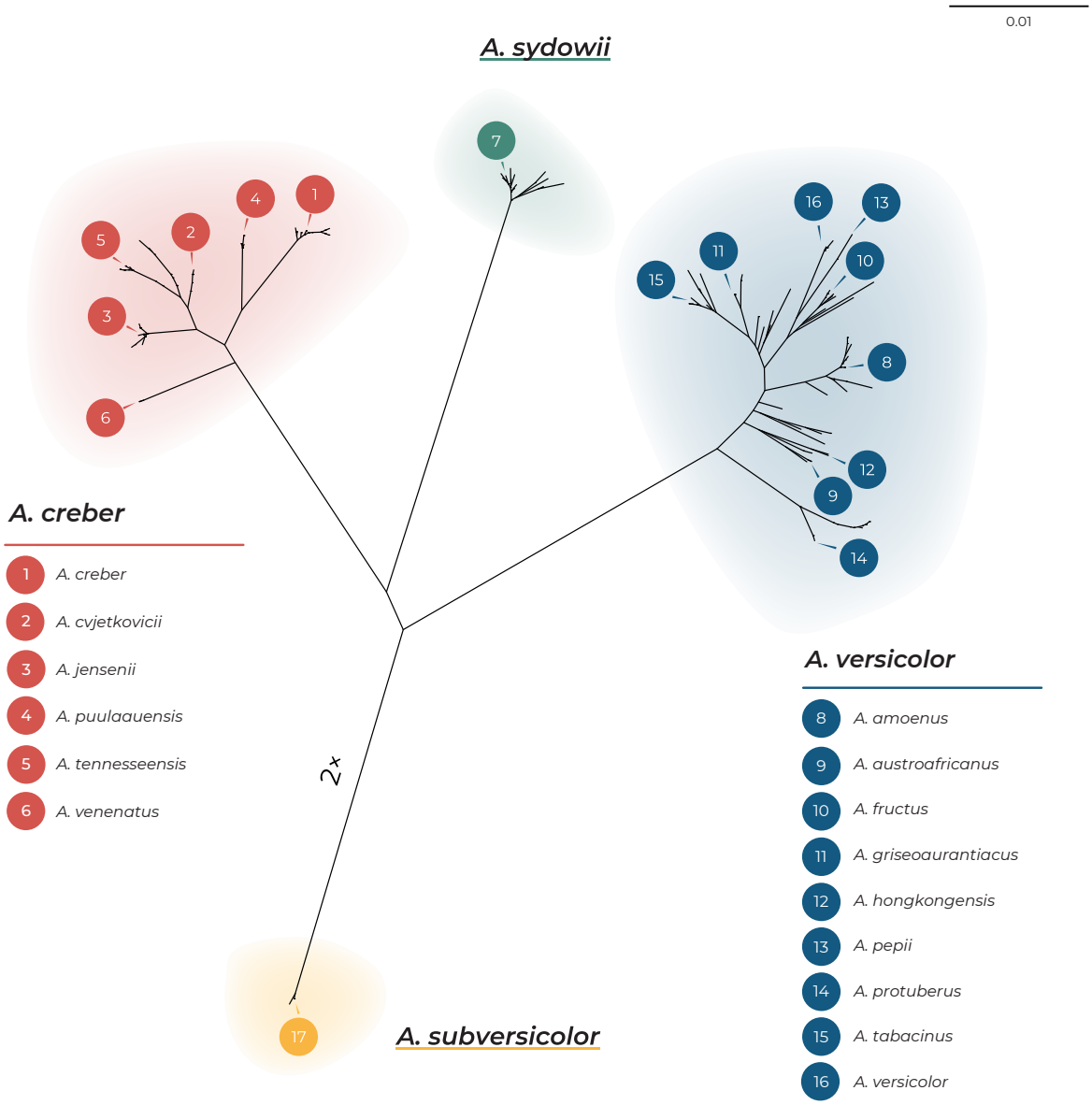

Fig. 19. Taxonomic re-arrangement of series *Versicolores* into four species with marked synonyms. The new taxonomy is schematically shown in the form of the radial tree (ML tree identical to that from Fig. 2).

As a result, a total of 13 species were put in synonymy, five with *A. creber* (*A. cvjetkovicii*, *A. jensenii*, *A. puulaauensis*, *A. tennesseensis*, and *A. venenatus*) and eight with *A. versicolor* (*A. amoenus*, *A. austroafricanus*, *A. fructus*, *A. griseoaurantiacus*, *A. hongkongensis*, *A. pepii*, *A. protuberus*, and *A. tabacinus*). The naming of the two broad species follows the priority rules of the International Code of Nomenclature for algae, fungi, and plants (Turland *et al.* 2018). *Aspergillus versicolor* is the oldest published name in the *A. versicolor* lineage and *A. creber*, simultaneously published with several other new species in its lineage (Jurjević *et al.* 2012), was the highest placed name in the taxonomy section of that article. This new taxonomy is schematically shown by a phylogenetic tree in Fig. 19. This tree is identical to the tree in Fig. 2 but displayed in a radial form, which nicely shows the presence of four wide clades and many small ones representing some of the 17 species accepted before this revision. Additionally, a new species belonging in series *Versicolores*, *A. qilianyuensis*, was described by Wang & Zhuang (2022) based on single strain, but we did not include the species in this study, since it was published during the final preparations of this article and we were unable to obtain the ex-type strain.

We believe that the user community will benefit from this new taxonomy with a lower number of cryptic species. Simplified classification with only four species will facilitate species identification in practices that was complicated by inconsistent identification results when using sequence data of different genes (Fig. 4) and the impossibility of finding species-specific mass spectra within *Aspergillus* when using the MALDI-TOF method (Shao *et al.* 2022). The four supported species in series *Versicolores* can be identified by all of the five genes we used in this study, however identification based on ITS remains problematic. To test the discriminatory power of ITS in the series, we obtained 48 ITS sequences of strains used in this study that are available in the GenBank database (Table 1; alignment available from the Dryad Digital Repository: https://doi.org/10.5061/dryad.63xsj3v5q). There are several substitutions distinguishing *A. sydowii* and *A. subversicolor* from the remaining species, however there is only one substitution separating *A. creber* and *A. versicolor* at the beginning of the ITS1 region and this position is not known for all the strains. A phylogenetic tree based on this dataset calculated by Maximum Likelihood in IQ-TREE (Supplementary Fig. S1) was

poorly resolved, and neither *A. creber*, nor *A. versicolor* formed separate clades. Overall, we cannot recommend ITS as a reliable marker for the identification of series *Versicolores* species, unlike all other loci used in this study.

DECLARATION ON CONFLICT OF INTEREST

The authors declare that there is no conflict of interest.

ACKNOWLEDGEMENTS

František Sklenář was supported by the project of Charles University Grant Agency (GAUK 380821). The project was supported by the Czech Ministry of Health (grant NU21-05-00681), the Charles University Research Centre program no. 204069 and Czech Academy of Sciences Long-term Research Development Project (RVO: 61388971). We are grateful to Radek Zmítko and Jan Karhan for the help with graphical adjustments of some analysis outputs. We thank Milada Chudíčková and Lenka Zídková for their invaluable assistance in the laboratory. VH is grateful for the support from the Japan Society for the Promotion of Science Postdoctoral Fellowships for Research in Japan (Standard) and the support from the Grant-in-aid for JSPS research fellows (grant No. 20F20772). Cobus M Visagie was financially supported by the Future Leaders - African Independent Research fellowship programme (FLAIR, FLR\R1\201831). The FLAIR Fellowship Programme is a partnership between the African Academy of Sciences and the Royal Society funded by the UK Government's Global Challenges Research Fund. We would like to acknowledge Keith A Seifert, Shivan Bezuidenhout, Renan Barbosa, Jiří Řehulka and David Nkwe who provided some strains used in this study.

REFERENCES

Ahlmann-Eltze C, Patil I (2021). ggsignif: R Package for Displaying Significance Brackets for'ggplot2'. *PsyArxiv doi: 10.31234/osf.io/7awm6*.

Ahrens D, Fujisawa T, Krammer HJ, *et al.* (2016). Rarity and incomplete sampling in DNA-based species delimitation. *Systematic Biology* **65**: 478–494.

Beck M (2017). ggord: Ordination Plots with ggplot2. *R package version* **1**: 588.

Boluda C, Rico V, Divakar P, *et al.* (2019). Evaluating methodologies for species delimitation: the mismatch between phenotypes and genotypes in lichenized fungi (*Bryoria* sect. *Implexae*, *Parmeliaceae*). *Persoonia* **42**: 75–100.

Bongomin F, Moore CB, Masania R, *et al.* (2018). Sequence analysis of isolates of *Aspergillus* from patients with chronic and allergic aspergillosis reveals a spectrum of cryptic species. *Future Microbiology* **13**: 1557–1563.

Borgohain P, Barua P, Dutta PJ, *et al.* (2019). Onychomycosis associated with superficial skin infection due to *Aspergillus sydowii* in an immunocompromised patient. *Mycopathologia* **184**: 683–689.

Bouckaert R, Heled J (2014). DensiTree 2: seeing trees through the forest. *bioRxiv* doi: 10.1101/012401.

Bouckaert R, Vaughan TG, Barido-Sottani J, *et al.* (2019). BEAST 2.5: An advanced software platform for Bayesian evolutionary analysis. *PLoS Computational Biology* **15**: e1006650.

Burbrink FT, Ruane S (2021). Contemporary philosophy and methods for studying speciation and delimiting species. *Ichthyology & Herpetology* **109**: 874–894.

Chambers EA, Hillis DM (2020). The multispecies coalescent over-splits species in the case of geographically widespread taxa. *Systematic Biology* **69**: 184–193.

Cicero C, Mason NA, Jiménez RA, *et al.* (2021). Integrative taxonomy and geographic sampling underlie successful species delimitation. *Ornithology* **138**: ukab009.

Danagoudar A, Pratap G, Shantaram M, *et al.* (2021). Antioxidant, cytotoxic and anti-choline esterase activity of green silver nanoparticles synthesized using *Aspergillus austroafricanus* CGJ-B3 (endophytic fungus). *Analytical Chemistry Letters* **11**: 15–28.

De Vries RP, Riley R, Wiebenga A, *et al.* (2017). Comparative genomics reveals high biological diversity and specific adaptations in the industrially and medically important fungal genus *Aspergillus*. *Genome Biology* **18**: 1–45.

Dobolyi C, Inotai K, Bata-Vidács I, *et al.* (2021). Isolation and detailed characterisation of the first sterigmatocystin hyperproducer mould strain in Hungary. *Acta Alimentaria* **50**: 247–258.

Domsch KH, Gams W, Anderson T-H (2007). *Compendium of soil fungi*. 2nd ed. edition. IHW-Verlag, Eching.

Drummond AJ, Xie W, Heled J (2012). Bayesian inference of species trees from multilocus data using *BEAST. *Molecular Biology and Evolution* **29**: 1969–1973.

Feng XY, Wang XH, Chiang YC, *et al.* (2021). Species delimitation with distinct methods based on molecular data to elucidate species boundaries in the *Cycas taiwaniana* complex (*Cycadaceae*). *Taxon* **70**: 477–491.

Fujisawa T, Barraclough TG (2013). Delimiting species using single-locus data and the Generalized Mixed Yule Coalescent (GMYC) approach: a revised method and evaluation on simulated datasets. *Systematic Biology* **62**: 707–724.

Gams W, Christensen M, Onions AHS, *et al.* (1985). Infrageneric taxa of *Aspergillus*. In: *Advances in Penicillium and Aspergillus Systematics.* (R.A. Samson, J.I. Pitt, eds). Plenum Press, New York: 55–62.

Géry A, Lepetit C, Heutte N, *et al.* (2022). Cellular cytotoxicity and oxidative potential of recurrent molds of the genus *Aspergillus* series *Versicolores*. *Microorganisms* **10**: 228.

Géry A, Rioult J-P, Heutte N, *et al.* (2021). First characterization and description of *Aspergillus* series *Versicolores* in French bioaerosols. *Journal of Fungi* **7**: 676.

Glass NL, Donaldson GC (1995). Development of primer sets designed for use with the PCR to amplify conserved genes from filamentous ascomycetes. *Applied and Environmental Microbiology* **61**: 1323–1330.

González-Abradelo D, Pérez-Llano Y, Peidro-Guzmán H, *et al.* (2019). First demonstration that ascomycetous halophilic fungi (*Aspergillus sydowii* and *Aspergillus destruens*) are useful in xenobiotic mycoremediation under high salinity conditions. *Bioresource Technology* **279**: 287–296.

Hall TA (1999). BioEdit: a user-friendly biological sequence alignment editor and analysis program for Windows 95/98/NT. *Nucleic Acids Symposium Series* **41**: 95–98.

Hong S-B, Cho H-S, Shin H-D, *et al.* (2006). Novel *Neosartorya* species isolated from soil in Korea. *International Journal of Systematic and Evolutionary Microbiology* **56**: 477–486.

Houbraken J, Kocsubé S, Visagie CM, *et al.* (2020). Classification of *Aspergillus*, *Penicillium*, *Talaromyces* and related genera (*Eurotiales*): An overview of families, genera, subgenera, sections, series and species. *Studies in Mycology* **95**: 5–169.

Huang C, Feng Y, Patel G, *et al.* (2021). Production, immobilization and characterization of beta-glucosidase for application in cellulose degradation from a novel *Aspergillus versicolor*. *International Journal of Biological Macromolecules* **177**: 437–446.

Hubka V, Barrs V, Dudová Z, *et al.* (2018). Unravelling species boundaries in the *Aspergillus viridinutans* complex (section *Fumigati*): opportunistic human and animal pathogens capable of interspecific hybridization. *Persoonia* **41**: 142–174.

Hubka V, Nováková A, Peterson SW, *et al.* (2016). A reappraisal of *Aspergillus* section *Nidulantes* with descriptions of two new sterigmatocystin-producing species. *Plant Systematics and Evolution* **302**: 1267–1299.

Imbert S, Normand AC, Gabriel F, *et al.* (2019). Multi-centric evaluation of the online MSI platform for the identification of cryptic and rare species of *Aspergillus* by MALDI-TOF. *Medical Mycology* **57**: 962–968.

Jakšić Despot D, Kocsubé S, Bencsik O, *et al.* (2017). New sterigmatocystin-producing species of *Aspergillus* section *Versicolores* from indoor air in Croatia. *Mycological Progress* **16**: 63–72.

Janda-Ulfig K, Ulfig K, Markowska A (2009). Extracellular enzyme profiles of xerophilic fungi isolated from dried materials of medicinal plants. *Polish Journal of Environmental Studies* **18**: 391–397.

Jia J, Chen M, Mo X, *et al.* (2019). The first case report of kerion-type scalp mycosis caused by *Aspergillus protuberus*. *BMC Infectious Diseases* **19**: 1–5.

Jones G (2017). Algorithmic improvements to species delimitation and phylogeny estimation under the multispecies coalescent. *Journal of Mathematical Biology* **74**: 447–467.

Jones G, Aydin Z, Oxelman B (2015). DISSECT: an assignment-free Bayesian discovery method for species delimitation under the multispecies coalescent. *Bioinformatics* **31**: 991–998.

Jurjević Ž, Kubátová A, Kolařík M, *et al.* (2015). Taxonomy of *Aspergillus* section *Petersonii sect. nov.* encompassing indoor and soil-borne species with predominant tropical distribution. *Plant Systematics and Evolution* **301**: 2441–2462.

Jurjević Ž, Peterson SW, Horn BW (2012). *Aspergillus* section *Versicolores*: nine new species and multilocus DNA sequence based phylogeny. *IMA Fungus* **3**: 59–79.

Jurjević Ž, Peterson SW, Solfrizzo M, *et al.* (2013). Sterigmatocystin production by nine newly described *Aspergillus* species in section *Versicolores* grown on two different media. *Mycotoxin Research* **29**: 141–145.

Kato H, Nakahara T, Sugimoto K, *et al.* (2015). Isolation of notoamide S and enantiomeric 6-epi-stephacidin A from the fungus *Aspergillus amoenus*: biogenetic implications. *Organic letters* **17**: 700–703.

Katoh K, Standley DM (2013). MAFFT multiple sequence alignment software version 7: improvements in performance and usability. *Molecular Biology and Evolution* **30**: 772–780.

Kekkonen M, Hebert PD (2014). DNA barcode-based delineation of putative species: efficient start for taxonomic workflows. *Molecular Ecology Resources* **14**: 706–715.

Klich M (1993). Morphological studies of *Aspergillus* section *Versicolores* and related species. *Mycologia* **85**: 100–107.

Klich M, Mullaney E, Daly C (1993). Analysis of intraspecific and interspecific variability of three common species in *Aspergillus* section *Versicolores* using DNA restriction fragment length polymorphisms. *Mycologia* **85**: 852–855.

Kozakiewicz Z (1989). *Aspergillus* species on stored products. *Mycological Papers* **161**: 1–188.

Kubatko LS, Degnan JH (2007). Inconsistency of phylogenetic estimates from concatenated data under coalescence. *Systematic Biology* **56**: 17–24.

Letunic I, Bork P (2016). Interactive tree of life (iTOL) v3: an online tool for the display and annotation of phylogenetic and other trees. *Nucleic Acids Research* **44**: W242–W245.

Li YC, Wen J, Ren Y, *et al.* (2019). From seven to three: Integrative species delimitation supports major reduction in species number in *Rhodiola* section *Trifida* (*Crassulaceae*) on the Qinghai-Tibetan Plateau. *Taxon* **68**: 268–279.

Li Z-X, Wang X-F, Ren G-W, *et al.* (2018). Prenylated diphenyl ethers from the marine algal-derived endophytic fungus *Aspergillus tennesseensis*. *Molecules* **23**: 2368.

Liu YJ, Whelen S, Hall BD (1999). Phylogenetic relationships among ascomycetes: evidence from an RNA polymerse II subunit. *Molecular Biology and Evolution* **16**: 1799–1808.

Magoga G, Fontaneto D, Montagna M (2021). Factors affecting the efficiency of molecular species delimitation in a species-rich insect family. *Molecular Ecology Resources* **21**: 1475–1489.

Mason NA, Fletcher NK, Gill BA, *et al.* (2020). Coalescent-based species delimitation is sensitive to geographic sampling and isolation by distance. *Systematics and Biodiversity* **18**: 269–280.

Micheluz A, Manente S, Tigini V, *et al.* (2015). The extreme environment of a library: Xerophilic fungi inhabiting indoor niches. *International Biodeterioration & Biodegradation* **99**: 1–7.

Minh BQ, Schmidt HA, Chernomor O, *et al.* (2020). IQ-TREE 2: new models and efficient methods for phylogenetic inference in the genomic era. *Molecular Biology and Evolution* **37**: 1530–1534.

Nguyen HT, Nguyen TD, Le TML, *et al.* (2021). Integrative taxonomy of *Mesocriconema onoense* (Tylenchida: Criconematidae) from Vietnam highly suggests the synonymization of *Mesocriconema brevistylus* and related species. *Infection*, *Genetics and Evolution* **95**: 105090.

Nováková A, Hubka V, Saiz-Jimenez C, *et al.* (2012). *Aspergillus baeticus sp. nov.* and *Aspergillus thesauricus sp. nov.*, two species in section *Usti* from Spanish caves. *International Journal of Systematic and Evolutionary Microbiology* **62**: 2778–2785.

Nováková A, Hubka V, Valinová Š, *et al.* (2018). Cultivable microscopic fungi from an underground chemosynthesis-based ecosystem: a preliminary study. *Folia Microbiologica* **63**: 43–55.

O'Donnell K, Cigelnik E (1997). Two divergent intragenomic rDNA ITS2 types within a monophyletic lineage of the fungus *Fusarium* are nonorthologous. *Molecular Phylogenetics and Evolution* **7**: 103–116.

Pante E, Puillandre N, Viricel A, *et al.* (2015). Species are hypotheses: avoid connectivity assessments based on pillars of sand. *Molecular Ecology* **24**: 525–544.

Paradis E (2010). pegas: an R package for population genetics with an integrated-modular approach. *Bioinformatics* **26**: 419–420.

Parker E, Dornburg A, Struthers CD, *et al.* (2022). Phylogenomic species delimitation dramatically reduces species diversity in an Antarctic adaptive radiation. *Systematic Biology* **71**: 58–77.

Peterson SW (2008). Phylogenetic analysis of *Aspergillus* species using DNA sequences from four loci. *Mycologia* **100**: 205–226.

Pitt JI, AD Hocking (2009). *Fungi and food spoilage*. Springer, Dordrecht, Heidelberg, London, New York.

Posada D (2008). jModelTest: phylogenetic model averaging. *Molecular Biology and Evolution* **25**: 1253–1256.

Puillandre N, Lambert A, Brouillet S, *et al.* (2012). ABGD, Automatic Barcode Gap Discovery for primary species delimitation. *Molecular Ecology* **21**: 1864–1877.

R Core Team (2015). *R: A language and environment for statistical computing*. R Foundation for Statistical Computing. Vienna, Austria. R Foundation for Statistical Computing, Vienna, Austria.

Rank C, Nielsen KF, Larsen TO, *et al.* (2011). Distribution of sterigmatocystin in filamentous fungi. *Fungal Biology* **115**: 406–420.

Raper KB, Fennell DI (1965). *The genus Aspergillus*. Williams & Wilkins, Baltimore, MD.

Reid NM, Carstens BC (2012). Phylogenetic estimation error can decrease the accuracy of species delimitation: a Bayesian implementation of the general mixed Yule-coalescent model. *BMC Evolutionary Biology* **12**: 196.

Sakhri A, Chaouche NK, Catania MR, *et al.* (2019). Chemical composition of *Aspergillus creber* extract and evaluation of its antimicrobial and antioxidant activities. *Polish Journal of Microbiology* **68**: 309.

Samson RA, Visagie CM, Houbraken J, *et al.* (2014). Phylogeny, identification and nomenclature of the genus *Aspergillus*. *Studies in Mycology* **78**: 141–173.

Seo T-K (2008). Calculating bootstrap probabilities of phylogeny using multilocus sequence data. *Molecular Biology and Evolution* **25**: 960–971.

Shao J, Wang Q, Wei L, *et al.* (2022). Limitations of matrix-assisted laser desorption/ionization time-of-flight mass spectrometry for the identification of *Aspergillus* species. *Medical Mycology* **60**: myab084.

Shehata AN, Abd El Aty AA, Darwish DA, *et al.* (2018). Purification, physicochemical and thermodynamic studies of antifungal chitinase with production of bioactive chitosan-oligosaccharide from newly isolated *Aspergillus griseoaurantiacus* KX010988. *International Journal of Biological Macromolecules* **107**: 990–999.

Schmitt I, Crespo A, Divakar P, *et al.* (2009). New primers for promising single-copy genes in fungal phylogenetics and systematics. *Persoonia* **23**: 35–40.

Schwab CJ, Straus DC (2004). The roles of *Penicillium* and *Aspergillus* in sick building syndrome. *Advances in Applied Microbiology* **55**: 215–238.

Siqueira JPZ, Sutton DA, García D, *et al.* (2016). Species diversity of *Aspergillus* section *Versicolores* in clinical samples and antifungal susceptibility. *Fungal Biology* **120**: 1458–1467.

Sklenář F, Jurjević Ž, Houbraken J, *et al.* (2021). Re-examination of species limits in *Aspergillus* section *Flavipedes* using advanced species delimitation methods and description of four new species. *Studies in Mycology* **99**: 100120.

Sklenář F, Jurjević Ž, Peterson SW, *et al.* (2020). Increasing the species diversity in the *Aspergillus* section *Nidulantes*: Six novel species mainly from the indoor environment. *Mycologia* **112**: 342–370.

Sklenář F, Jurjević Ž, Zalar P, *et al.* (2017). Phylogeny of xerophilic aspergilli (subgenus *Aspergillus*) and taxonomic revision of section *Restricti*. *Studies in Mycology* **88**: 161–236.

Struck TH, Feder JL, Bendiksby M, *et al.* (2018). Finding evolutionary processes hidden in cryptic species. *Trends in Ecology & Evolution* **33**: 153–163.

Sukumaran J, Holder MT, Knowles LL (2021). Incorporating the speciation process into species delimitation. *PLoS Computational Biology* **17**: e1008924.

Sukumaran J, Knowles LL (2017). Multispecies coalescent delimits structure, not species. *Proceedings of the National Academy of Sciences of the United States of America* **114**: 1607–1611.

Swain SK, Debta P, Sahu MC, *et al.* (2020). Otomycosis due to *Aspergillus versicolor*. *International Journal of Health & Allied Sciences* **9**: 192.

Thom C, Church MB (1926). *The Aspergilli*. Williams & Wilkins, Baltimore, MD.

Thom C, Raper KB (1945). *A manual of the Aspergilli*. Williams &Wilkins, Maryland, MD.

Tsang C-C, Hui TWS, Lee K-C, *et al.* (2016). Genetic diversity of *Aspergillus* species isolated from onychomycosis and *Aspergillus hongkongensis sp. nov.*, with implications to antifungal susceptibility testing. *Diagnostic Microbiology and Infectious Disease* **84**: 125–134.

Turland NJ, Wiersema JH, Barrie FR, *et al.* (2018). International Code of Nomenclature for algae, fungi, and plants (Shenzhen Code) adopted by the Nineteenth International Botanical Congress Shenzhen, China, July 2017. Koeltz Botanical Books, Glashütten.

van Rossum G, Drake FL (2019). *Python language reference, version 3*. Python Software Foundation.

Venables WN, Ripley BD (2002). *Modern applied statistics with S*. Fourth edition. Springer, New York.

Veršilovskis A, De Saeger S (2010). Sterigmatocystin: occurrence in foodstuffs and analytical methods–an overview. *Molecular Nutrition & Food Research* **54**: 136–147.

Vidal-Acuña MR, Ruiz-Pérez de Pipaón M, Torres-Sánchez MJ, *et al.* (2018). Identification of clinical isolates of *Aspergillus*, including cryptic species, by matrix assisted laser desorption ionization time-of-flight mass spectrometry (MALDI-TOF MS). *Medical Mycology* **56**: 838–846.

Visagie CM, Hirooka Y, Tanney JB, *et al.* (2014). *Aspergillus*, *Penicillium* and *Talaromyces* isolated from house dust samples collected around the world. *Studies in Mycology* **78**: 63–139.

Wang PM, Liu XB, Dai YC, *et al.* (2018). Phylogeny and species delimitation of *Flammulina*: taxonomic status of winter mushroom in East Asia and a new European species identified using an integrated approach. *Mycological Progress* **17**: 1013–1030.

Wang X-C, Zhuang WY (2022). New species of *Aspergillus* (*Aspergillaceae*) from tropical islands of China. *Journal of Fungi* **8**: 225.

Wickham H (2016). *ggplot2: elegant graphics for data analysis*. Springer-Verlag, New York.

Yang Z (2015). The BPP program for species tree estimation and species delimitation. *Current Zoology* **61**: 854–865.

Zahradnik E, Kespohl S, Sander I, *et al.* (2013). A new immunoassay to quantify fungal antigens from the indoor mould *Aspergillus versicolor*. *Environmental Science: Processes & Impacts* **15**: 1162–1171.

Zhang J, Kapli P, Pavlidis P, *et al.* (2013). A general species delimitation method with applications to phylogenetic placements. *Bioinformatics* **29**: 2869–2876.

Supplementary Material: https://studiesinmycology.org/

Fig. S1. Phylogenetic tree based on 48 ITS sequences of series *Versicolores* strains available from the NCBI GenBank database (Table 1). The tree was calculated in IQ-TREE v. 2.1.2 with 100 000 ultrafast bootstrap replicates (only support values higher than 70 % are shown). TrNef was selected as the most suitable model of evolution by jModelTest v 2.1.7. The ex-type strains are designated with a superscript T.

Table S1. Strains from *Aspergillus* series *Versicolores* used for calculation of phylogenetic tree based on the partial calmodulin sequences (Fig. 1).

Table S2. Growth rates of selected strains on eight cultivation media after 14 d in mm (average values from at least three measurements).

Table S3. Production of Hülle cells on eight cultivation media after 3 wk of cultivation at 25 °C in the dark.

Table S4. Maximum sequence dissimilarity between isolates of the same *Aspergillus* species whose species limits have been delimited using methods based on multispecies coalescent model; only species represented by isolates from at least three countries were included.